6-2013

Conductive Polymer Blends and Their Use in Memory Devices

Mohammad Yousef Al-Haik

UAEU

جامعة الإمارات العربية المتحدة
United Arab Emirates University

United Arab Emirates University

Deanship of Graduate Studies

Conductive Polymer Blends and Their Use in Memory Devices

By

Mohammad Yousef Al-Haik

Supervised by

Dr. Saud Aldajah

Mechanical Engineering Department

Faculty of Engineering, UAEU

Dr. Ahmad Ayesh

Physics Department

Faculty of Science, UAEU

Dr. Mahmoud Mohsin

Chemistry Department

University of Sharjah

A Thesis Submitted to the Deanship of Graduate Studies in Partial Fulfillment of the Requirements for the Degree of Master of Science in

Mechanical Engineering

June 2012

ES/F11

United Arab Emirates University
Faculty of Engineering, Graduate Studies
M.S.c. Program in Mechanical Engineering

THESIS EXAMINATION REPORT

Student ID : 200950069

Student Name : Mohammad Yousef Al- Haik

Title of the Thesis : Conductive Polymer Blends and Their Use in Memory Devices

The Thesis Examination as A Partial Fulfillment of M. Sc. Degree in Mechanical Engineering Was conducted on 07/06/2011 Based on Examining the Thesis and the Students Presentation and the Subsequent Discussion, The Committee Recommends:

- [x] Thesis is Satisfactory as is.
- [ ] Thesis is Satisfactory After Minor Modifications.
- [ ] Thesis should be Re-Evaluated After Major Modifications.
- [ ] Thesis is Rejected.

Examining Committee Members:

Thesis Supervisor: Dr Saud Al-Dajah Signature: ..... Date: 7/6/2012

Member: Dr. Ahmad Alawar Signature: ..... Date: 7/06/2012

Member: Dr Nayef Ghasem Signature: ..... Date: 7/6/2012

Member: Dr. Dagou Zeze, Durham University. UK Signature: ..... Date: 25/06/12

Approval of Program Coordinator:

Dr. Salahaddin Al-Omari Signature: ..... Date: 7/6/2012

APPROVAL:

Associate Dean for Research and Graduate Studies ..... Date : 25/6/2012

DEDICATION

This work is dedicated to my beloved parents, especially my father 'Yousef Haik', who never gave up on me and believed in me. To my wife and kids, the love and joy of my life, who have sacrificed so much for me to accomplish this work, I greatly appreciate their support and encouragement.

ABSTRACT

The aim of this project is to synthesize and characterize conductive polymers made out of blending non conductive polymers with ionic liquids. An application to demonstrate the use of these novel conductive polymers is to create an organic memory device.

Attempts to synthesize conductive polymers have been reported in the literature; several of these approaches include doping a polymer with arsenic or iodine based dopant. In this work, ionic liquids, known as plasticizer, are used as the dopant for non-conductive polymers. There are several advantages of employing the ionic liquids over other dopants, including the maintenance of organic based blends (both the polymers and ionic liquids are organic) and maintaining biocompatibility of the blends for bio-related applications.

In this work, conductive polymers were synthesized by blending non-conductive mixture of poly vinyl alcohol (PVA) and Poly-acrylamide-co-acrylic acid (PAA) with different weight percentages of glycerol, sorbitol and imidazolium bromide). The percentage of the dopant plasticizers were varied from 0-5% by wt ratio. The solution casting method was used to form thin films, which were examined with nanoindentation, differential scanning calorimetry (DSC), thermo gravimetric analysis (TGA), Fourier Transform Infrared spectroscopy (FT-IR) and *ac* impedance spectroscopy. It was found that the thermal properties (glass transition, T_g, melting point, T_m, and decomposition temperature, T_d) for the blended PVA/PAA showed a decrease proportional to the percentages of the three plasticizers used in this project. The hardness and elastic modulus obtained from the nanoindentation test were also found to decrease with increase in plasticizer concentration. FT-IR confirmed the reduction in hydrogen bonding between

combined polymer chains in favor of formation new bonding between the plasticizers and the polymer blend chains.

The novelty of doping nonconductive polymers with ionic liquid stems from the ability to modulate the degree of electrical conductivity, mechanical and thermal properties of the blends by controlling the percentage of the ionic liquid introduced into the polymer will open a new field of polymer studies; hence, organic polymer blends.

Once blends with favorable electrical properties were identified; they were then utilized in producing an organic storage memory device. A hysteresis loop approximately ±20V wide was observed as a charge element based under ±20V sweep range when CNT was blended, but ±5 to ±10 when gold (*Au*) and zinc oxide (*ZnO*) were blended along with the mixture of the polymers and the glycerol. The impedance measurements showed that the ionic conductivity of PVA/PAA polymer membrane can be controlled by addition of plasticizer. Hence, the novel conductive polymer presented in this thesis formed a solution to overcome challenges associated with a total organic memory device. The doped polymers were substituted for the silicon base semiconductor in a conventional memory device, however with enhanced performance compared to the silicon based device.

ACKNOWLEDGEMENTS

I would like to start off by thanking the Almighty Allah for giving me the ability and the possibility to fulfill the tasks needed to complete this work.

I am sincerely thankful for all my advisors for their unlimited and continuous support and guidance. I wish to thank them for taking time from their busy schedules to help me finish this work on time. I'm very thankful for their support while preparing the thesis and publications.

I am also very thankful for all the technicians and engineers, Tahir Abdul-Rahman, Habib Abdul-Rahman, Vinitha Baboo, Mohammad Shaar, for helping me when I needed their help the most. I would like to thank the technician, Gamal Sorour for his help in the SEM imaging.

Lastly, I would like to thank my family and friends for their support as well, especially my parents and wife for their continuous belief in me.

TABLE OF CONTENTS

LIST OF FIGURES

Figure **Page**

LIST OF TABLES

Table **Page**

LIST OF SCHEMES

Scheme **Page**

Chapter 1:

INTRODUCTION

In the last few years, researches on both blended polymers and semiconductors have fascinated widespread interest due to their applications in electronic device [1]. The conjugated organics polymers are used in many applications, such as in memory devices [2, 3] sensors and fuel cells. A few polymers exhibit hydrophilic characteristics that received much attention for membrane electrolytes in recent years [4]. One of the main advantages of polymeric electrolytes are their good mechanical, electrical and thermal properties, their ease to synthesis into thin films of desirable sizes, and the ability to form good electrode contact for impedance/ conductivity testing.

In this study, non-conductive polymers are doped with organic plasticizers to modulate their electrical conductivity. Two non-conductive polymers were blended with three different plasticizers at different weight ratios, respectively. The two polymers used were poly-vinyl alcohol (PVA) and poly-acrylamide-co-acrylic acid (PAA) which were mixed together to make the blend, the mixture ratio was 1:1. The plasticizers used were glycerol, sorbitol and 1-methyl-3-n-decyl-imidazolium bromide which were added to the polymer mixture with varying weight percentages of 1%, 2%, 3% and 5%. These two polymers were selected due to their biodegradability and solubility in water. Previously, the mechanical and thermal properties for PVA as a function of the dopant concentration were reported.

A key element of the property of a polymer blend is the miscibility of its components, because it affects the mechanical properties, the morphology, its permeability and degradation [5, 6]. A large scale of investigations regarding the miscibility in multi-component polymer systems has

been carried out using scanning electron microscope (SEM). The blends are of particular significance because they can be used as biomedical and biodegradable materials [7-17].

Diff

conductivity of polymer films such as preparation of polymer blends and preparation of composite polymer electrolytes (CPE), by means of blending in organic plasticizers and/or fillers [18]. Investigation is being focused on polymer films to enhance the ambient temperature conductivity by blending of polymers [19] cross-linking [20] insertion of ceramic filters [21] plasticization [22], etc. Polymer blend is the most valid and feasible approach to producing high ionic conduction.

In this chapter, brief introduction about the polymer blends as well as the dopants will be introduced.

1.1 Poly-vinyl alcohol (PVA)

PVA is a hydrophilic semi-crystalline polymer produced by polymerization of vinyl acetate monomer to form poly (vinyl acetate) (PVAc), and subsequent hydrolysis of PVAc to form PVA [23]. PVA is soluble in water and its solubility in water is being influenced by a number of factors such as; the degree of hydrolysis, molecular weight and molecular weight distribution, particle size distribution and crystallinity [24]. When formed as thin films, the properties of PVA are extremely affected by the molecular weight and the degree of hydrolysis [25]. PVA is a great polymer to choose for making biodegradable blends with natural polymers due to its good film-forming capability [26] and water solubility. Several studies show that PVA has been used on biopolymer based materials produced by casting or extrusion [27]. In the case of casting

produced polymer films from aqueous solution, the research shows PVA to have been blended with polysaccharides, such as starch [26, 28-30], gellan [31] and with proteins, such as wheat gluten [32], collagen [33,34]and gelatin [35-37]. The conductivity of PVA polymer films are modulated when blending the polymer with ionic liquids such as the ones studies for this project.

1.2 Poly-acrylamide-co-acrylic acid (PAA)

Poly (acrylamide-co-acrylic) acid is a type of anionic polymer and has a wide range of applications, such as, the stabilizer and a flocculent in many technological and ecological processes. It is capable of absorbing a lot of water; many times its weight in water and this is used in disposable diapers [38]. PAA as a film affects the properties by the change of molecular weight and the degree of hydrolysis. As the molecular weight of PAA increases above 1,000,000; it finds applications as a flocculent [39]. By controlling the hydrogel behavior of PAA, it is a useful method to prepare polymer blends. Both PVA and PAA are currently being used in many biomedical applications as active hydrogels since both are hydrophilic polymers [40]. PAA may be treated in PVA network while crosslinking and also forming new bonds.

1.3 Ionic Liquids

Room temperature ionic liquids (RTILs) are salts with melting points close or below room temperature, 30°C. Most polymers in the industry have shown to display hydrophilic characteristics which have had more scientists paying much attention for membrane electrolyte during the past few years. The first work to become published in the study for solid polymer electrolyte was carried out by Wright and co-workers [41, 42] and was devoted to the ionic nature for their conducting behavior. Scientists have used ionic liquids, also known as

plasticizers, as organic solvents and supporting electrolytes in many fields due to their exceptional properties like high conductivity, non-volatility, non-flammability, etc. [43-48]. Due to the significant development of plasticizers to the conductivity, thermal and electrochemical properties of polymers, the merging of plasticizers into different polymers has been reported [49-51]. In order to overcome the brittleness of polymer films, the addition of plasticizers is important to improve flow and flexibility, and to increase toughness, to impact resistance of film coasting, and to prevent them from cracking during packaging and transportation [52, 53]. The compatibility and permanence is normally based on the selection of plasticizer for a specified system, the amount needed for plasticization, and the desired physical properties of the films [54].

Ionic liquids when blended with polymers show a promising class of new materials with a bright technological future. The blends are now being used in application that are enabled by their presence, as well as in application where device or process performance outweighs their higher cost [55].

The main driving force to explore ionic liquids is the fact that these compounds have a very low vapor pressure, so that they are candidates to replace volatile organic solvents in organic reactions, because the properties of ionic liquids (miscibility with water and other solvents, dissolving ability, polarity, viscosity, density) can be tuned by an appropriate choice of the anion and the cation. Ionic liquids are often considered as designer solvents. These ionic liquids can also be used to immobilize transition metal catalysts in the liquid phase of biphasic catalytic reactions. Other applications include their use as solvents for extraction processes and as an

electrolyte for batteries, fuel cells, and dye-sensitized solar cells. Also they are neutral organic compounds.

Ionic liquid are a class of liquid salt that contain anions and cations. The ionic character means that some of the properties of the ionic liquid differ significantly from that of conventional organic liquids.

1.3.1 Glycerol

Glycerol is a syrupy, colorless, water soluble high-boiling point liquid with a distinctly sweet taste. It's often used in many industrial applications, such as shaving cream, soaps, and has been reported to be used in most medical applications, namely, cough drops, and children syrups (fever medicines). It's also widely used as a plasticizer and it's a natural produced material.

1.3.2 Sorbitol

Sorbitol, also known as glucitol, is a combination of compounds found naturally in many fruit plants, it's a sweet-tasting crystalline alcohol which is produced commercially by the reduction of glucose, and it is used as a sugar substitute because of its slow metabolism rate. It is a non-sticky, nonconductive solution found in apples, pears, peaches, and prunes [56]. Sorbitol is also non-toxic and rapidly metabolized; it contains no antimicrobial or bacteriostatic agents. It is used in many clinical applications, similarly, to treat urinary bladder and prostatic infections. It, similar to glycerol is a widely used plasticizer and it's naturally produced.

1.3.3 Imidazolium Bromide

Imidazole is an organic compound with the formula $(CH)_2N(NH)CH$. It is a colorless solid that dissolves in water to give mildly basic solution. It is known to chemists as an aromatic heterocycle, classified as a diazole and as an alkaloid. Imidazole has been used extensively as a corrosion inhibitor on certain transition metals, such as copper. Preventing copper corrosion is important, especially in aqueous systems, where the conductivity of the copper decreases due to corrosion. Imidazole is used to synthesis many ionic liquids, one for example is 1-methyl-3-n-decyl-imidazolium bromide $(C_{14}H_{27}N_2)^+Br^-$, which is used as a semiconductor in this project, where it and the other plasticizers give the s-shape for a hysteresis loop.

2. Scope of the Thesis

In this work, the effect of the three ionic liquids (glycerol, sorbitol and imidazolium bromide) the percentages on mechanical, thermal, and electrical properties of PVA alone, PAA alone and the combination of the blended films are investigated. Both DSC and TGA were used to analyze the thermal properties of the solid state PVA/PAA polymer membrane blends. Nanoindentation was carried out to analyze the mechanical properties, hardness and toughness of the polymer blends. SEM was used to examine the surface morphology and the cross-sectional view of the blends. The resulting membrane of this blend polymer electrolyte showed very high ionic conductivity. The ionic conductivity of the polymer blend electrolyte membrane with the three plasticizers was measured by an *ac* impedance spectroscopy. The characteristic properties for the PVA/PAA polymer membrane electrolyte with different composition ratios have been systemically studied and are discussed.

Organic memory devices that employ the conductive character of the doped polymers have been utilized to replace the conventional silicon dioxide wafers used in a memory device to produce a total complete organic memory device.

Chapter 2:

MATERIALS AND EXPERIMENTAL METHODS

This chapter discusses the experimental methods utilized in this work to synthesis and characterizes the conductive polymer.

2.1. Materials

All three plasticizers (Glycerol, Sorbitol and 1-methyl-3-n-decyl-Imidazolium Bromide) were obtained from Quartek Corp., NC. Polyvinyl alcohol (PVA) and poly (acrylamide-co-acrylic) acid (PAA) were purchased from Sigma-Aldrich Chemical Co. PVA having an average molecular weight of 61,000 g/mol with a 99% rate of acetyl hydrolysis and PAA with an average molecular weight of 5,000,0000 g/mol were used in this study. All other reagents that were used in the laboratory were also purchased from Sigma-Aldrich and used as needed. De-ionized water was used in the preparation of the polymer films.

2.2 Materials and Membrane Preparation

PVA and PAA were dissolved separately in deionized water. 100ml of water was used to dissolve 5 grams of each polymer in conical flasks. Undergoing vigorous stirring and heating continuously at 90°C for several hours until both show homogeneous nature. Blending both together to obtain a jelly type substance (PVA/PAA combined). All three plasticizer were used as dopants with weight percentages of 1%, 2%, 3% and 5%. 10ml of each polymer solution was mixed with the percentages mentioned; PVA blended with the three plasticizers and their weight percentages. Same procedure was followed for PAA and the blended polymer (PVA-PAA). They were then casted into films by spreading the suspension on glass plates (microscope slide plates) and keeping in a hot air vacuum oven at 80°C for 24 hours to remove any excess water. After which, the films were visually inspected for their dryness and free standing nature.

2.3. Thermogravimetric Analysis (TGA)

Weight decomposition percentage was analyzed using the Thermogravimetric analyzer TGA (Q50, TA Instruments, Water LLC) that contains a TGA Heat Exchanger system for analyzing PVA, PAA and the blend that contained the plasticizers. Each sample, approximately 5-8 mg in weight was placed on a ceramic plate inside the tube furnace, which was heated from 25°C to 600°C at a rate of 10°c/min under nitrogen atmosphere. The results were analyzed using TA Universal Analysis 2000 V4.5A build 4.5.05 (TA Instruments) software. All PVA-PAA, PVA-PAA-Glycerol, PVA-PAA-Sorbitol, PVA-PAA-Imidazolium bromide polymer membrane samples were tested at least three times for average readings.

2.4. Differential Scanning Calorimetry (DSC)

DSC analysis of polymeric membranes were carried out using a differential scanning calorimeter DSC Q200 V24.4 Build 116 Model (TA Instruments, Water LLC) containing a refrigerator cooling system. Each sample, approximately 5-8mg in weight was placed in a hermetically sealed aluminum pans and were then heated from -50°C to 400°C at a rate of 10°C/min under nitrogen atmosphere [57]. Placed inside the furnace next to the filled pan is an empty hermetically sealed aluminum pan as a reference cell. The results were analyzed using TA Universal Analysis 2000 V4.5A Build 4.5.05 (TA Instruments) software. All PVA-PAA, PVA-PAA-Glycerol, PVA-PAA-Sorbitol, PVA-PAA-Imidazolium bromide polymer membrane samples were tested at least three times for average readings.

2.5. Nanoindentation

All nanoindentation testing of PVA, PAA, PVA-PAA, PVA-PAA-Glycerol, PVA-PAA-Sorbitol and PVA-PAA-Imidazolium Bromide membrane films were performed by a Nano Test Materials Testing Platform Two (Micro materials LTD, Wrexham, UK) that was equipped with a three-sided pyramid diamond indenter tip (Berkovich type) [58]. The nanoindentation tests were carried out as follows: a constant displacement rate of 0.01607 mN/s was maintained during the increment of load until the indenter reached a depth of 1827nm into the surface of the films. The load was then held at maximum value (1mN) for 30s in order to avoid the creep that may significantly affect the unloading behavior. The indenter was then withdrawn from the surface at the same rate as indenting until 10% of the maximum load, followed by the indenter being completely removed from the material. Here, constant displacement rate was chosen to load the samples to avoid stain-hardening effects on the measurements [59]. At least five indents were performed on each sample and the distance between the indentations was 50 μm to avoid the interaction.

Both the hardness (H) and reduced modulus (E), elastic modulus, were obtained from the load-displacement spread sheet. As the indenter penetrated into the sample, both the elastic and plastic deformation occurred, however, the elastic portion was the only section of the displacement that recovered during the unloading of the indenter. Nanoindentation hardness is defined as follows [4].

$$H - \frac{P_{\max}}{A} = \frac{P_{\max}}{24.5 h_c^2} \qquad (1)$$

Where P_{max} is the load measured at a maximum depth of penetration (h) in an indentation cycle, A is the projected contact area; and h_c is the contact depth of the indentation, which is given by

$$h_c = h - 0.75 \frac{P_{\max}}{S} \qquad (2)$$

Where S is the slope, $\frac{dP}{dh}$, of the initial portion of the unloading curve at $h=h_{max}$ and 0.75 is a constant that depends on the indenter geometry. The elastic modulus of the sample was inferred from the initial unloading contact stiffness S. the relationship among contact stiffness, contact area, and the elastic modulus was derived as follows [60].

$$S = 2\beta E_r \sqrt{\frac{A}{\pi}} \qquad (3)$$

Where β is a constant that depends on the geometry of the indenter (β=1.034 for a Berkovich indenter) and E_r is the reduced elastic modulus, taking into account the elastic deformation of both the specimen and the indenter. For evaluating E_r, the contact stiffness (S), and the contact area (A) could be determined accurately from load against displacement graph measured during the indentation process. The specimen's elastic modulus (E_s) was then calculated as follows [61],

$$E_s = \frac{1 + v_s^2}{\frac{1}{E} - \frac{1 - v_i^2}{E_i}} \qquad (4)$$

Where v_s and v_i (0.07) [62] are the Poisson's ratios of the specimen and indenter, respectively, whereas E_i is the modulus of the diamond indenter (1141 GPa). In all the calculations, the estimated value of v_s of semi-crystalline polymeric materials is 0.35 [63].

2.6. Fourier Transform Infrared Spectroscopy (FTIR)

FTIR spectroscopy is an analytical technique used to identify organic and inorganic materials. The analysis results in an absorption spectra which provides information about the chemical bonds and molecular structure of a material whether organic or inorganic. The technique works on the fact that bonds and groups of bonds vibrate at characteristic frequencies. A molecule that is exposed to infrared rays absorbs infrared energy at frequencies which are characteristic to that molecule. The specimen's transmittance and reflectance of the infrared rays at different frequencies is translated into an IR absorption bands.

The spectroscopy was used to characterize the presence of specific chemical groups in the materials. Transmission infrared spectra of all films were recorded at room temperature using a NEXUS-470 (Thermo Nicolet Corporation) Spectrophotometer in the range of wave number from 4000 to 400 cm^{-1} during 32 scans, with 2 cm^{-1} resolution. Each film was sandwiched between two KBr plates and placed in the sample holder mounted in the instrument. The infrared

spectra were recorded after scanning the background. The background scan was used as a reference.

2.7. Scanning Electron Microscopy (SEM)

SEM was carried out using a Jeol Model JSM-5600 instrument at an accelerating voltage of 10KV and 18-300,000 magnifications with guaranteed resolution of 3.5 nm. Sample film was dehydrated at room temperature using ethanol for 1 hr, dried in air and then sputter-coated with a thin film of gold. The film was cut and SEM was examined on the surface of the cut.

2.8. ac Impedance Measurements

A Solarton 1260A Impedance/Gain-Phase Analyzer was used to conduct the *ac* measurement within a frequency range of 1-10^6 Hz as a function of temperature between 25°C to 125°C. Z-60 and Z-View software package was used to control measurements which provide the complex impedance ($Z(\omega)$) and the phase angle (θ) as a function of frequency ($f = \omega/2\pi$). The total ac impedance of a material provides a quantitative measure of the induction and capacitance parts and given by the relation, $Z(\omega) = Z'(\omega) - iZ''(\omega)$. Where $Z'(\omega)$ and $Z''(\omega)$ are the real and imaginary parts of the impendence. The software was also used to fit the measurements, and to simulate the results with equivalent circuits. The polymer films were placed between two stainless-steel electrodes (the surface area of the top electrode as a constant 9.62×10^{-6} m^2 while the area of the bottom electrode is large to ease the electrode alignment). The total impedance was resolved into $Z'(\omega)$ and $Z''(\omega)$ using the phase versus frequency measurements which were used to draw Nyquist plots (frequency is an implicit function).

Chapter 3:

RESULTS AND DISCUSSION

This chapter presents the results obtained for characterizing the conductive polymer blends.

3.1. Thermal Properties

The properties of the polymers used in this project have shown that when adding plasticizers to them causes them to reduces the interaction between macromolecules which introduces favorable properties such as decrease in hardness, elastic modulus, and melting properties. Thermal degradation of polymeric materials is a consequence of the fact that the organic macromolecules within the polymer matrix as well as low-molecular-weight organic molecules are stable only up to a certain temperature range. Their stability depends on the inherent characteristics of the sample as well as the specific interactions associated between the different macromolecules or molecules present in the polymer. These interactions are due to the dipole-dipole interaction, van der Waals, London, and hydrogen bonding forces. Since molecules/macromolecules consist of atoms or group linked together by covalent bonds, and the strength of these bonds are limited, a high thermal stability of the blend can be explained at the molecular level because of the less scission of chemical bonds under the influence of heat. Chain scission or bond dissociation takes place when the supplied thermal energy exceeds the bond dissociation energy of the respective bond or group. The plasticizers are low-molecular-weight molecules, that when added to polymeric materials modifies the tridimensional organization of the polymeric matrix, decreasing the intermolecular attraction forces and consequently, increasing the free volume and the mobility of the polymeric hydroxyl groups and the polar functional groups of some amino acids residues [64-66].

3.1.1. TGA Analysis

The TGA thermographs for neat PVA, neat PAA, neat PVA-PAA, and various composition ratios for PVA-PAA-Glycerol, PVA-PAA-Sorbitol, and PVA-PAA-Imidazolium Bromide membrane blends have been conducted and analyzed to determine their thermal stability and the corresponding degradation stages in response to temperature as well as their moisture content in the membrane. The aim is to understand quantitatively the chemical reactions occurring during the thermal treatment of polymer blends. All polymer membranes exhibited two-stage degradation. Figure 3.1(*a-d*) shows all the combined TGA curves of neat PVA, PAA and the blend PVA-PAA membranes. Figure 3.2(*a-e*) depicts all the TGA curves with various composition ratios of PVA-PAA-Glycerol membranes. Figure 3.3(*a-e*) illustrates all the TGA curves of various composition ratios of PVA-PAA-Sorbitol membranes. And Figure 3.4(*a-e*) exhibits all the TGA curves of various composition ratios of PVA-PAA-Imidazolium Bromide membranes. The percentage weight loss of each sample with temperature range is rendered in Tables 3.1-3.4 for all polymeric membranes conducted in the order as respectively mentioned in the order of the Figures.

All the Tables show a three-step degradation process. All demonstrated an initial loss of about 3-6% weight occurring from 25-150^{o}C except for the polymers that were blended with glycerol, they showed dramatic weight loss of 8-13% between that range. The initial range was related to both the loss of non-bound water and to the formation of intra and intermolecular anhydrides.

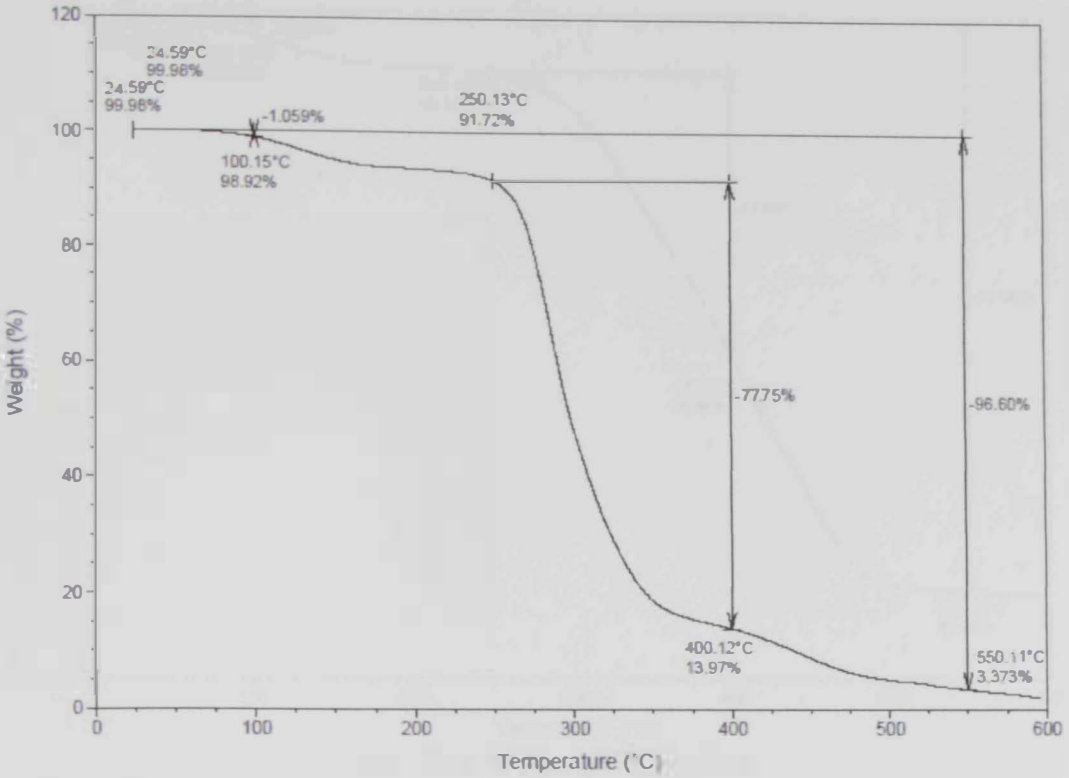

a) TGA of Neat PVA

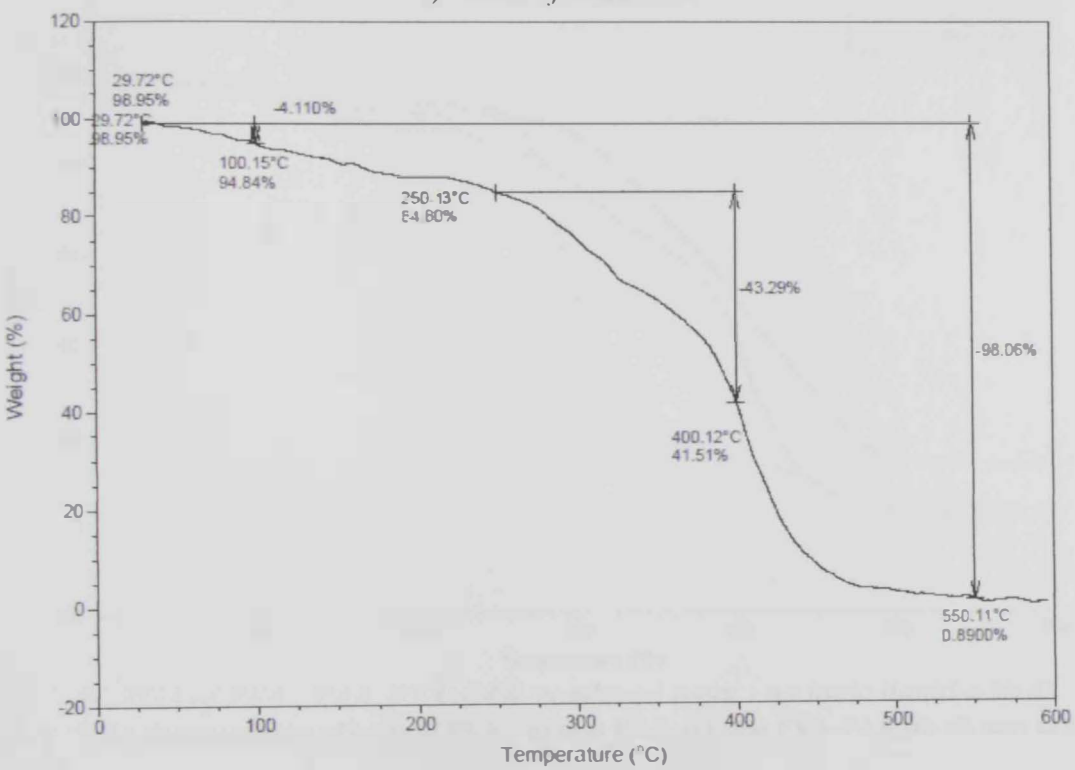

b) TGA of Neat PAA

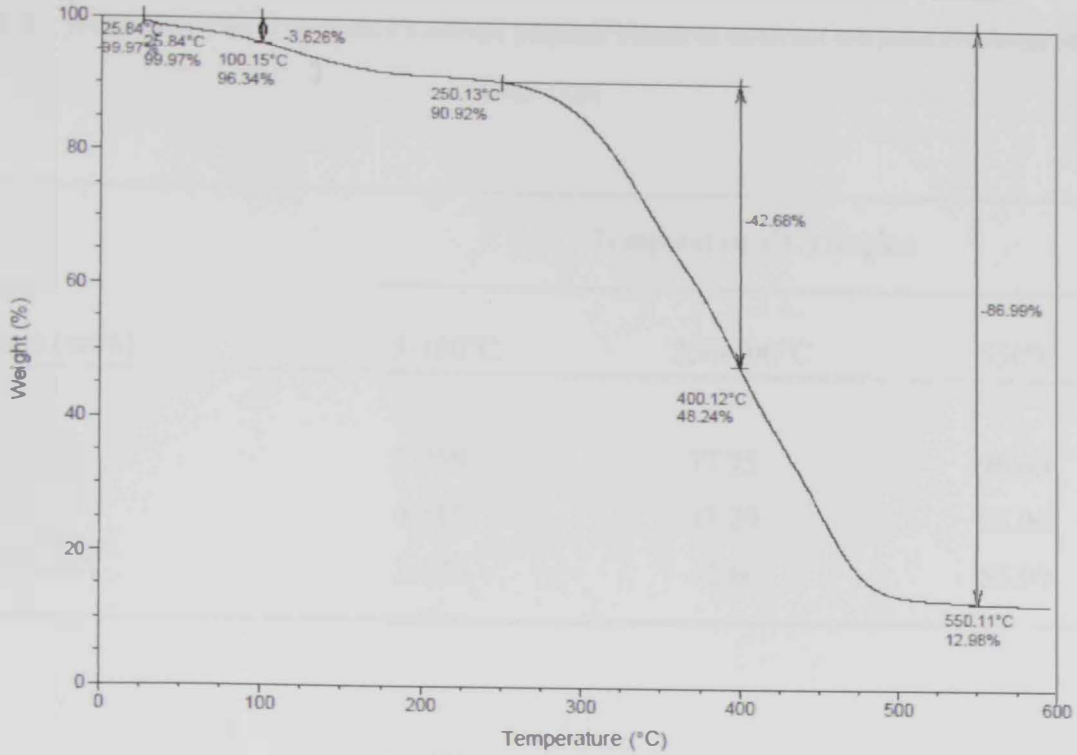

c) TGA of Neat PVA & PAA

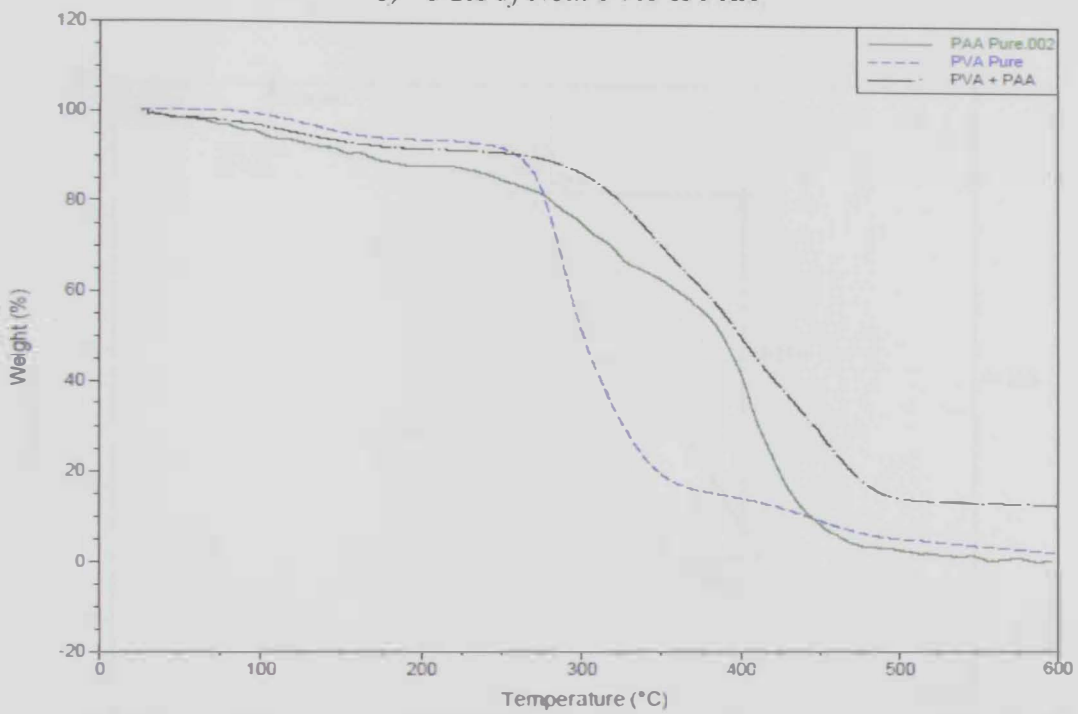

d) TGA of PVA , PAA, PVA-PAA combined (neat - no ionic liquid added)

Figure 3. 1 TGA thermographs of (a) neat PVA, (b) neat PAA, (c) neat PVA-PAA (d) all neat combined

Table 3. 1 Weight loss (%) of the neat PVA-PAA polymer blends at different temperature range obtained from TGA

IL Weight Percentage (wt%)	Temperature (°C) Region		
	25-100°C	250-400°C	550°C
0.0 PVA	1.059	77.75	96.60
0.0 PAA	4.110	43.29	98.06
0.0 PVA+PAA	3.626	42.66	86.99

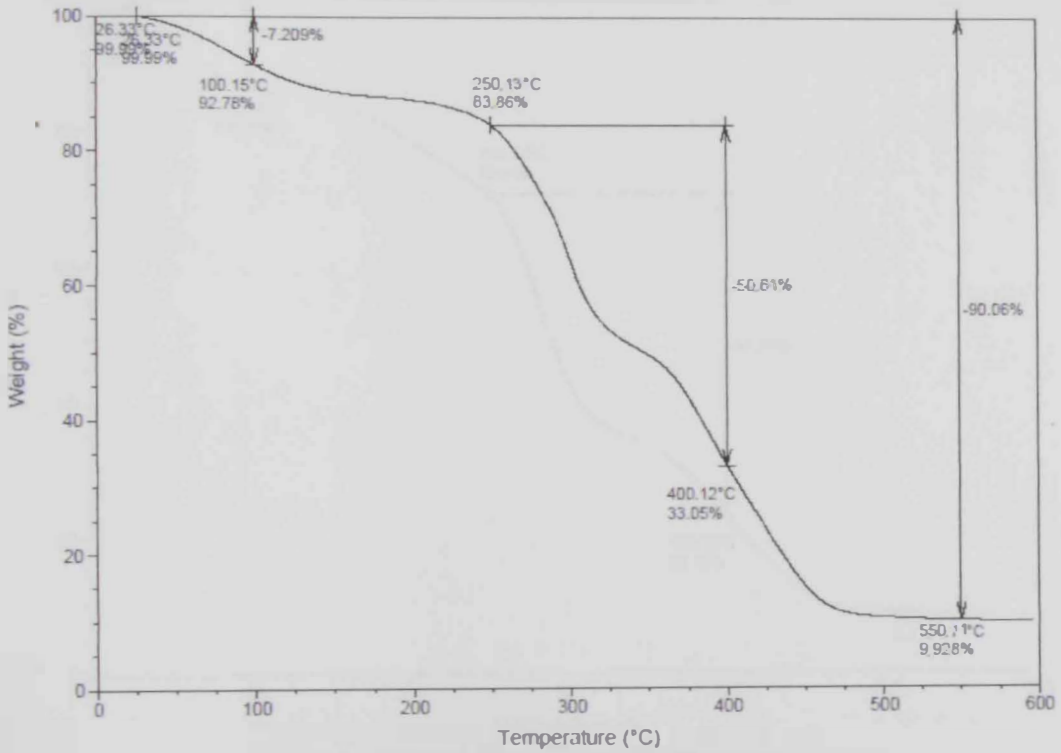

a) TGA of PVA-PAA-1% Glycerol

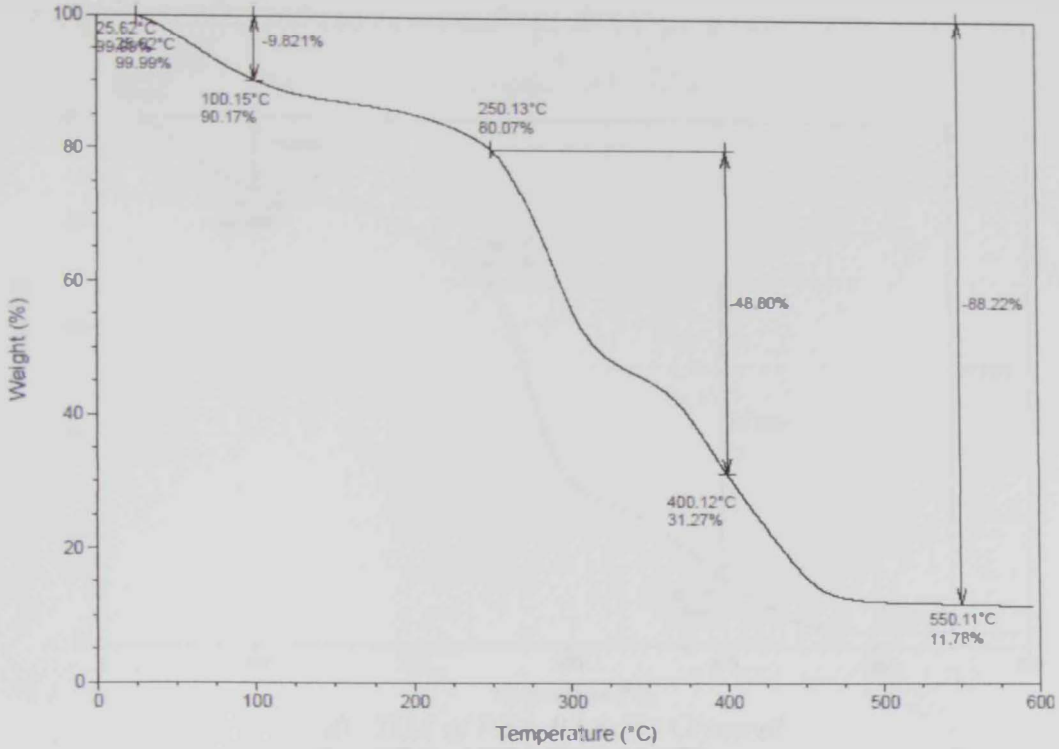

b) TGA of PVA-PAA-2% Glycerol

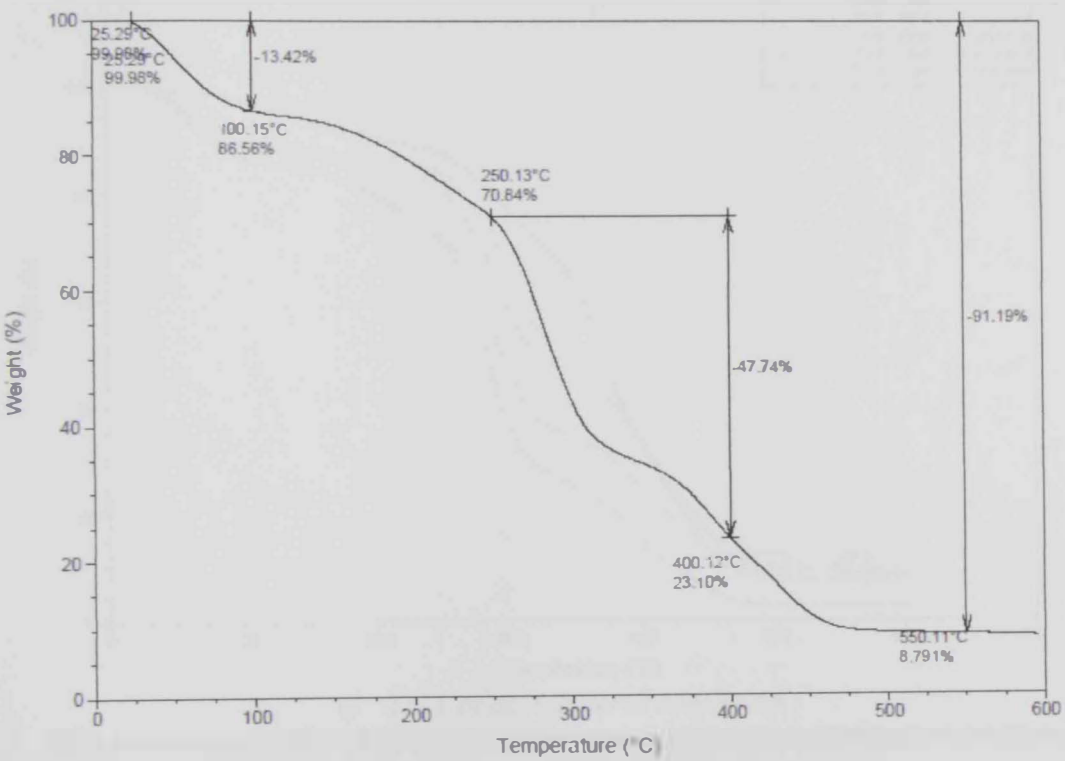

c) TGA of PVA-PAA- 3% Glycerol

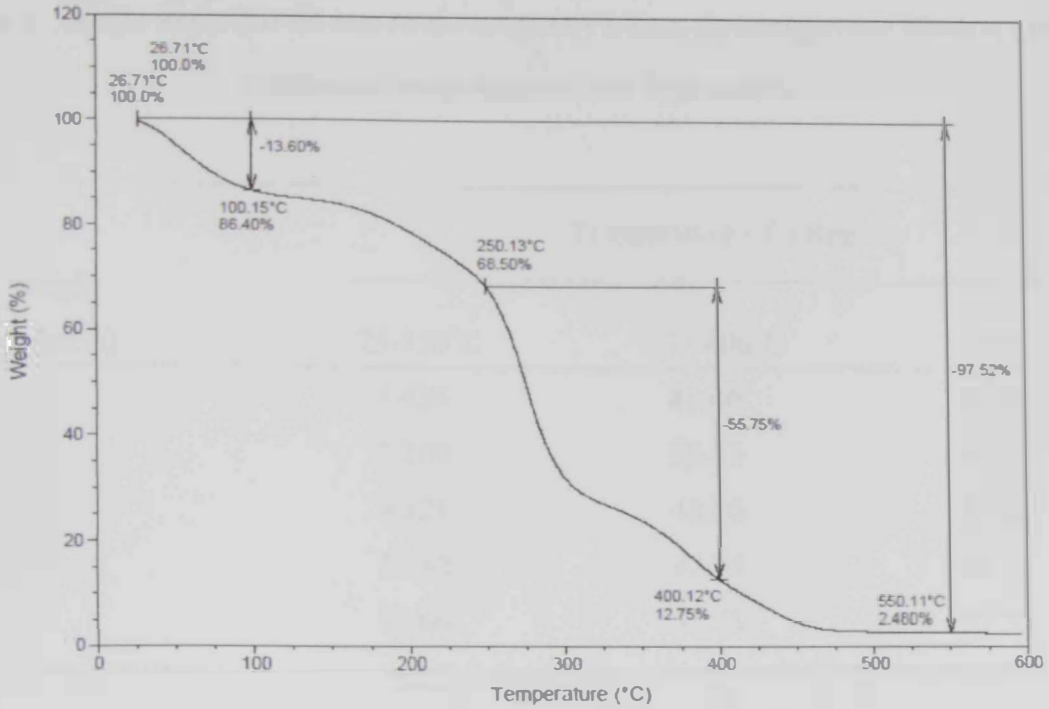

d) TGA of PVA-PAA-5% Glycerol

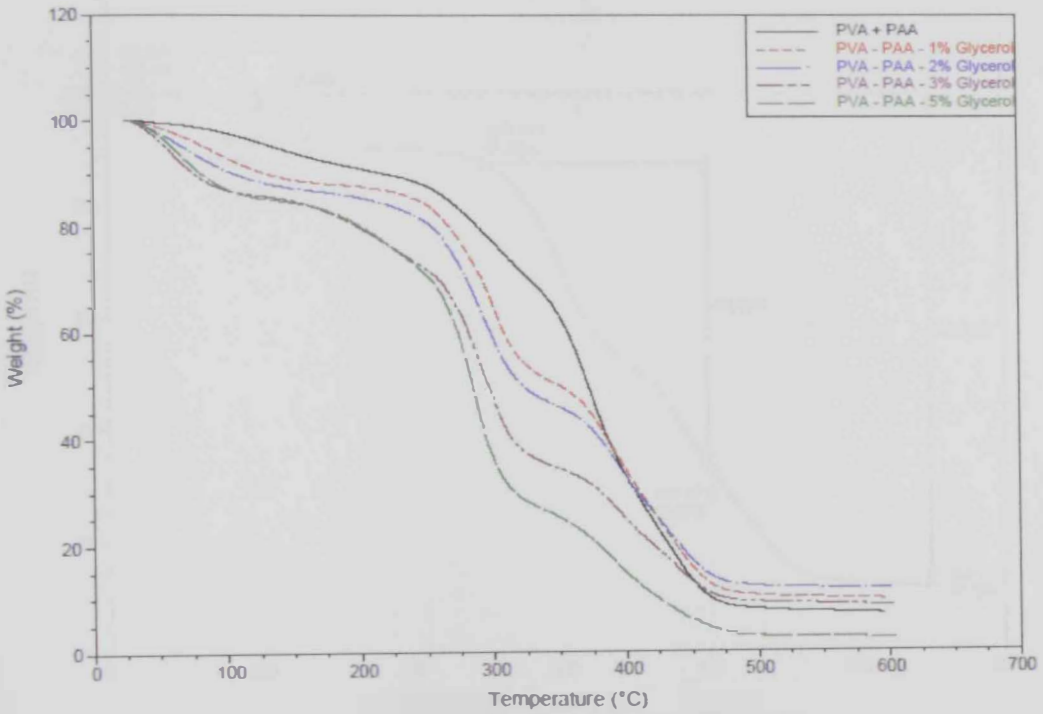

e) TGA of all Glycerol combined

Figure 3. 2 TGA thermographs of (a) PVA-PAA-1%Glycerol, (b) PVA-PAA-2%Glycerol, (c) PVA-PAA-3%Glycerol, (d) PVA-PAA- 5% Glycerol, (e) all Glycerol composition ratio membranes combined

Table 3. 2 Weight loss (%) of the neat PVA-PAA and PVA-PAA-Glycerol polymer blends at different temperature range obtained from TGA analysis

Glycerol Weight Percentage (wt%)	Temperature (°C) Region		
	25-150°C	250-400°C	550°C
0.0	3.626	42.66	86.99
1.0	7.209	50.81	90.06
2.0	9.821	48.80	88.22
3.0	13.42	47.74	91.19
5.0	13.60	55.75	97.52

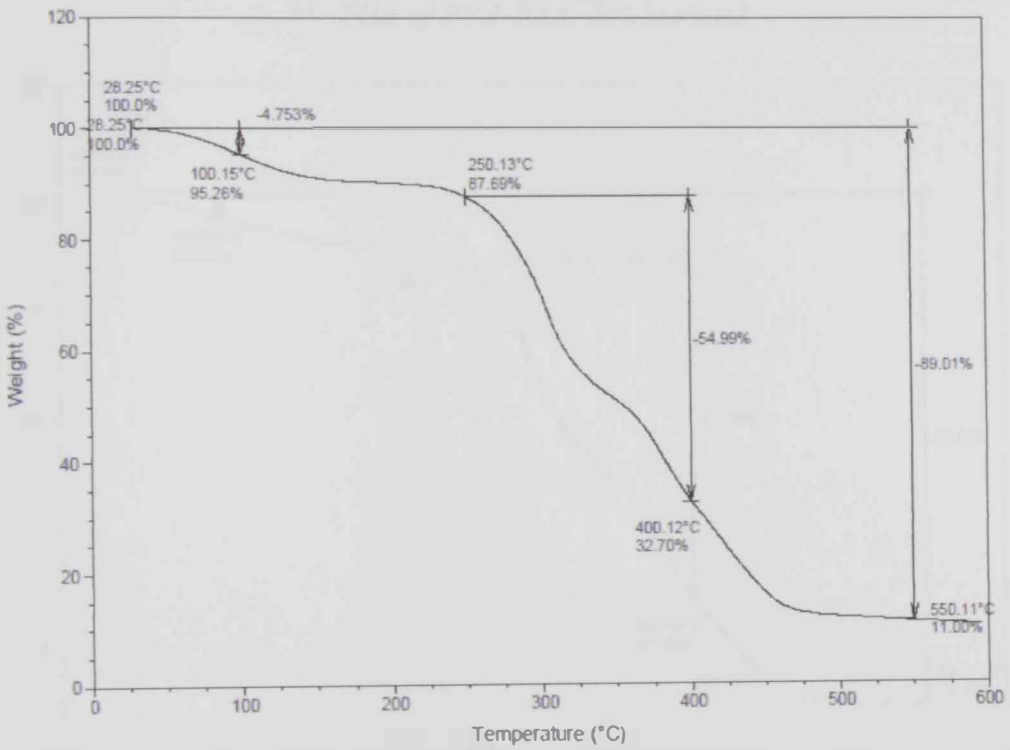

a) TGA of PVA-PAA- 1% Sorbitol

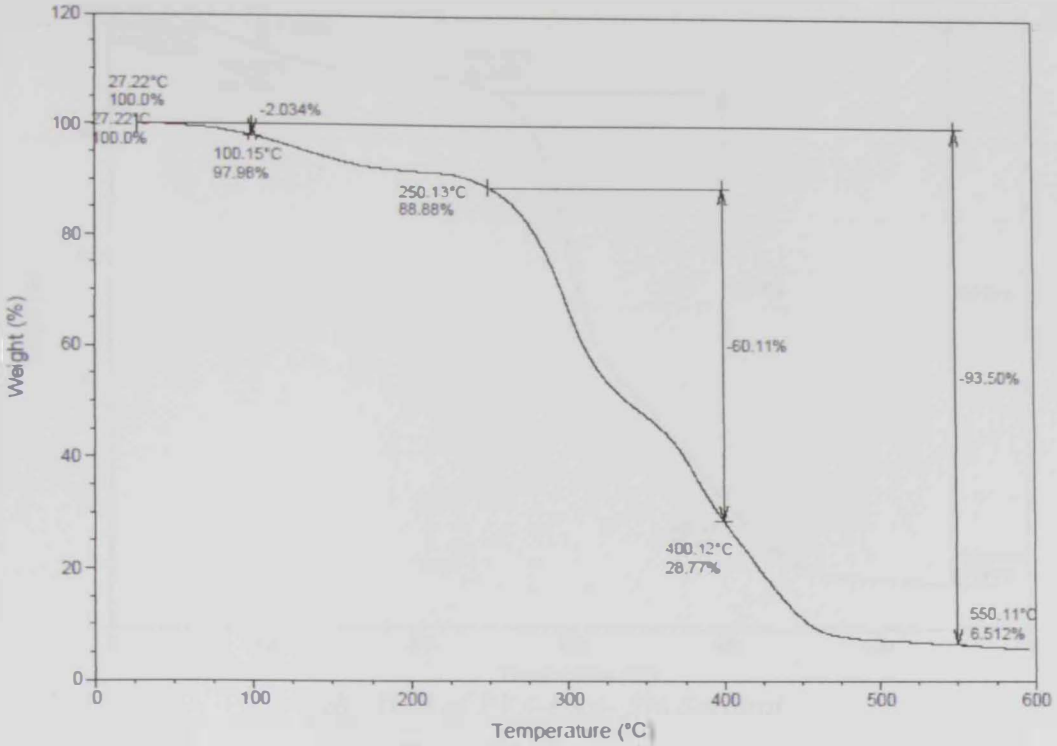

b) TGA of PVA-PAA- 2% Sorbitol

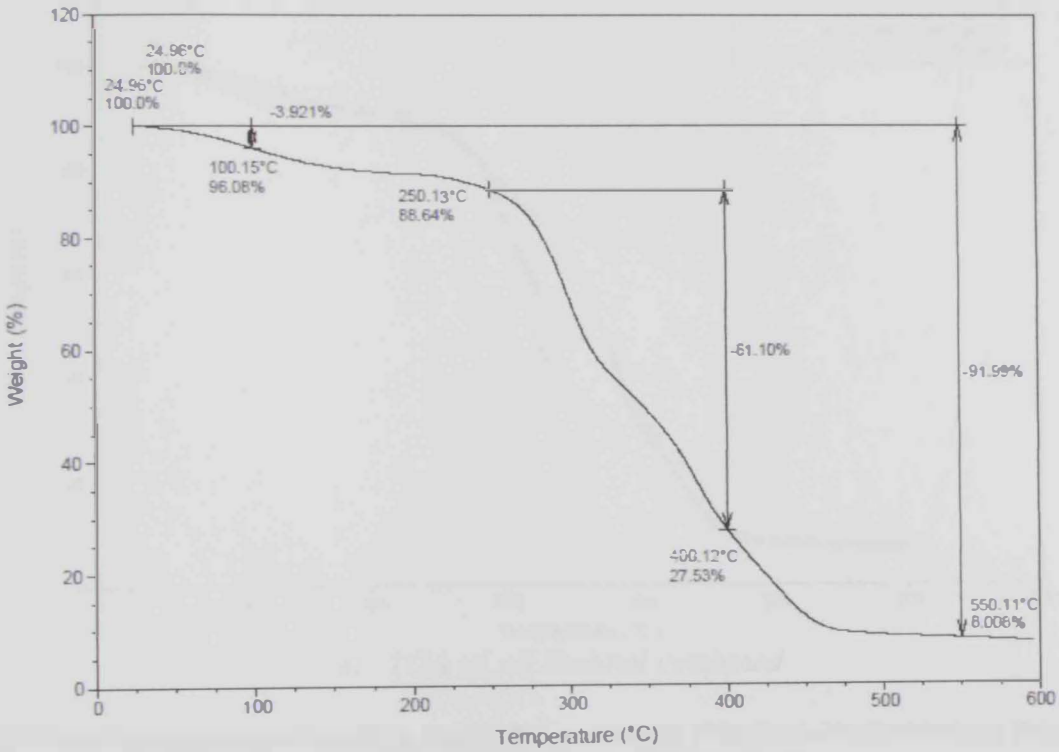

c) TGA of PVA-PAA- 3% Sorbitol

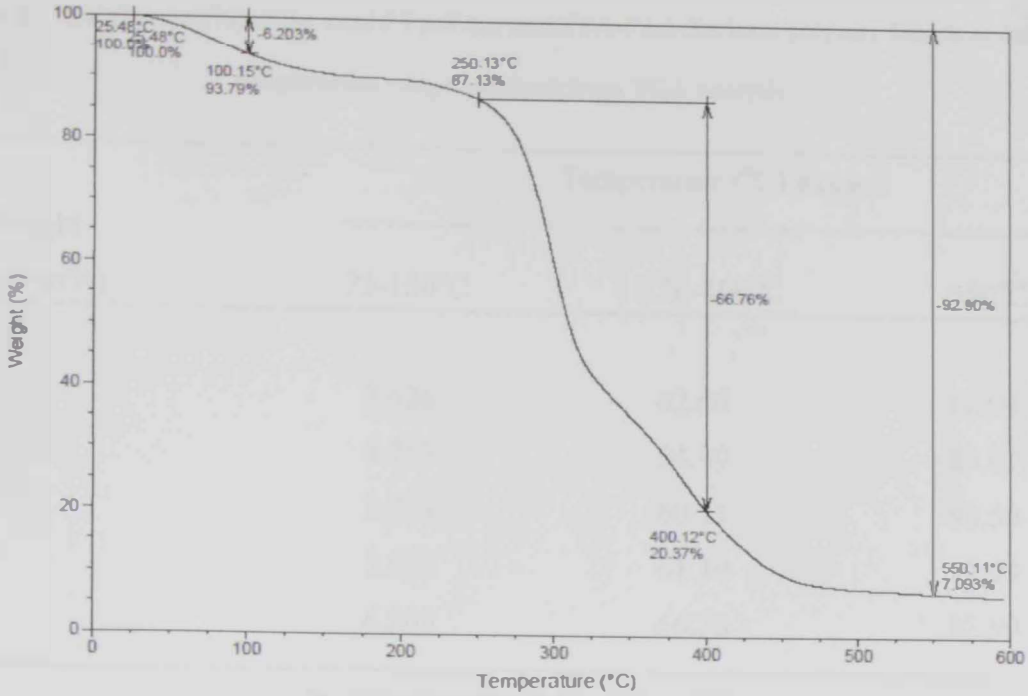

d) TGA of PVA-PAA- 5% Sorbitol

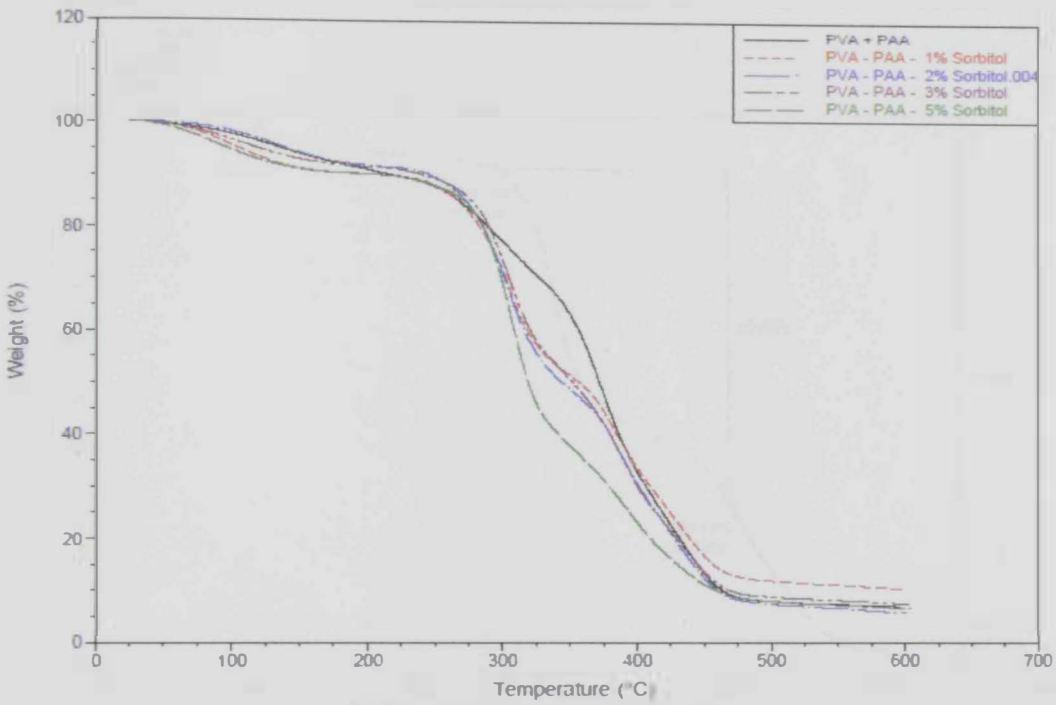

e) TGA of all Sorbtiol combined

Figure 3. 3 TGA thermographs of (a) PVA-PAA- 1% Sorbitol, (b) PVA-PAA-2% Sorbitol, (c) PVA-PAA-3% Sorbitol, (d) PVA-PAA- 5% Sorbitol, (e) all Sorbitol composition ratio membranes combined

Table 3. 3 Weight loss (%) of the neat PVA-PAA and PVA-PAA-Sorbitol polymer blends at different temperature range obtained from TGA analysis

Sorbitol Weight Percentage (wt%)	Temperature (°C) Region		
	25-150°C	250-400°C	550°C
0.0	3.626	42.66	86.99
1.0	4.753	54.99	89.01
2.0	2.034	60.11	93.50
3.0	3.921	61.10	91.99
5.0	6.203	66.76	92.90

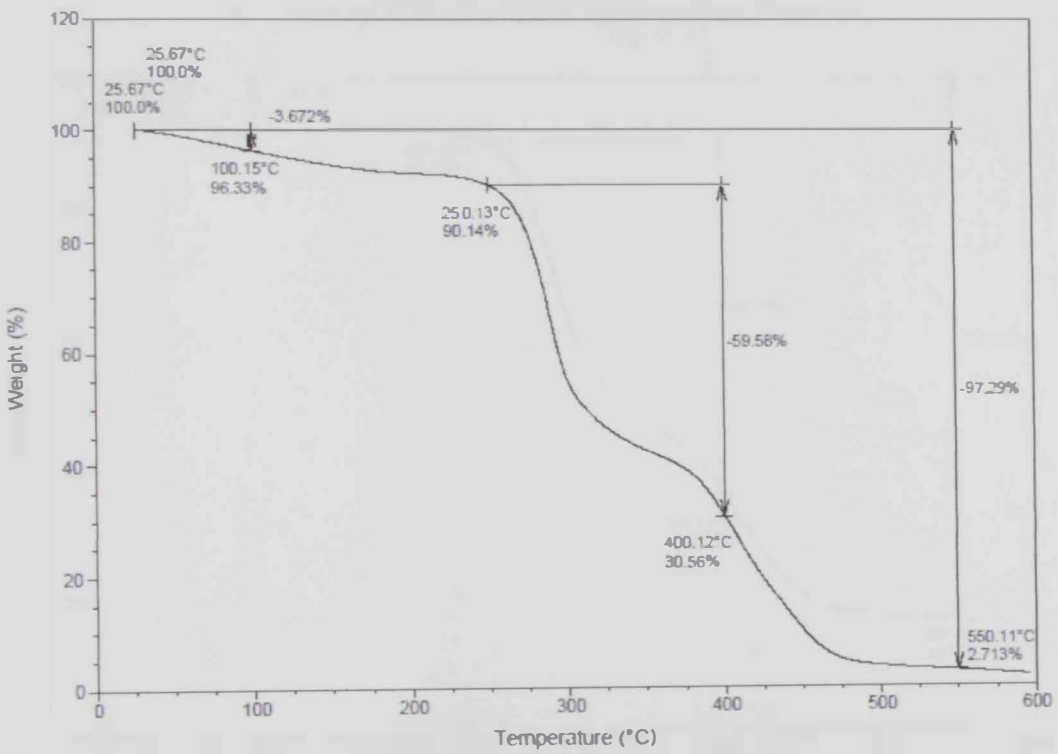

a) TGA of PVA-PAA- 1% Imidazolium Bromide

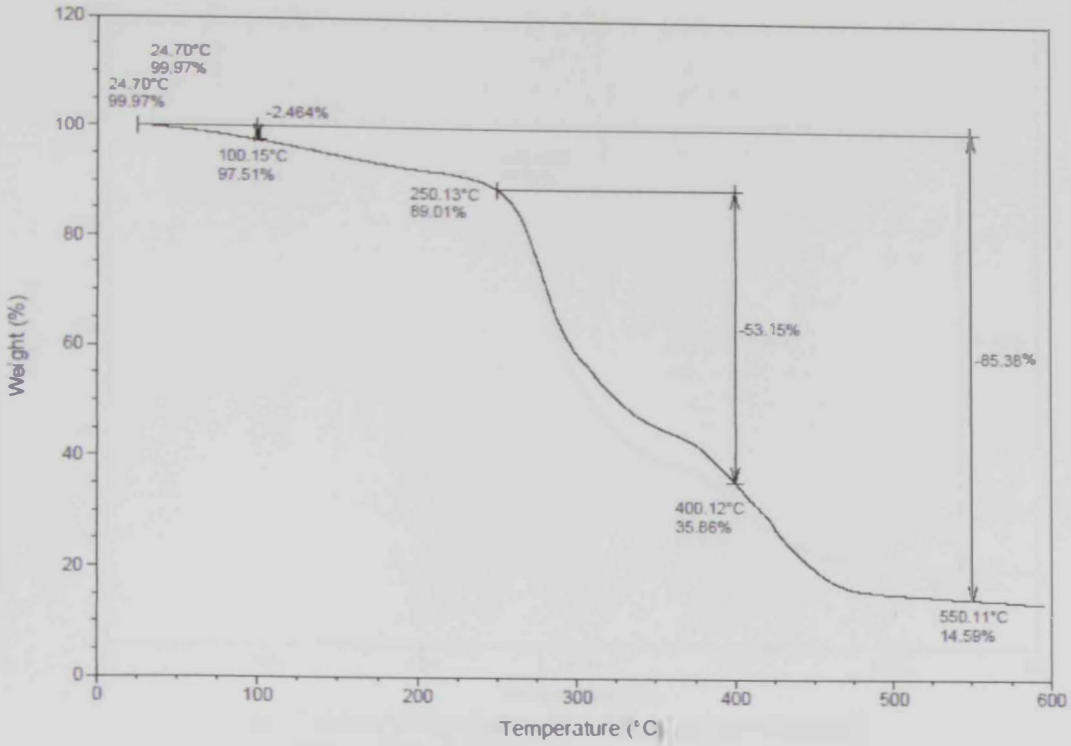

b) TGA of PVA-PAA- 2% Imidazolium Bromide

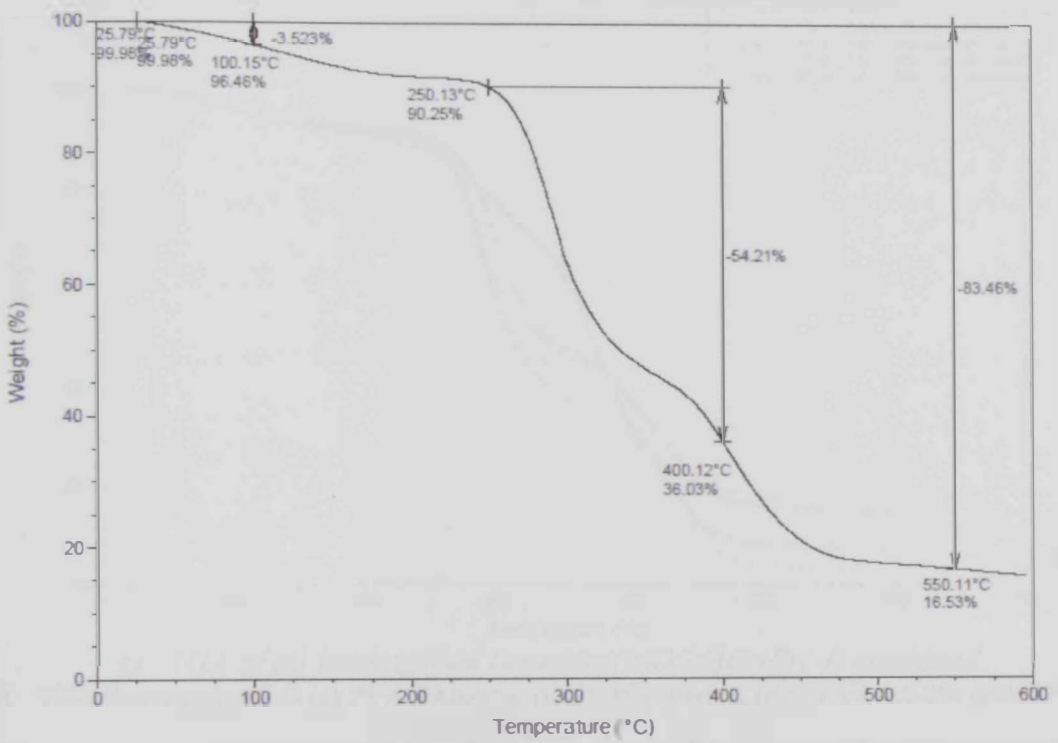

c) TGA of PVA-PAA- 3% Imidazolium Bromide

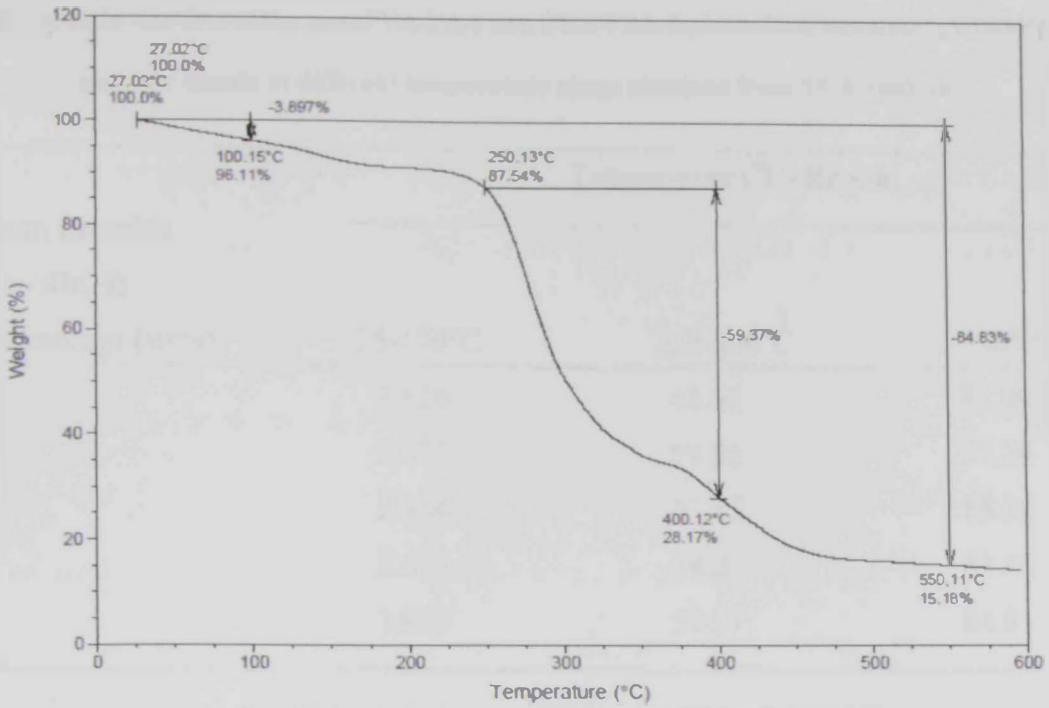

d) TGA of PVA-PAA- 5% Imidazolium Bromide

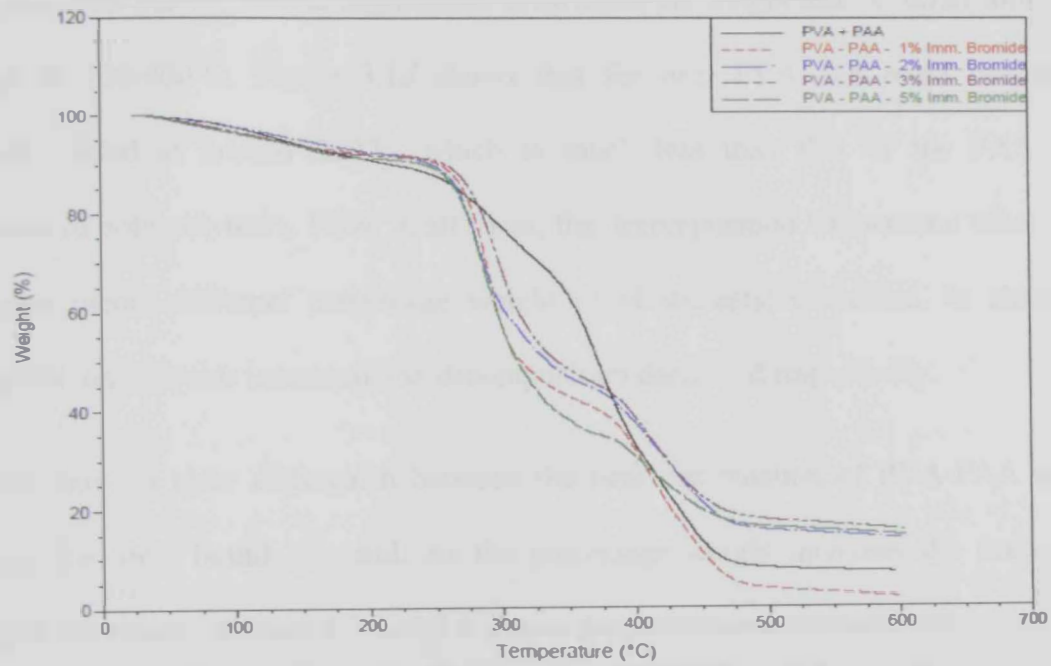

e) TGA of all Imidazolium Bromide([MDIM](+)Br(-)) combined

Figure 3. 4 TGA thermographs of (a) PVA-PAA-1% (|MDIM|(+)Br(-)), (b) PVA-PAA-2% (|MDIM|(+)Br(-)) , (c) PVA-PAA-3% (|MDIM|(+)Br(-)), (d) PVA-PAA- 5% (|MDIM|(+)Br(-)), (e) all (|MDIM|(+)Br(-)) composition ratio membranes combined

Table 3. 4 Weight loss (%) of the neat PVA-PAA and PVA-PAA-Imidazolium Bromide ([MDIM](+)Br(-)) polymer blends at different temperature range obtained from TGA analysis

Imidazolium Bromide ([MDIM](+)Br(-)) Weight Percentage (wt%)	Temperature (°C) Region		
	25-150°C	250-400°C	550°C
0.0	3.626	42.66	86.99
1.0	3.672	59.56	97.29
2.0	2.464	53.15	85.38
3.0	3.523	54.21	83.46
5.0	3.897	59.37	84.83

It is also observed that the second degradation in all cases the weight loss occurred somewhere in the range of 250-400°C. Figure 3.1*d* shows that for neat PVA, the onset decomposition temperature stated at around 250°C, which is much less than that of the PAA and the combination of both polymers. Now, in all cases, the decomposition temperature when added to the polymer blends different percentage weight of plasticizers; decreased. In short, as the percentage of ionic liquids increased, the decomposition decreased respectively.

Figure 3.2 shows a clear distinguish between the neat combination of PVA-PAA and when added to it the ionic liquid, glycerol. As the percentage weight increases the decomposition temperature decreases. Figures 3.3 and 3.4 shows the same pattern, so in accordance to adding plasticizers, the decomposition temperature started at approximately 250°C in all cases, this is directly related to the plasticizing effect of the ionic liquids causing the decomposition temperature to decrease to a lower value. The second stage around 350-450°C was due to the

carbonation of polymer matrix followed by a final decomposition of the polymer chains that begins around 550°C. The second stages were associated to the decarboxylation process of intra and inter molecular anhydrides formed during the previous dehydration and related to the dehydration of the OH groups of the copolymer [67]. There was an 85% or more weight loss for all samples at above 550°C. TGA data are given above in tables 3.1-3.4.

The onset decomposition temperature for PVA-PAA blends starts at 300°C. After this temperature, the PVA-PAA-glycerol, PVA-PAA-sorbitol, PVA-PAA-imidazolium bromide polymer membrane becomes greatly degraded. It has been clearly evidenced that the polymer blends with ionic liquids membrane samples are relatively stable in the temperature range of 100-275°C.

3.1.2. DSC Analysis

The samples of the blended films were analyzed by DSC to determine the glass transition (T_g), melting point (T_m), and decomposition temperature (T_d) which were extracted from the instrument's software. All thermographs were obtained from the initial heating run from -50 to 400°C. Three endothermic peaks were observed on the DSC curves of the blended polymer membranes. The first peak from 75-150°C, is due to the relaxation in the polymer crystalline domains. The second relaxation in the temperature range of 180-225°C is caused by the melting of the crystalline domains of the PVA-PAA polymer membranes, and the third relaxation peak starting from 250°C and higher is due to the decomposition of the polymer blends. A smaller peak area of T_m for the polymer membrane indicates a smaller fraction of crystalline phase and a larger fraction of amorphous phase, which may benefit anionic transportation [68].

In Figure 3.5, the neat polymer membrane films; it is observed that when the polymer PVA and PAA were blended together showed a shift to a higher temperature for the melting point than that of the combined polymer film. As for the transition peak, it's seen that the temperature of the combined is in between the PVA and PAA polymer membranes. The glass transition temperature for neat PAA is much less than that of neat PVA which when mixed together leads to the interaction of molecules of PAA to take the lead. Same pattern is seen for the melting temperature, but for the decomposition temperature (T_d), the dominating polymer is neat PVA at about 330°C and neat PAA at around 279°C, so when blended, gave a temperature range in between the two.

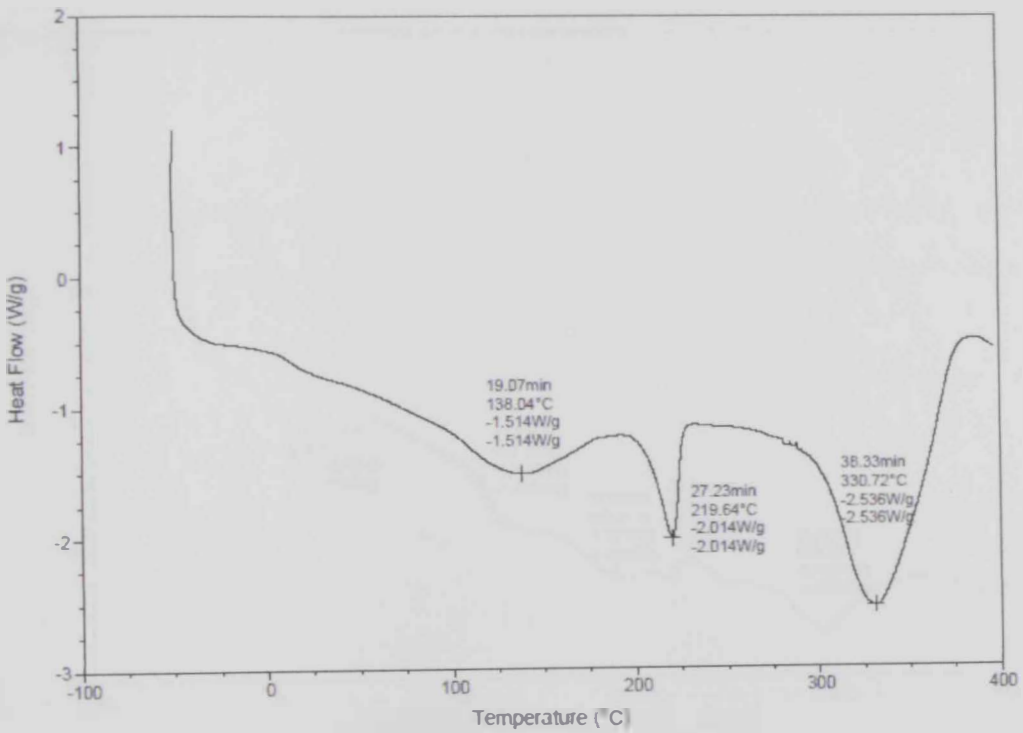

a) DSC of Neat PVA

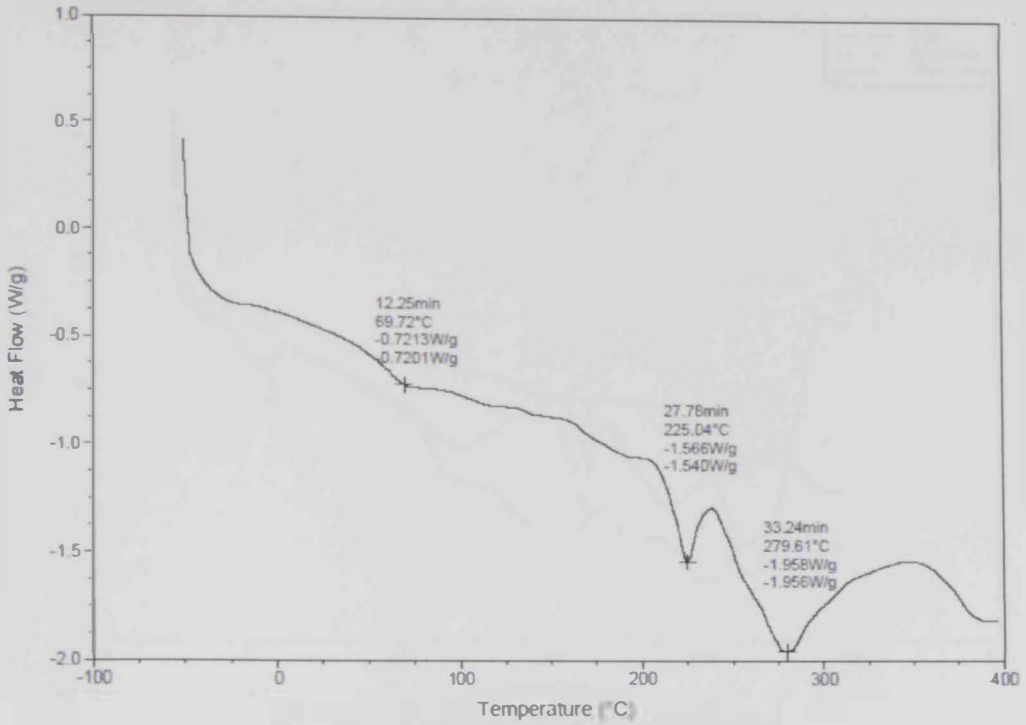

b) DSC of Neat PAA

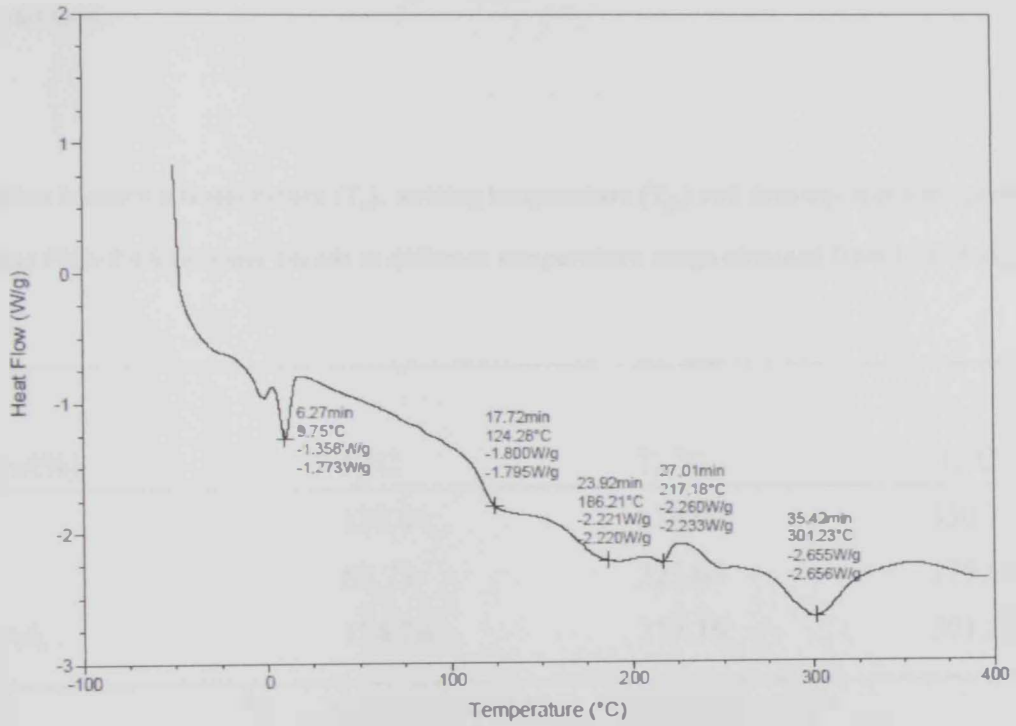

c) DSC of Neat PVA - PAA

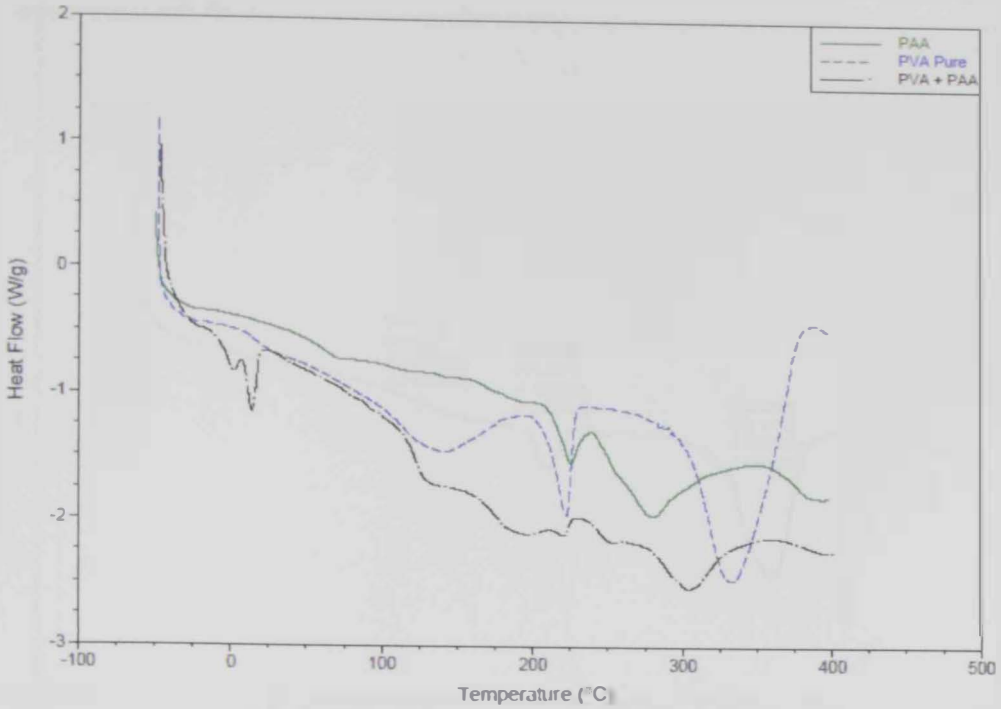

d) DSC of all neat polymers combined

Figure 3. 5 DSC thermographs of (a) neat PVA, (b) neat PAA, (c) neat PVA-PAA, (d) all neat polymer membranes combined.

Table 3. 5 Glass transition temperature (T_g), melting temperature (T_m) and decomposition temperature (T_d) of the neat PVA-PAA polymer blends at different temperature range obtained from DSC Analysis

IL Weight Percentage (wt%)	T_g °C	T_m °C	T_d °C
0.0 PVA	138.04	219.69	330.72
0.0 PAA	69.72	225.04	279.61
0.0 PVA+PAA	124.28	217.16	301.23

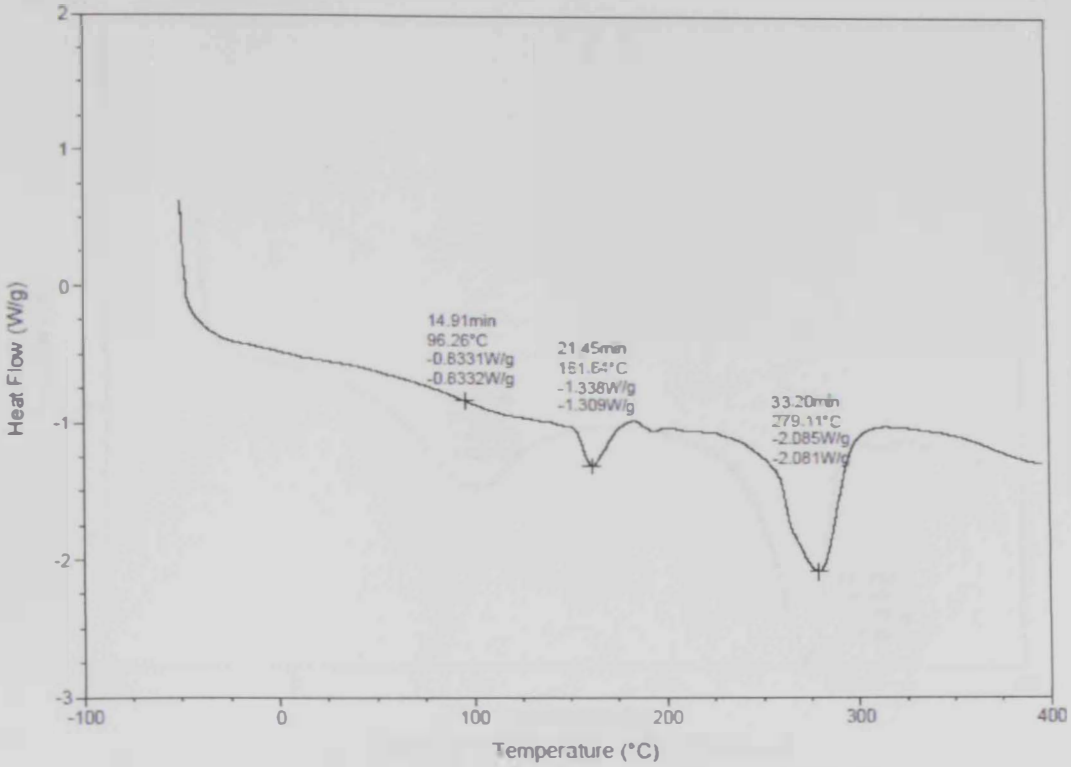

a) DSC of PVA-PAA-1% Glycerol

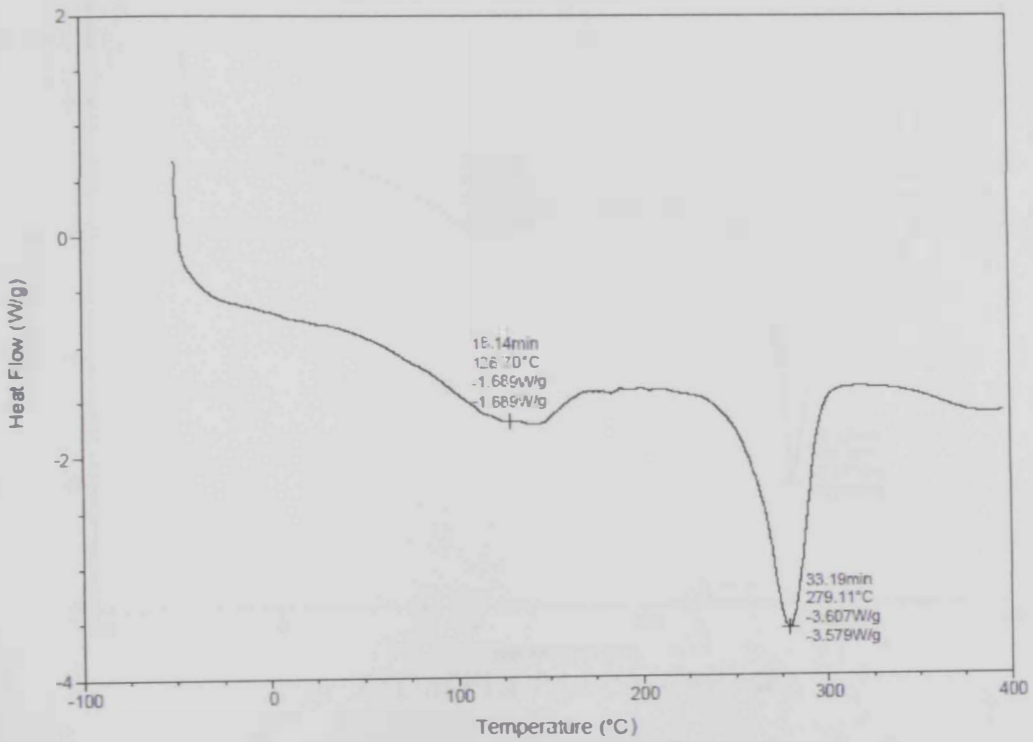

b) DSC of PVA-PAA-2% Glycerol

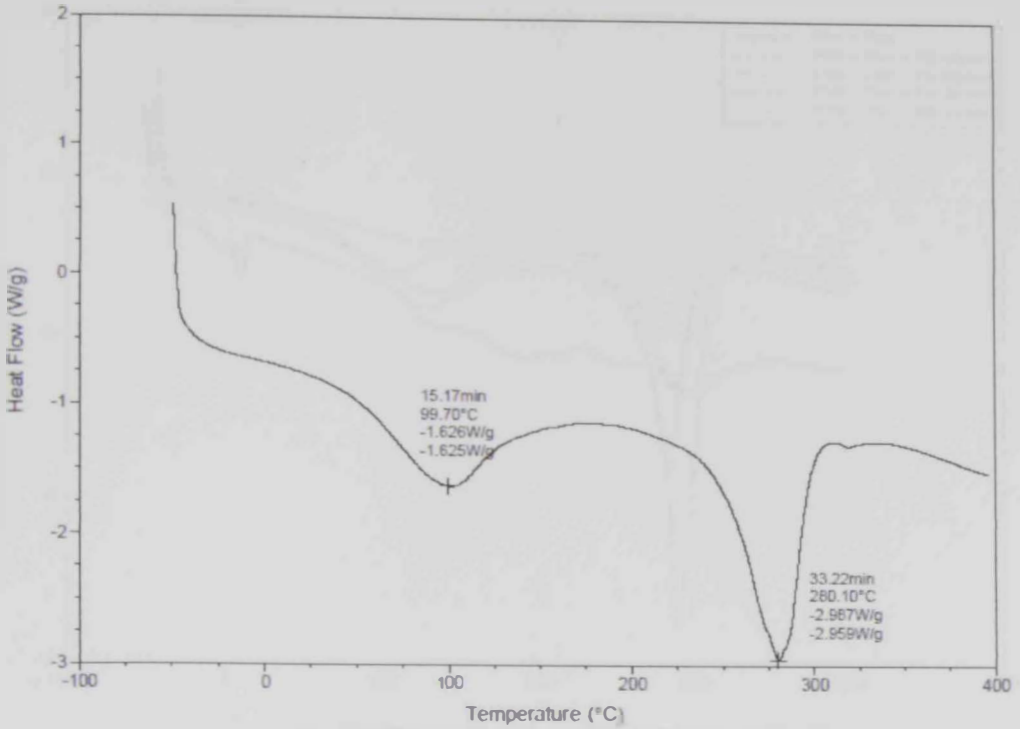

c) DSC of PVA-PAA -3% Glycerol

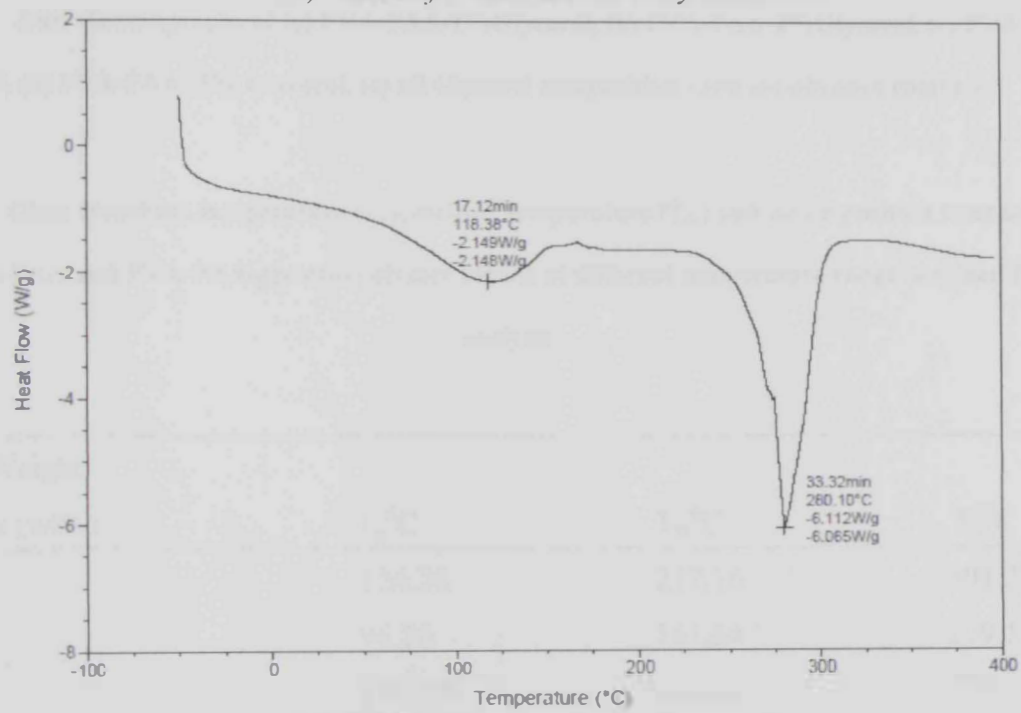

d) DSC of PVA-PAA -5% Glycerol

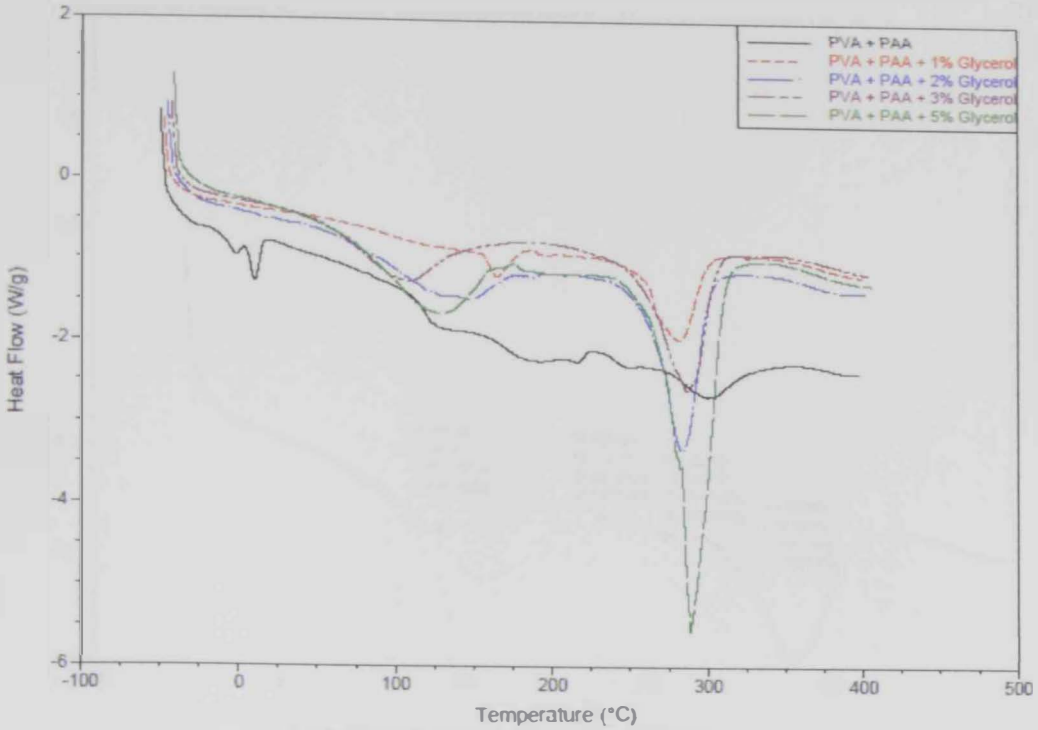

e) DSC of PVA-PAA - all Glycerol combined

Figure 3. 6 DSC thermographs of (a) PVA-PAA-1%Glycerol, (b) PVA-PAA-2%Glycerol, (c) PVA-PAA-3%Glycerol, (d) PVA-PAA- 5% Glycerol, (e) all Glycerol composition ratio membranes combined

Table 3. 6 Glass transition temperature (T_g), melting temperature (T_m) and decomposition temperature (T_d) of the PVA-PAA and PVA-PAA-glycerol polymer blends at different temperature range obtained from DSC analysis

Glycerol Weight Percentage (wt%)	T_g °C	T_m °C	T_d °C
0.0	124.28	217.16	301.23
1.0	96.26	161.64	279.11
2.0	126.70	---------	279.11
3.0	99.70	---------	280.10
5.0	116.36	---------	280.10

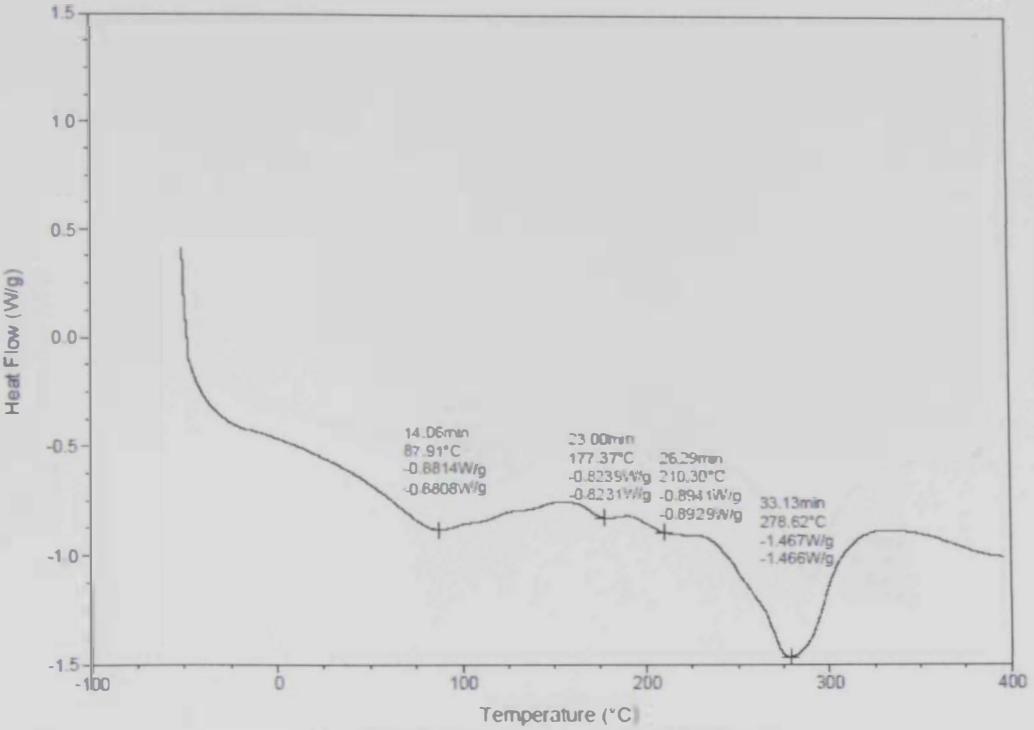

a) DSC of PVA-PAA - 1% Sorbitol

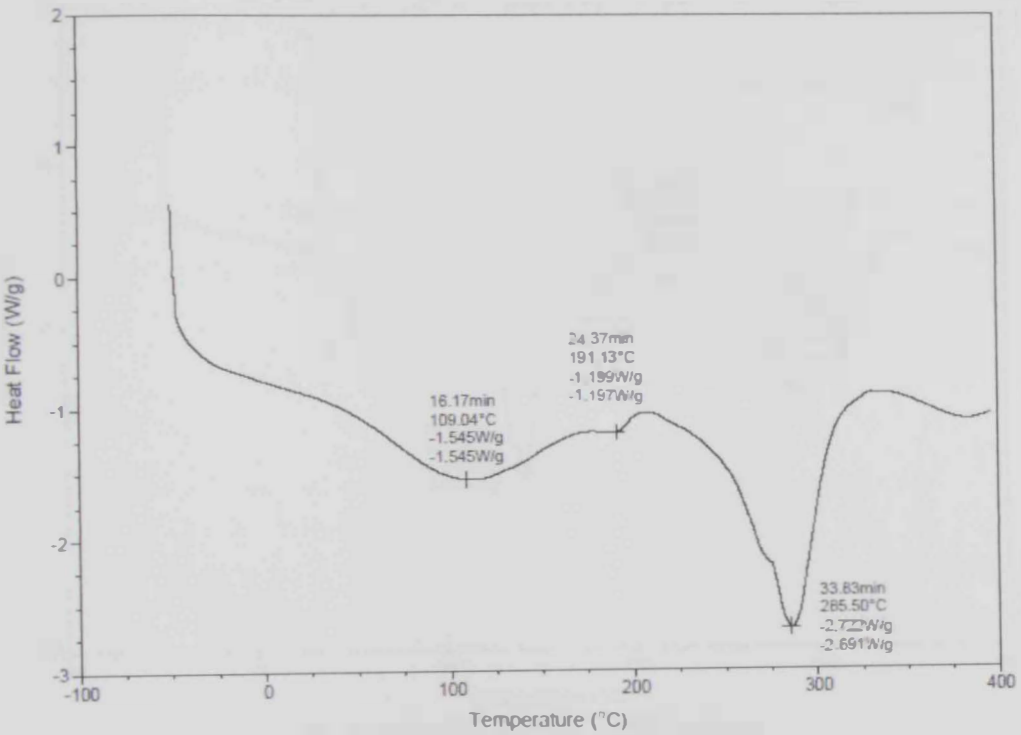

b) DSC of PVA-PAA - 2% sorbitol

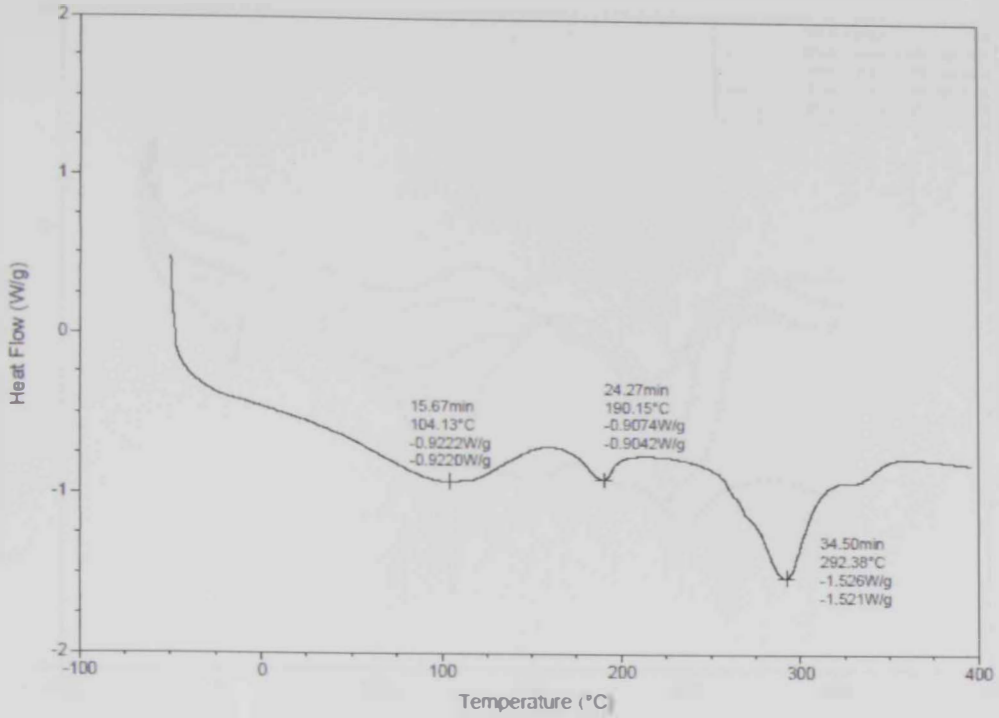

c) DSC of PVA-PAA - 3% Sorbitol

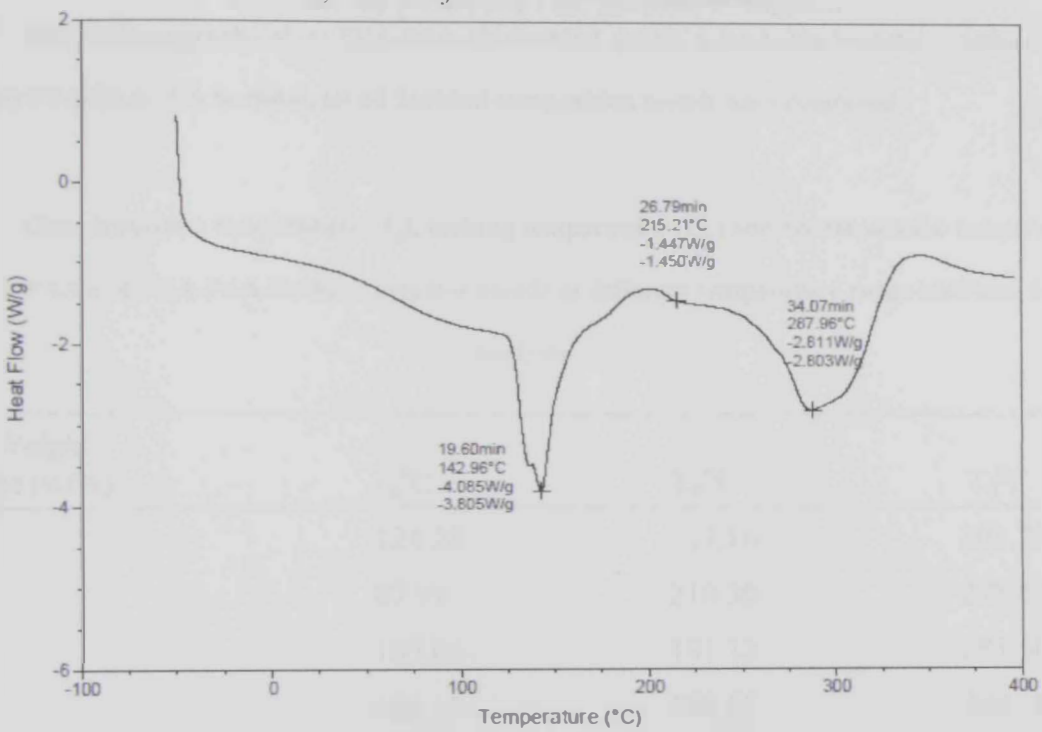

d) DSC of PVA-PAA - 5% Sorbitol

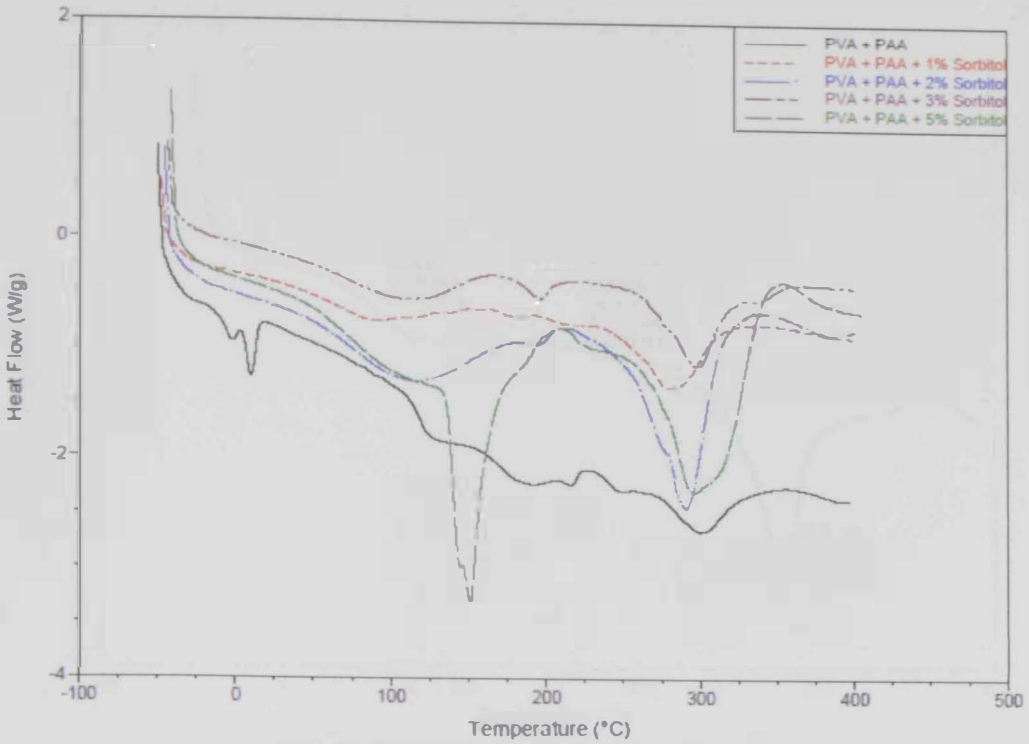

e) *DSC of PVA-PAA - all Sorbitol Combined*

Figure 3. 7 DSC thermographs of (a) PVA-PAA-1%Sorbitol, (b) PVA-PAA-2% Sorbitol, (c) PVA-PAA-3% Sorbitol, (d) PVA-PAA- 5% Sorbitol, (e) all Sorbitol composition membranes combined

Table 3. 7 Glass transition temperature (T_g), melting temperature (T_m) and decomposition temperature (T_d) of the PVA-PAA and PVA-PAA-Sorbitol polymer blends at different temperature range obtained from DSC analysis

Sorbitol Weight Percentage (wt%)	T_g °C	T_m °C	T_d °C
0.0	124.28	217.16	301.23
1.0	87.91	210.30	278.67
2.0	109.04	191.13	285.50
3.0	104.13	190.15	292.38
5.0	142.96	215.21	287.96

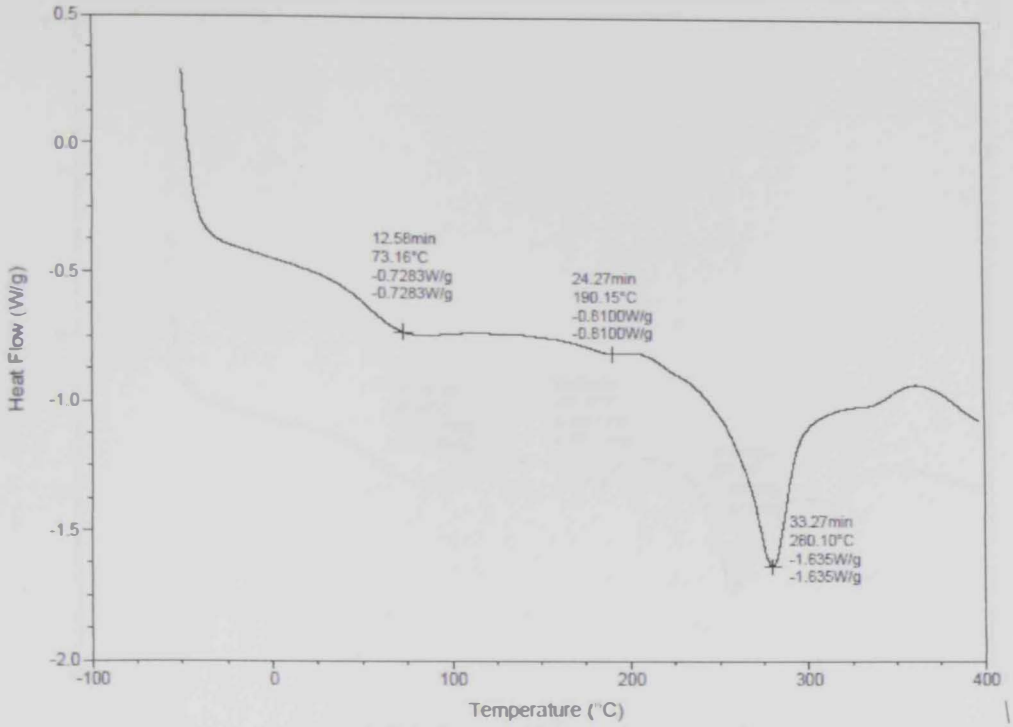

a) DSC of PVA-PAA - 1% imidazolium bromide

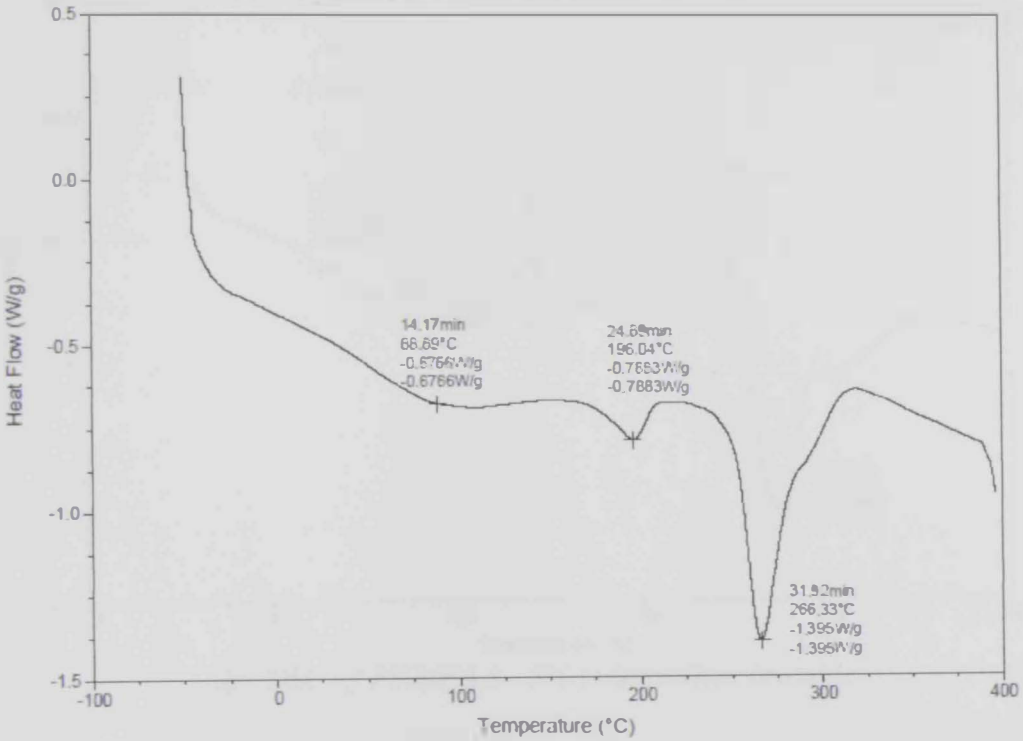

b) DSC of PVA-PAA - 2% imidazolium bromide

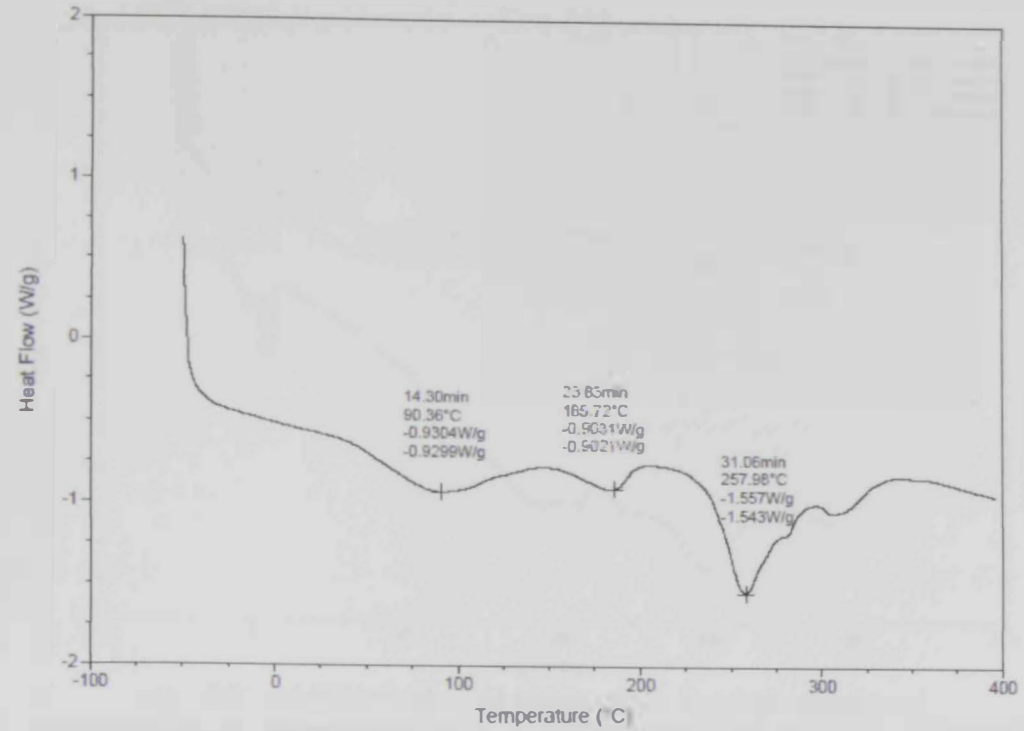

c) DSC of PVA-PAA - 3% imidazolium bromide

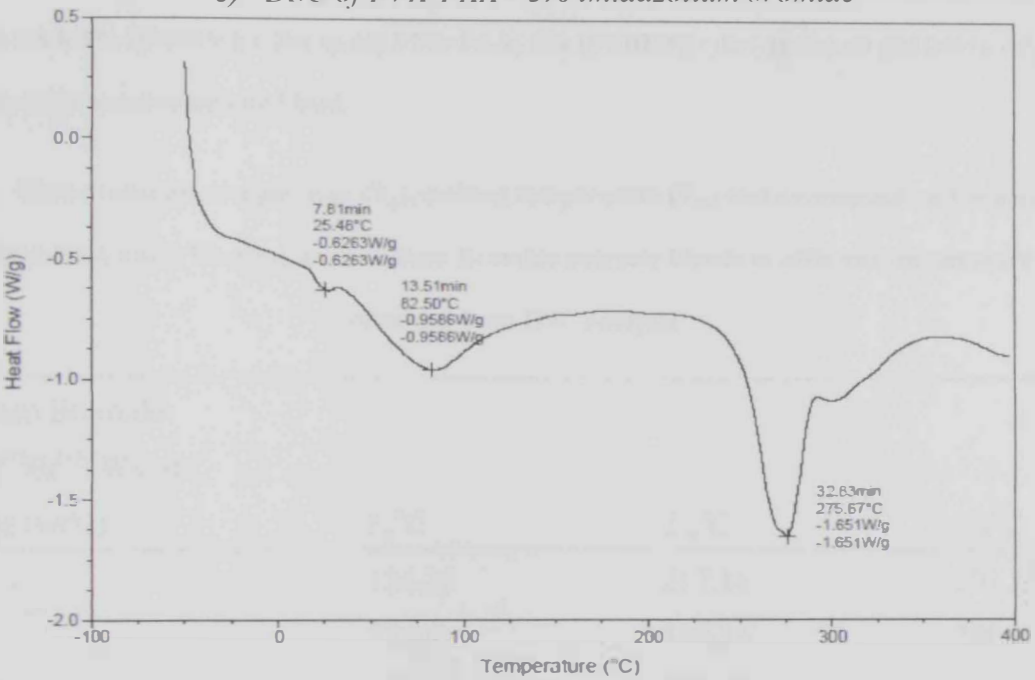

d) DSC of PVA-PAA - 5% imidazolium bromide

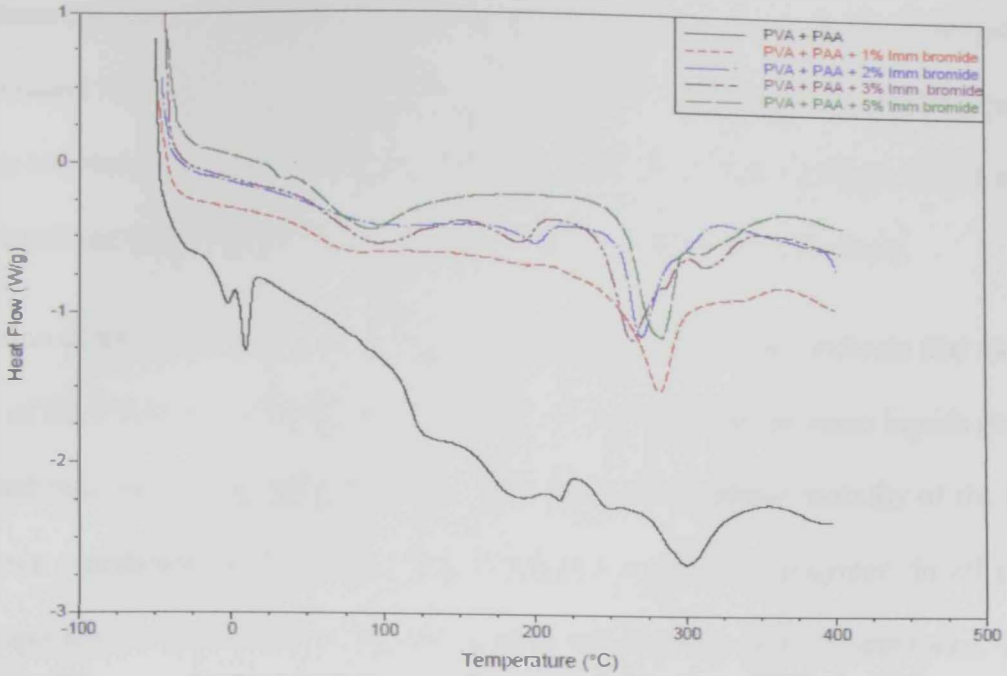

e) DSC of PVA-PAA – all imidazolium bromide combined

Figure 3. 8 DSC thermographs of (a) PVA-PAA-1% (|MDIM|(+)Br(-)), (b) PVA-PAA-2% (|MDIM|(+)Br(-)) , (c) PVA-PAA-3% (|MDIM|(+)Br(-)), (d) PVA-PAA- 5% (|MDIM|(+)Br(-)), (e) all (|MDIM|(+)Br(-)) composition ratio membranes combined.

Table 3. 8 Glass transition temperature (T_g), melting temperature (T_m) and decomposition temperature (T_d) of the PVA-PAA and PVA-PAA-Imidazolium Bromide polymer blends at different temperature range obtained from DSC analysis

Imidazolium Bromide ($[MDIM]^{(+)}Br^{(-)}$) Weight Percentage (wt%)	T_g °C	T_m °C	T_d °C
0.0	124.28	217.16	301.23
1.0	73.16	190.15	280.10
2.0	88.89	196.04	266.33
3.0	90.36	185.72	257.98
5.0	82.50	---------	275.67

When the ionic liquids are incorporated into the PVA-PAA films, it can be seen that the thermal degradation onset is shifted to a higher temperature, while the melting peak is shifted to a lower temperature, and that these effects increase with increasing ionic liquid content. These behaviors are better visualized in the peak temperature data shown in Tables 3.5-3.8 above.

The depression of the melting temperature (T_m) and the peak broadening indicate that the ordered association of the PVA molecules was decreased by the presence of the ionic liquids [69]. It can be interpreted that the ionic liquids introduced increases the segmental mobility of the PVA and PAA polymer membranes and decreases the crystallite region of a polymer. In all cases, the water is evaporated by dehydration; the plasticizers will become more concentrated. Thus, the formation of the biopolymeric matrix will take place via electrostatic, hydrophobic, and Van der Walls interactions, as well as hydrogen bonds among adjacent polymer chains and between the ionic liquids [62]. FTIR spectroscopy results confirmed the formation of hydrogen bonding between the ionic liquids and the polymer membranes (PVA-PAA) blends as explained in more details in section FTIR Characterization.

3.2. Mechanical Properties

The mechanical properties of neat PVA, neat PAA, neat PVA-PAA, and all PVA-PAA blended with ionic liquids were performed by nanoindentation. The purpose for these tests was to determine the hardness and elastic modulus of the polymer blend membranes. It is extremely important to know the ductility and hardness of these polymer blends. The nanoindentation of loading-unloading curves for neat polymers PVA, neat PAA and the blend of neat PVA-PAA and PVA-PAA with ionic liquids with various percentage ratios of 1%, 2%, 3% and 5%

respectively. Neat PVA, neat PAA and neat PVA-PAA are shown in Figures 3.9(*a-d*), PVA-PAA-Glycerol are shown in Figures 3.10(*a-d*), PVA-PAA-Sorbitol in Figures 3.11(a-d), PVA-PAA-Imidazolium Bromide $[MDIM]^{(+)}Br^{(-)}$ in Figures 3.12(*a-d*); Figures 3.10-3.12 have various polymer blended ionic liquids.

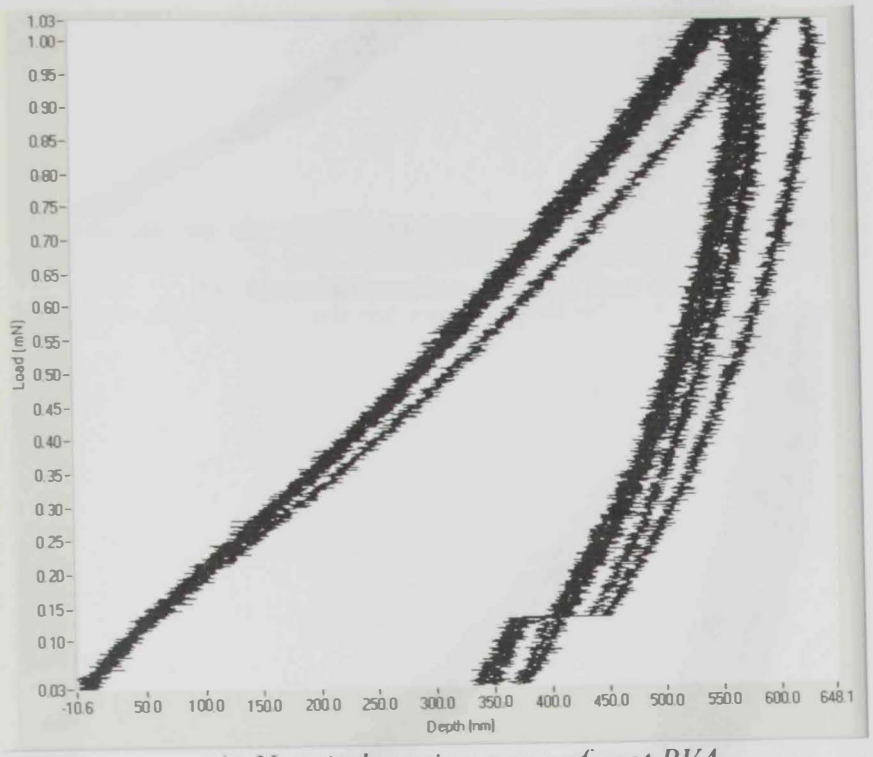

a) Nanoindentation curve of neat PVA

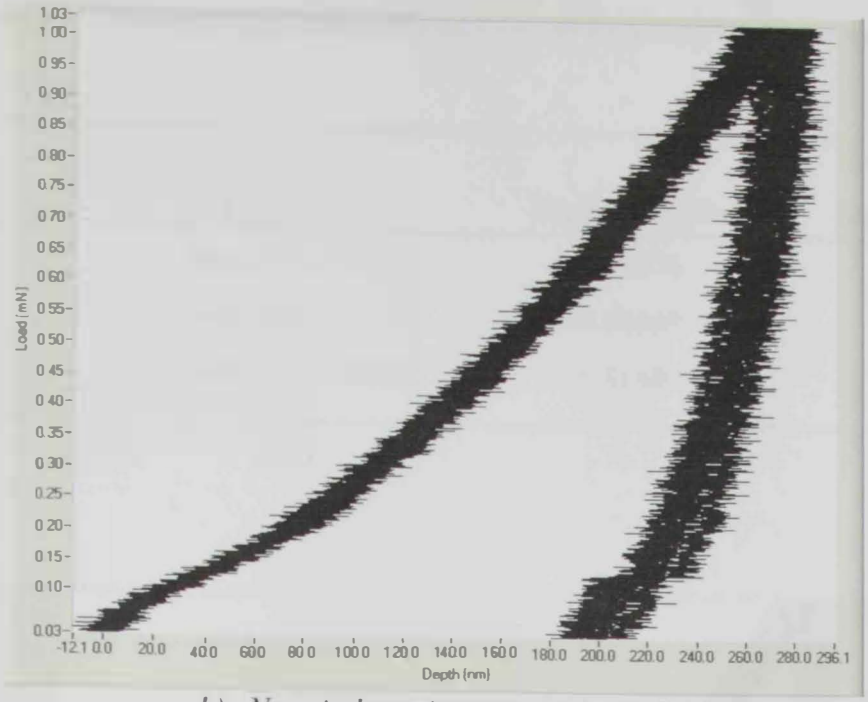

b) Nanoindentation curve of neat PAA

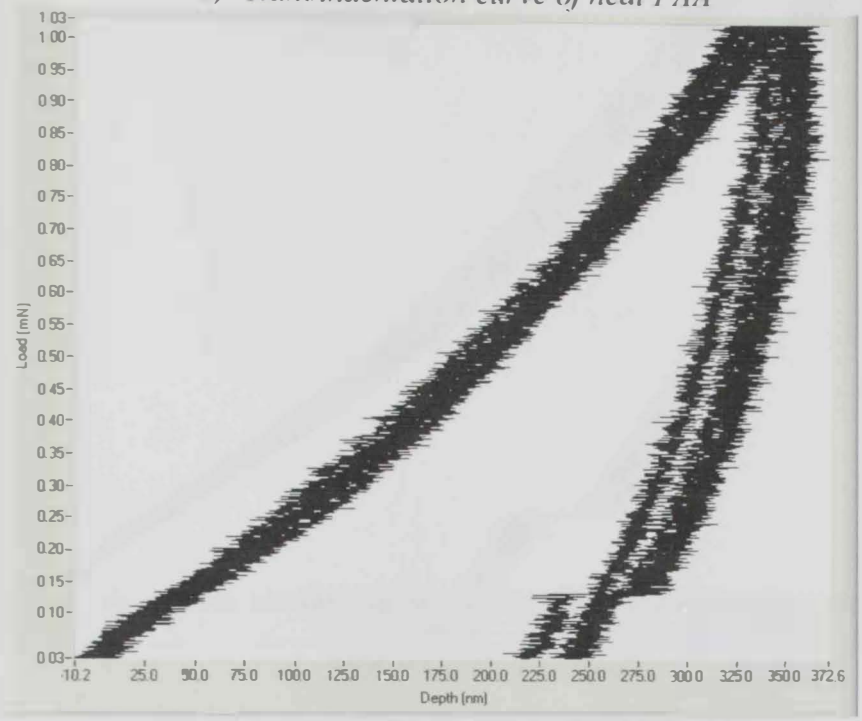

c) Nanoindentation curve of neat PVA–PAA

Figure 3. 9 Nanoindentation (loading-unloading curves) of the neat PVA and neat PAA polymer. (a) Nanoindentation curve of neat PVA. (b) Nanoindentation curve of neat PAA. (c) The combination of 1:1 ratio of neat PVA and PAA blends

Table 3. 9 Nanoindentation results of neat PVA and PAA and PVA-PAA blends

Data	Weight%	Hardness (GPa)	Reduced (elastic) Modulus (GPa)
a	Neat PVA	0.16674	2.80228
b	Neat PAA	0.66869	15.90223
c	Neat PVA - PAA	0.41489	9.2022

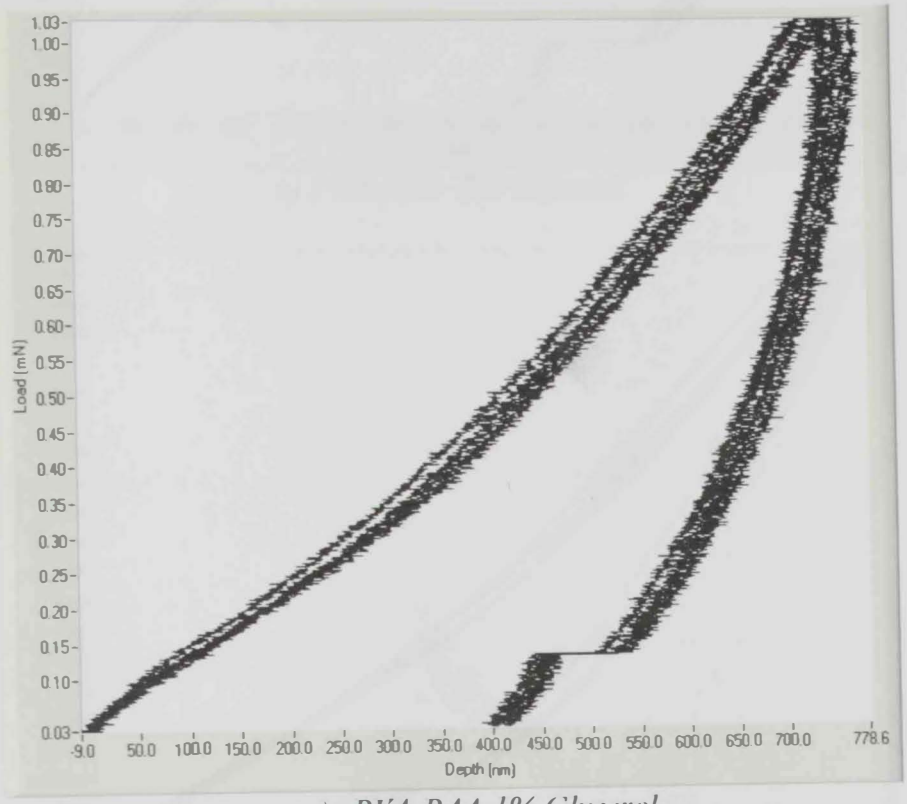

a) PVA-PAA-1% Glycerol

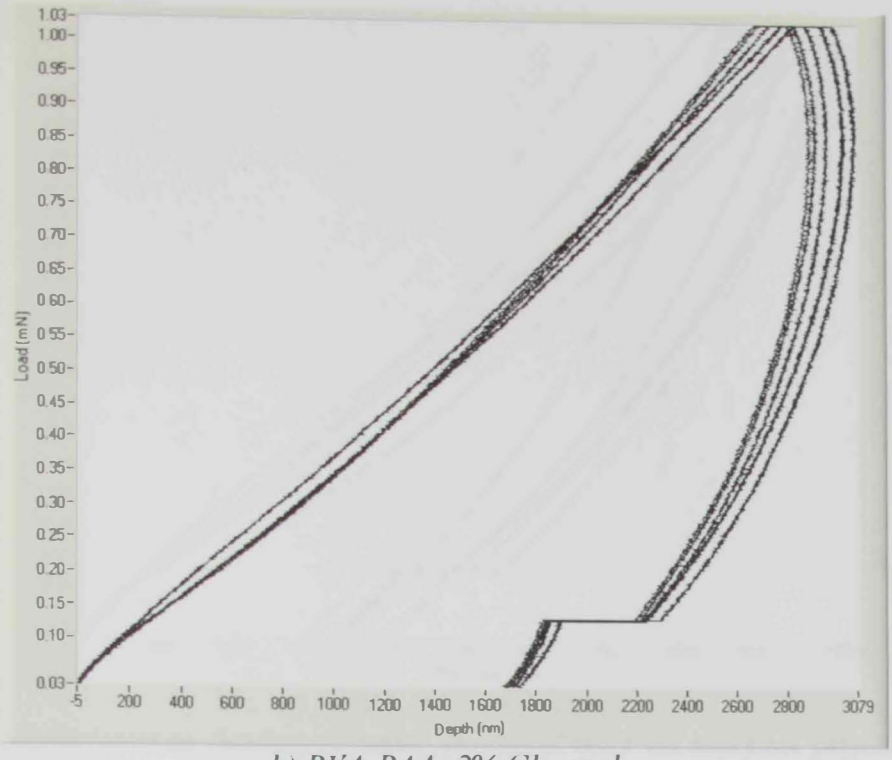

b) PVA-PAA- 2% Glycerol

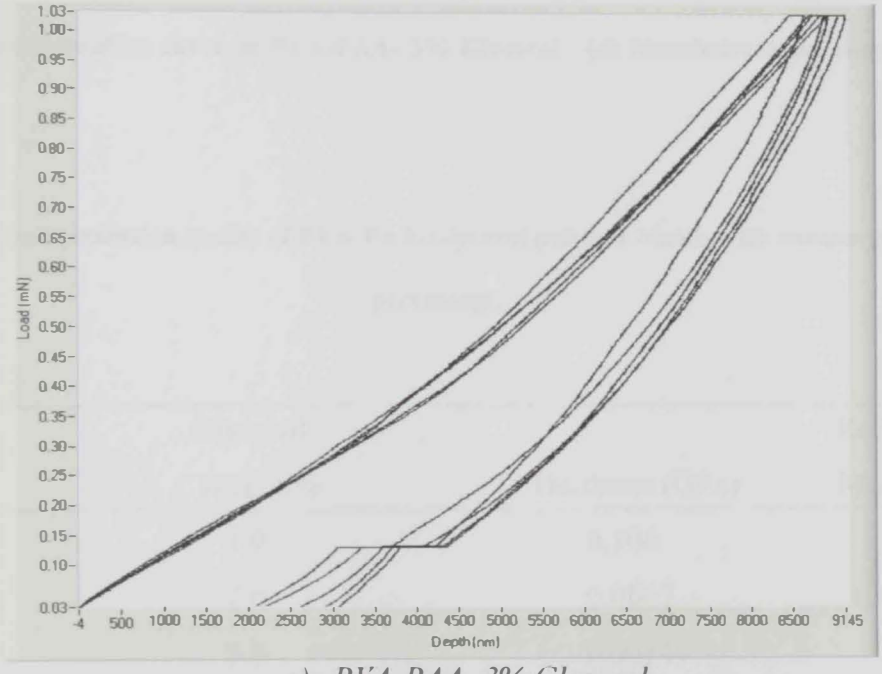

c) PVA-PAA- 3% Glycerol

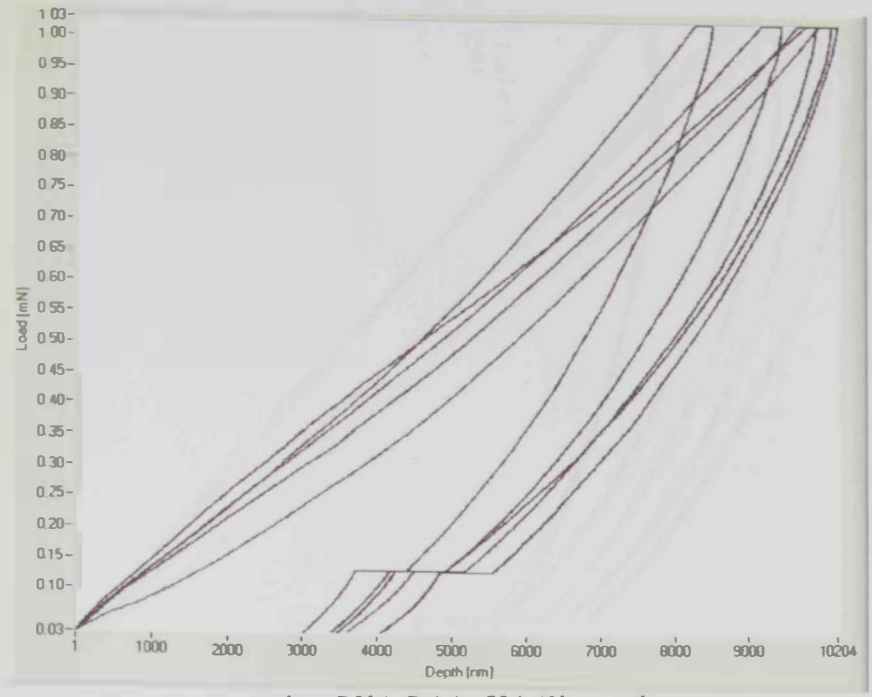

d) PVA-PAA- 5% Glycerol

Figure 3. 10 Nanoindentation (loading-unloading curves) of the PVA and PAA polymer blended with glycerol. (a) Nanoindentation curve of PVA-PAA- 1% Glycerol. (b) Nanoindentation curve of PVA-PAA- 2% Glycerol. (c) Nanoindentation curve of PVA-PAA- 3% Glycerol . (d) Nanoindentation curve of PVA-PAA- 5% Glycerol.

Table 3. 10 Nanoindentation results of PVA-PAA-Glycerol polymer blends with various glycerol weight percentage.

Data	Glycerol Weight%	Hardness (GPa)	Reduced (elastic) Modulus (GPa)
a	1.0	0.104	1.6865
b	2.0	0.0067	0.121
c	3.0	0.00149	0.00767
d	5.0	0.00117	0.00643

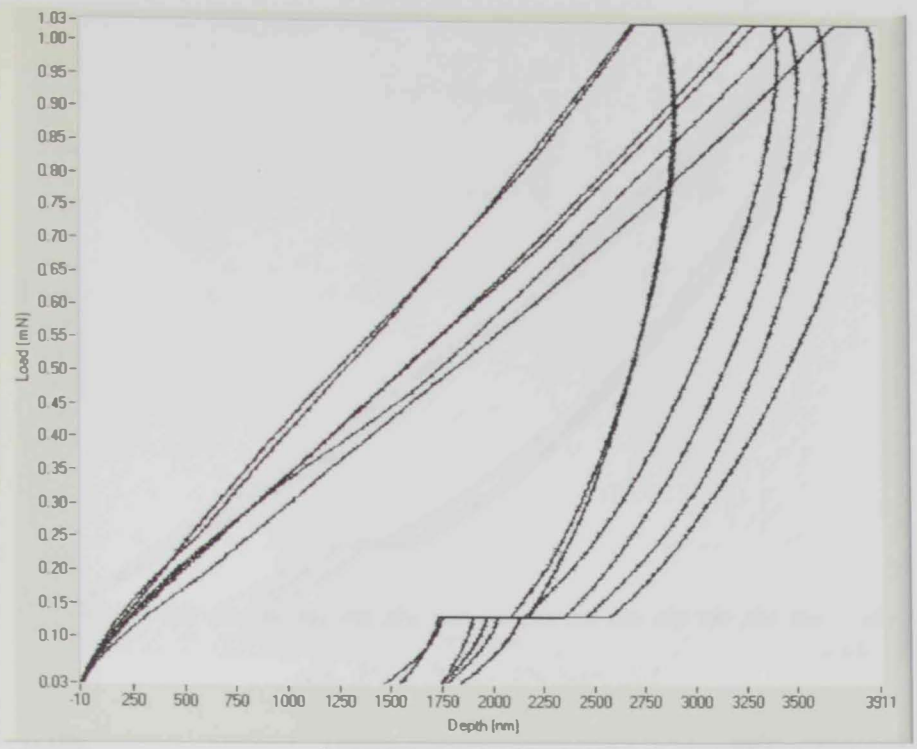

a) *PVA-PAA- 1% Sorbitol*

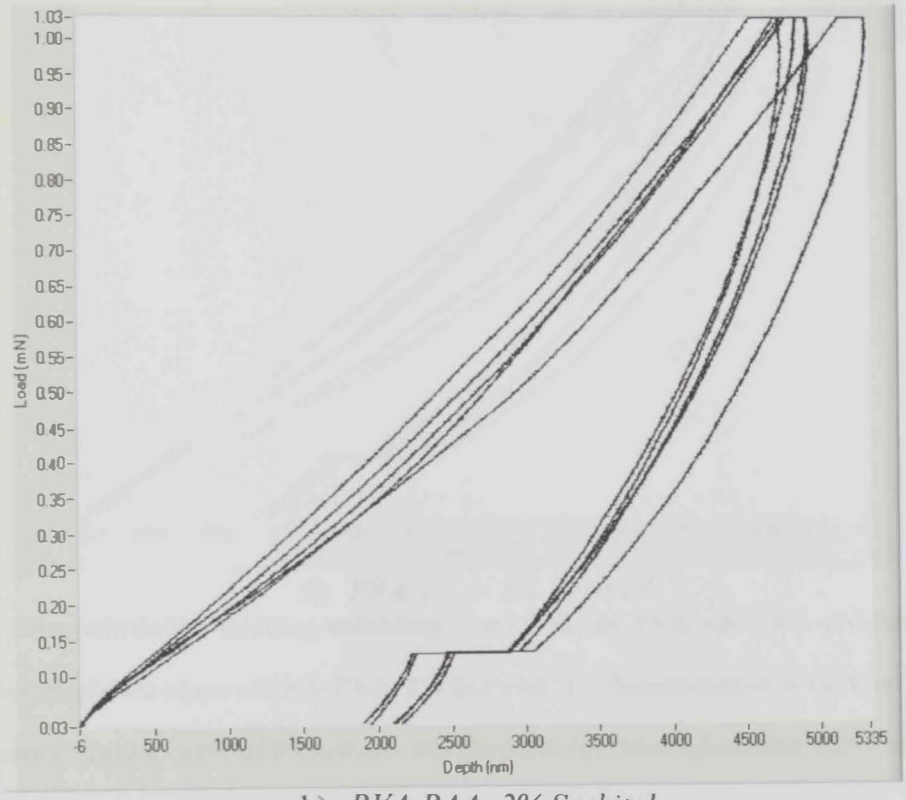

b) *PVA-PAA- 2% Sorbitol*

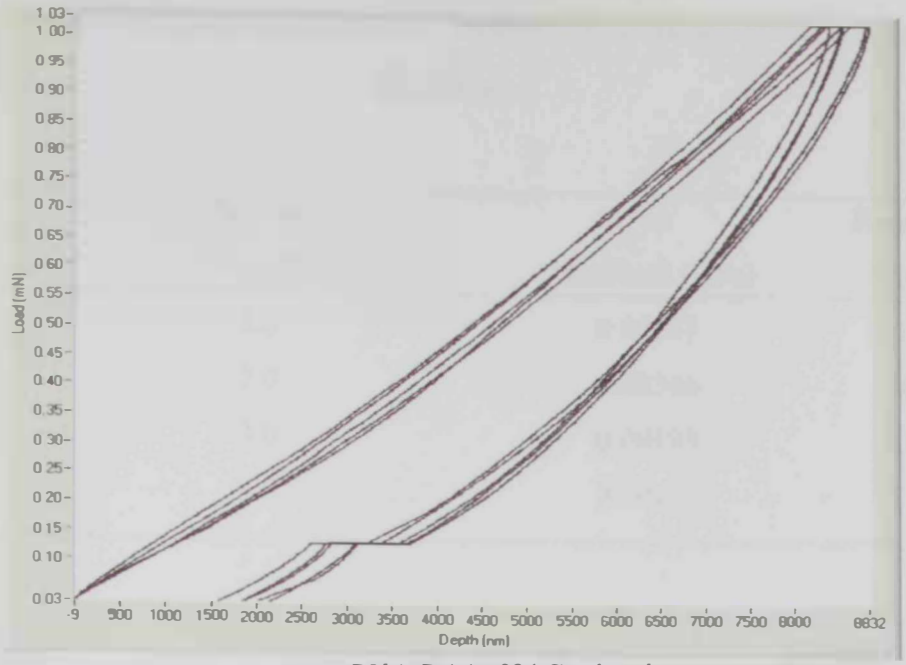

c) *PVA-PAA- 3% Sorbitol*

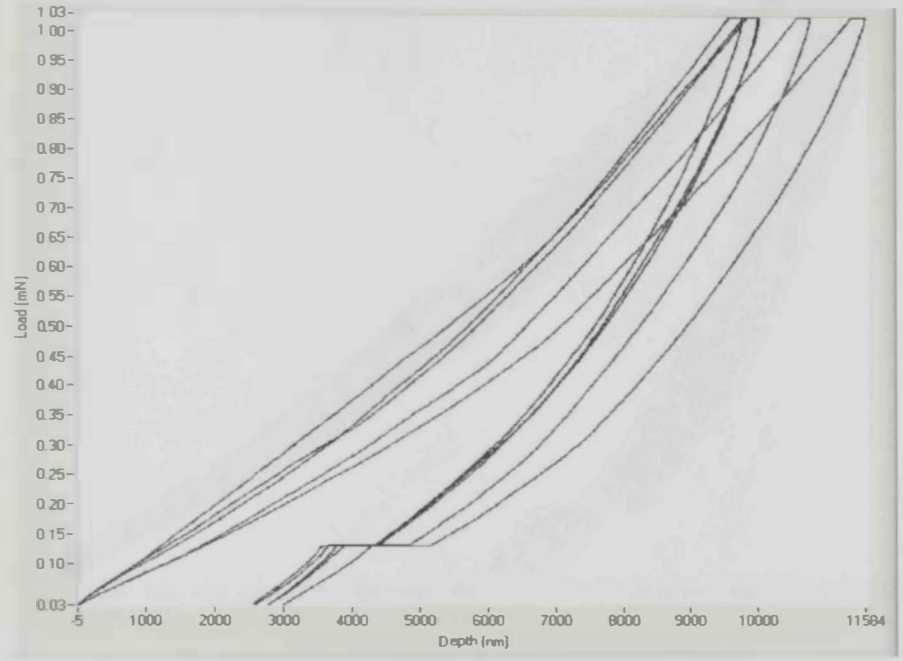

d) *PVA-PAA- 5% Sorbitol*

Figure 3. 11 Nanoindentation (loading-unloading curves) of the PVA and PAA polymer blended with Sorbitol. (a) Nanoindentation curve of PVA-PAA- 1% Sorbitol. (b) Nanoindentation curve of PVA-PAA- 2% Sorbitol. (c) Nanoindentation curve of PVA-PAA- 3% Sorbitol, (d) Nanoindentation curve of PVA-PAA-5% Sorbitol

Table 3. 11 Nanoindentation results of PVA-PAA- Sorbitol polymer blends with various sorbitol weight percentages.

Data	Sorbitol Weight%	Hardness (GPa)	Reduced (elastic) Modulus (GPa)
a	1.0	0.00587	0.08091
b	2.0	0.00346	0.02697
c	3.0	0.00193	0.00755
d	5.0	0.00122	0.00525

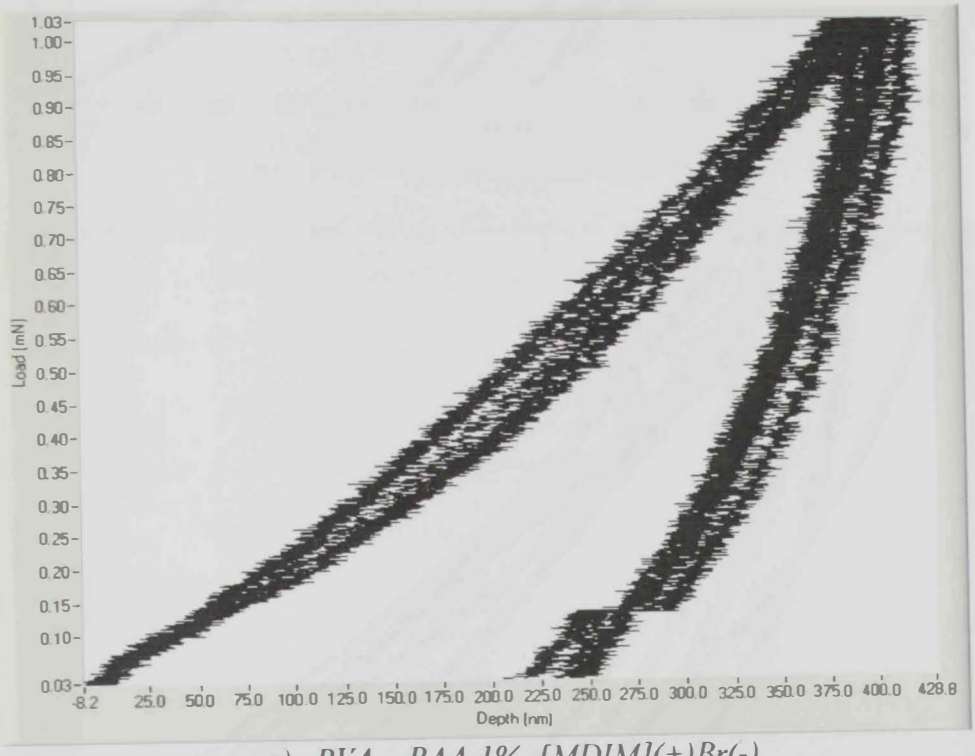

a) PVA – PAA-1% [MDIM](+)Br(-)

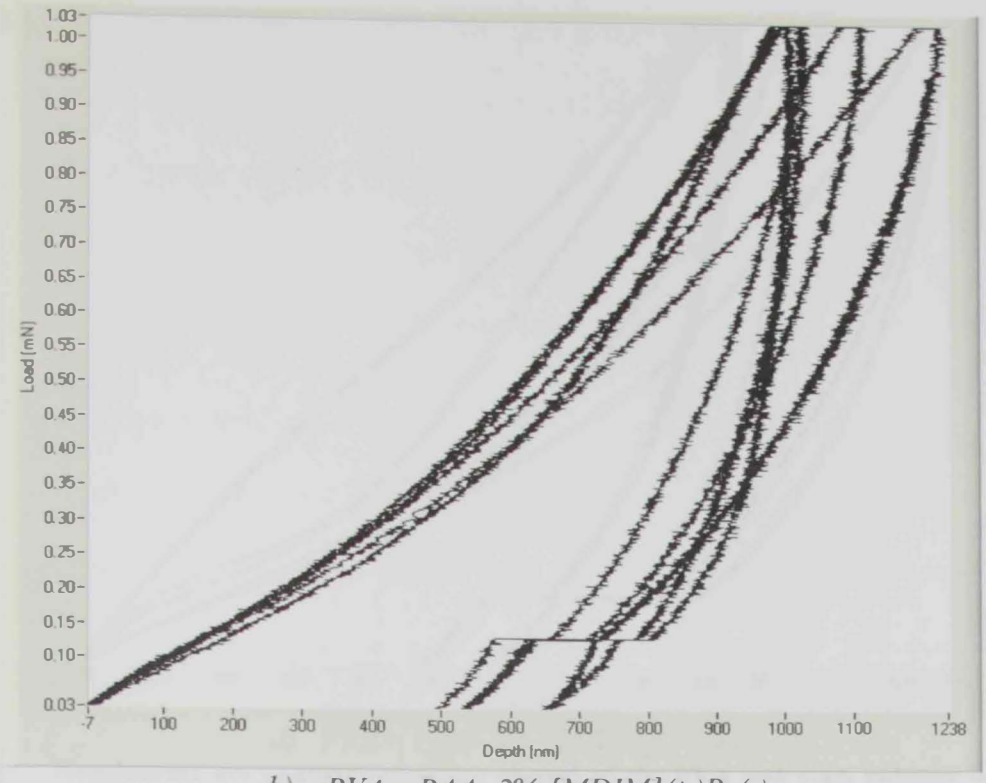

b) PVA – PAA- 2% [MDIM](+)Br(-)

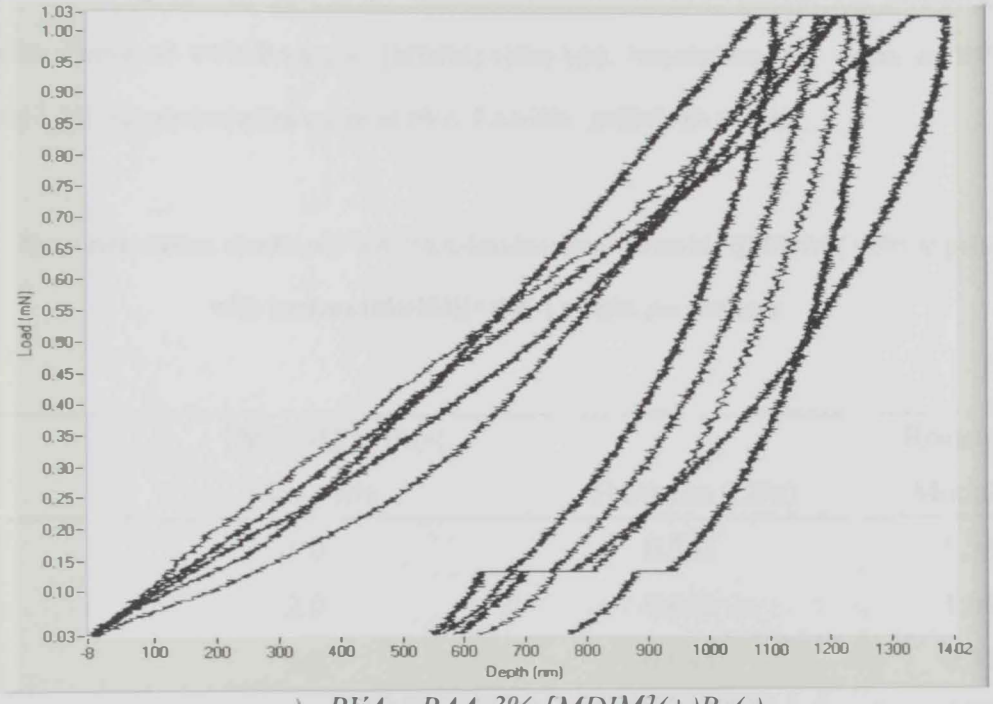

c) PVA – PAA-3% [MDIM](+)Br(-)

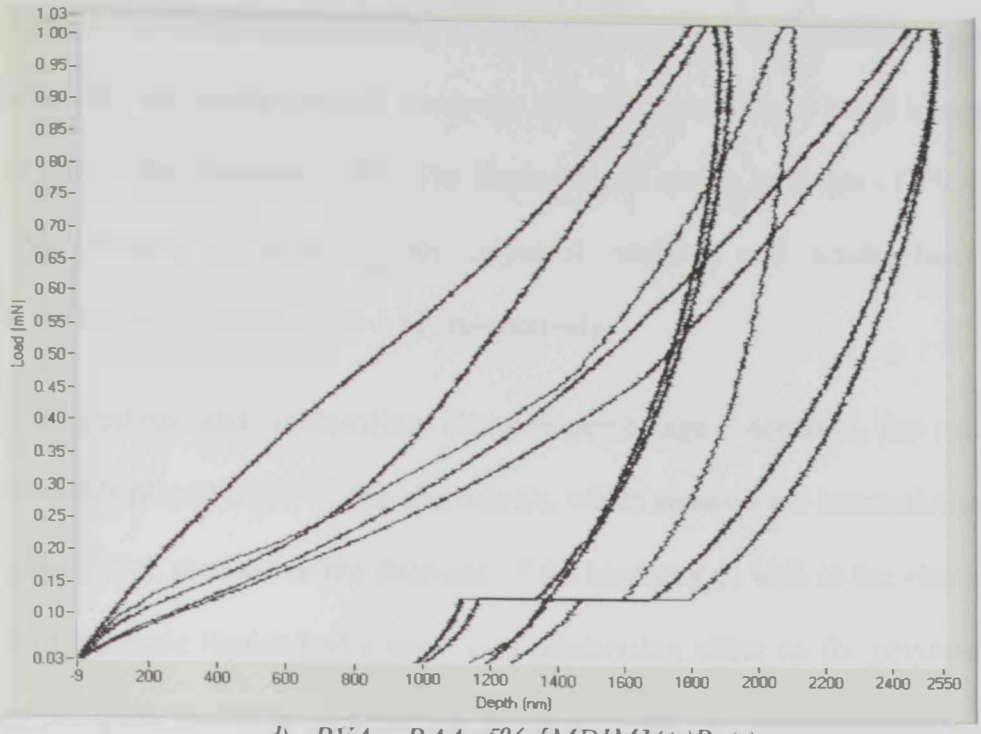

d) PVA - PAA- 5% [MDIM](+)Br(-)

Figure 3. 12 **Nanoindentation (loading-unloading curves) of the PVA and PAA polymer blended with Imidazolium Bromide - (|MDIM|(+)Br(-)). (a) Nanoindentation curve of PVA-PAA-1% |MDIM|(+)Br(-). (b) Nanoindentation curve of PVA-PAA-2% |MDIM|(+)Br(-).(c) Nanoindentation curve of PVA-PAA-3% |MDIM|(+)Br(-). (d) Nanoindentation curve of PVA-PAA-5% |MDIM|(+)Br(-)).**

Table 3. 12 **Nanoindentation results of PVA-PAA-Imidazolium Bromide (|MDIM|(+)Br(-)) polymer blends with various |MDIM|(+)Br(-) weight percentages**

Data	[MDIM](+)Br(-) Weight%	Hardness (GPa)	Reduced (elastic) Modulus(GPa)
a	1.0	0.363	5.543
b	2.0	0.052	1.013
c	3.0	0.044	0.575
d	5.0	0.013	0.225

It has been known that the plasticizers play an important role on the mechanical properties of polymers. Generally, the tensile strength decreases and the elongation at break increased as the percentage of plasticizers increased [70]. The hardness and elastic modulus of PVA and PAA blends as the function of ionic liquids (glycerol, sorbitol and imidazolium bromide) concentration are shown in Tables 3.10-3.12, respectively.

As the glycerol, sorbitol and imidazolium bromide percentages increased, the residual ionic liquids in the blends played a role as the plasticizers, which reduced the interactions among the macromolecules, which resulted in the decrease of the hardness as well as the elastic modulus. The presence of the ionic liquids had a significant plasticizing effect on the polymer blends by reducing both the glass transition and melting temperature of the polymer membranes and the storage modulus drop.

This plasticizing effect could be attributed to their low molecular-weight and hydroxyl groups leading to the formation of polymer-plasticizer interactions to the detriment of polymer-polymer interactions. Smaller molecules of the ionic liquids embed themselves between the polymer blend chains, increasing the spacing and free volume, and allowing them to move past one another even as lower temperatures.

It is essential to determine the mechanical properties of the polymer blends to determine the structural texture of the polymer. Due to there being conductive polymers commercially available, but they are very rigid and are extremely difficult to synthesize; whereas these blended polymers carried out in this work are much softer and easier to produce.

3.3. Fourier Transform Infrared Spectroscopy Characterization

Fourier transform infrared spectroscopy (FTIR) was used to characterize the presence of specific chemical groups in the materials. Moreover, it was used to analyze the interactions among the atoms or ions in the polymer films. Neat polymer membranes and polymer blends with various composition ratios of ionic liquids were obtained as 1-2 mm thick films and analyzed by FTIR Transmittance mode. Polymer complex formation has been confirmed from the below analysis. The dried films of neat polymer and blends were peeled off and cut into strips and sandwiched between the potassium bromide (KBr) powder before placing in the spectrophotometer. On blending the ionic liquid salts as dopant with the polymer solution, the cations of the plasticizers are expected to coordinate with the polar hydroxyl groups of the host polymers (PVA-PAA) resulted in the formation of a more ordered and coordinating complex blend. This type of interactions between the polymer blend and the dopant will influence the local structure of the polymer main chain and a specific infrared active vibration mode will be altered by either shifting the frequency or to some extent reducing the band intensity and broadness. The infrared spectroscopic studies will give evidence on the chain order and coordination which occurs between the polymer blends and the plasticizers.

It should be noted that the FTIR spectroscopy is used as a qualitative analysis to study the dispersion and coordination of the dopant within the polymer depending on the blending ratios. To explain the extent of dopant incorporation in the polymer matrix and its effect on electrical properties of the polymer blends, the microstructure and the presence of important functional groups in all samples were analyzed. The FTIR spectrum of neat PVA, neat PAA and neat PVA-

PAA are shown in Figure 3.13, PVA-PAA-Glycerol are shown in Figure 3.14, PVA-PAA-Sorbitol in Figure 3.15, PVA-PAA-Imidazolium Bromide $[MDIM]^{(+)}Br^{(-)}$ in Figure 3.16; Figures 3.14-3.16 have various polymer blended ionic liquids in them.

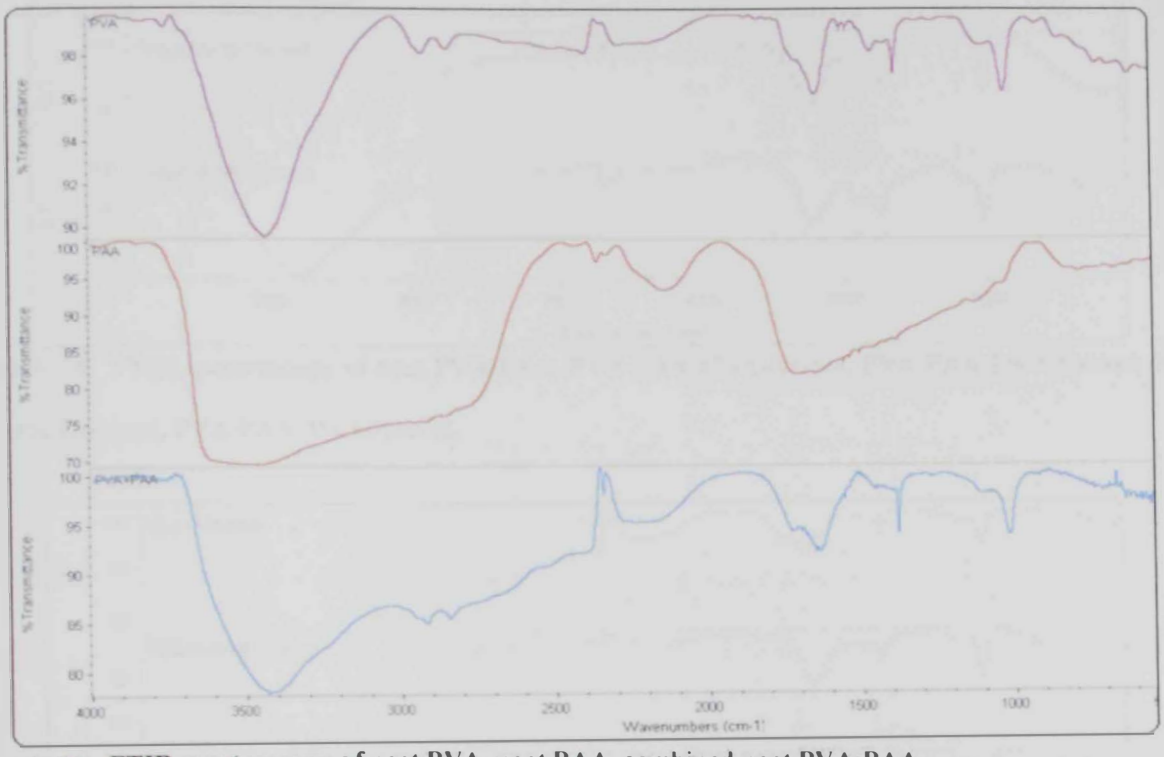

Figure 3. 13 FTIR spectroscopy of neat PVA, neat PAA, combined neat PVA-PAA

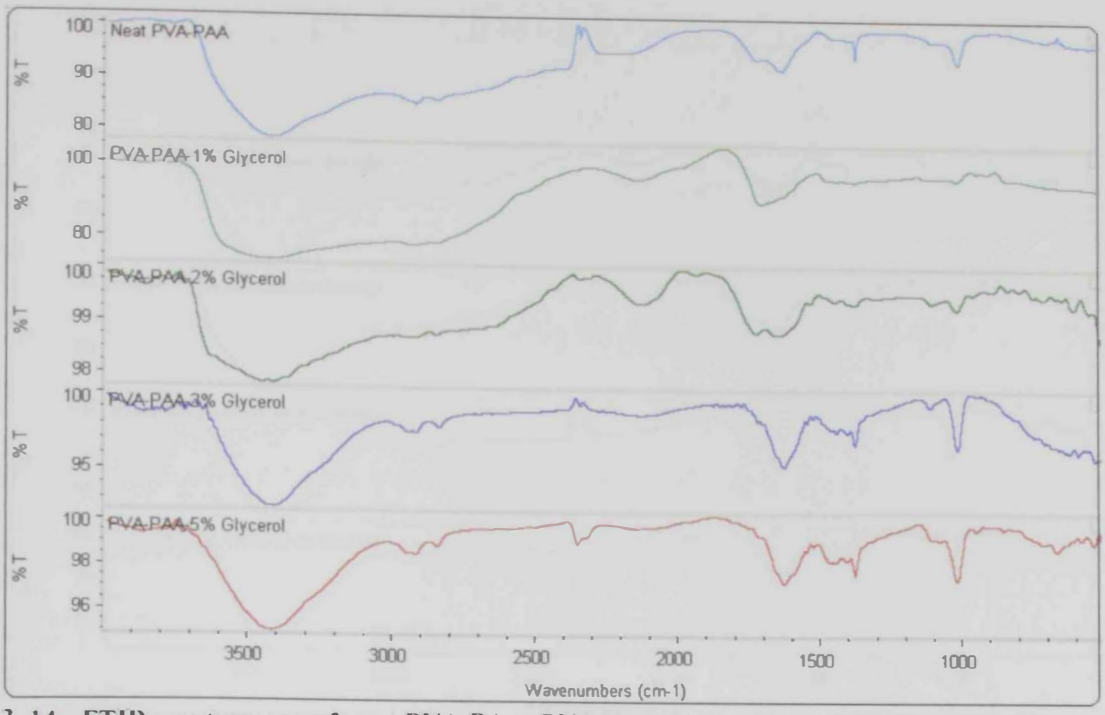

Figure 3. 14 FTIR spectroscopy of neat PVA-PAA, PVA-PAA-1% Glycerol, PVA-PAA-2% Glycerol, PVA-PAA-3% Glycerol, PVA-PAA-5% Glycerol.

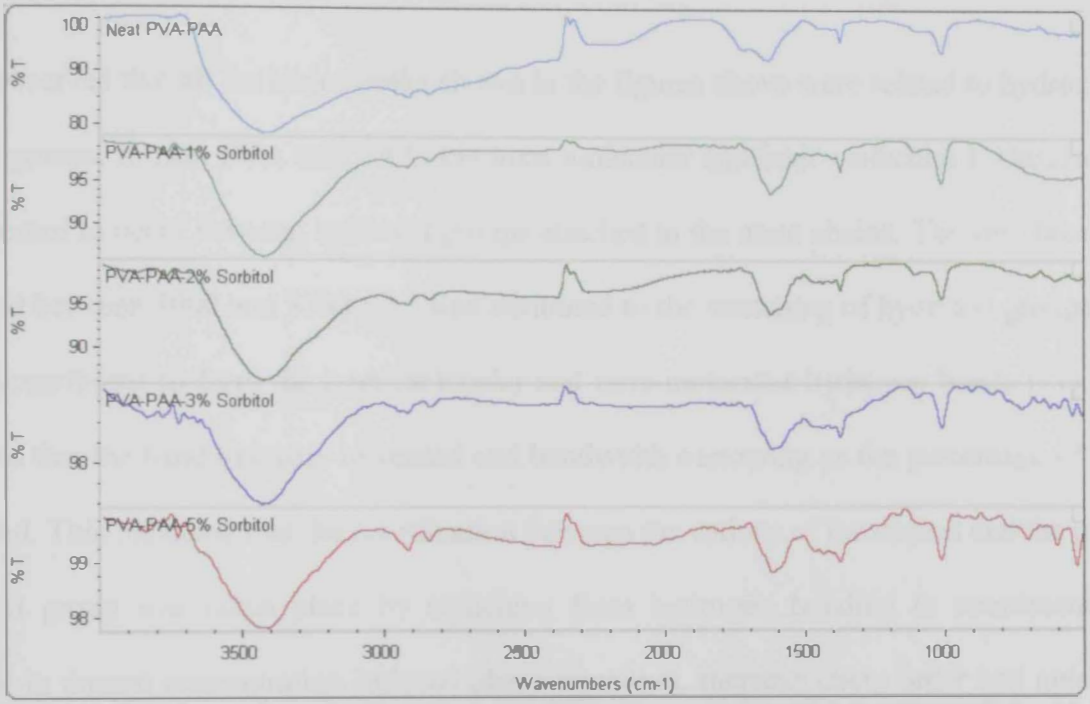

Figure 3. 15 FTIR spectroscopy of neat PVA-PAA, PVA-PAA-1% Sorbitol, PVA-PAA-2% Sorbitol, PVA-PAA-3% Sorbitol, PVA-PAA-5% Sorbitol.

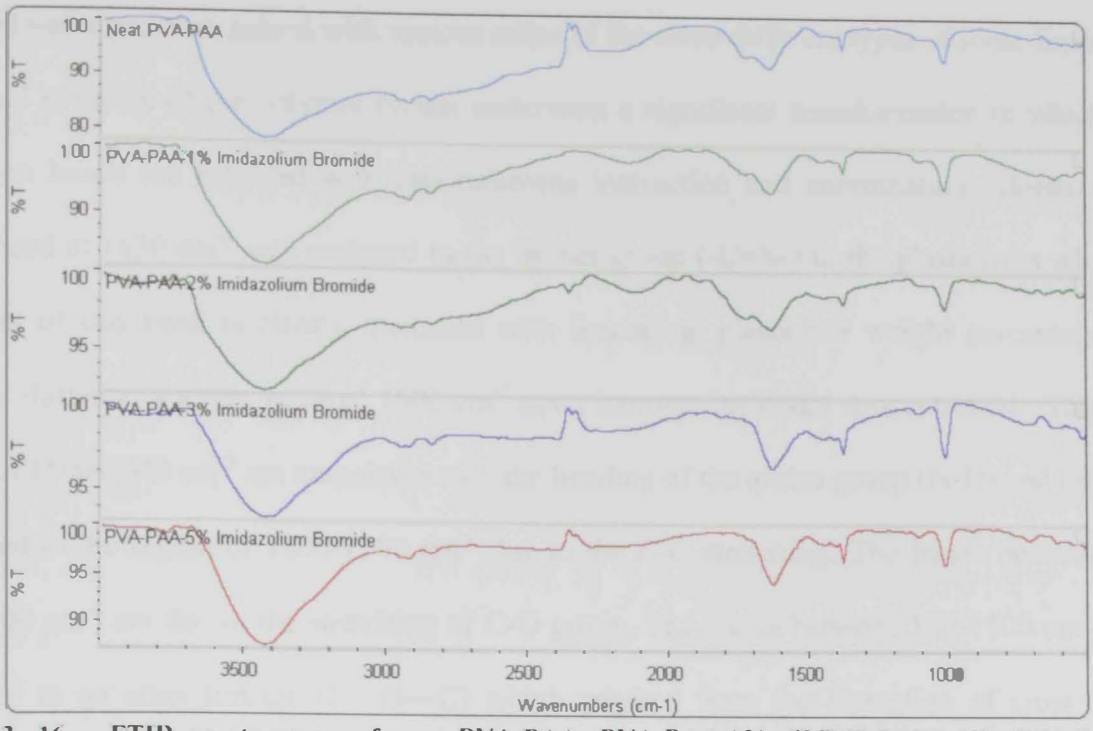

Figure 3. 16 FTIR spectroscopy of neat PVA-PAA, PVA-PAA-1% ([MDIM](+)Br(-)), PVA-PAA-2% ([MDIM](+)Br(-)), PVA-PAA-3% ([MDIM](+)Br(-)), PVA-PAA- 5% ([MDIM](+)Br(-)).

It was observed that all the major peaks shown in the figures above were related to hydroxyl, and methyl groups. In neat PVA and PAA, the intra-molecular and inter-molecular hydrogen bonds are expected to occur between hydroxyl groups attached to the main chains. The very broad band observed between 3000 and 3700 cm^{-1} was attributed to the stretching of hydroxyl groups (O-H) which contributed to form the inter-molecular and intra-molecular hydrogen bonds [71]. It was observed that the band intensity increased and bandwidth narrowing as the percentage of dopant increased. This indicated that the coordination between the cations of the dopant and the polymer hydroxyl group was taken place by switching from hydrogen bonding to coordination. An increase in dopant concentration induced phase transition, increase chain order and anisotropic environment in the blend structure. When the polymer blend (PVA-PAA) were dissolved in

distilled water and then mixed with various ratios of the three different types of ionic liquids, the chemical structure of the polymer blends underwent a significant transformation in which most hydrogen bonds are replaced with cations/anions interaction and coordination. Moreover, the small band at 1630 cm^{-1} was assigned to the imines group (-C=N-) in the plasticizers where the intensity of this band is clearly increased with increasing plasticizer weight percentages and slightly shifted to a lower value of 1600 cm^{-1} upon increase in dopant concentration. The bands between 1500-1640 cm^{-1} are associated with the bending of the amine group (N-H) and the peaks observed in the region of 1600-1700 cm^{-1} due to the C-C stretching. The bands between 1350 and 1400 cm^{-1} are due to the stretching of C-O group. The bands between 100-1100 cm-1 were assigned to an ether linkage (C—O—C) which resulted from the formation of cross linking reaction between the ionic liquids and its blend with poly(acrylic acid) and poly(vinyl alcohol). As the weight percent of ionic liquids increases, the intensity of this band increased. The ester formation between poly(vinyl alcohol) and poly(acrylic acid) is detectable due to the ester (C=O) vibrations and (C—O—C) ether vibrations at 1600 cm-1 and 1000 cm-1, respectively.

The main reason for determining the molecular structure of the polymer blends using FTIR spectroscopy is to relate the structural changes due to addition of the ionic liquids in order to enhance the electrical properties of the blends due to the cations/anions coupling mechanism which leads to a continuous loss of the hydrogen O-H and the formation of the complications and chain alignment.

3.4. Conductivity measurement (ac impedance)

Systematic *ac* impedance measurements at different temperatures were performed for neat PVA, neat PAA, the blended neat PVA-PAA and the doped polymer blend with the three ionic liquids were measured as a function of frequency. The room temperature measurements of the ionic liquids doped films produced Nyquist plots with one and/or two semi-circles. The semi-circles were used to determine the dc resistivity of each semi-circle as a function of temperature. Different temperature readings were needed to conduct the activation energy measurements. The activation energy determines the conductivity of the polymer blended ionic liquids. The conductivity is inversely proportional the resistivity, meaning as the resistivity increases, conductivity decreases and vise versa. The conductivity spectra of neat PVA, neat PAA and neat PVA-PAA are shown in Figure 3.17 (a-c), PVA-PAA- various ratios of glycerol are shown in Figure 3.18 (a-d), PVA-PAA- various ratios of sorbitol in Figure 3.19(a-d), PVA-PAA- various ratios of imidazolium bromide $[MDIM]^{(+)}Br^{(-)}$ in Figure 3.20(a-d); Figures 3.18-3.20 have various polymer membrane blended with ionic liquids in them.

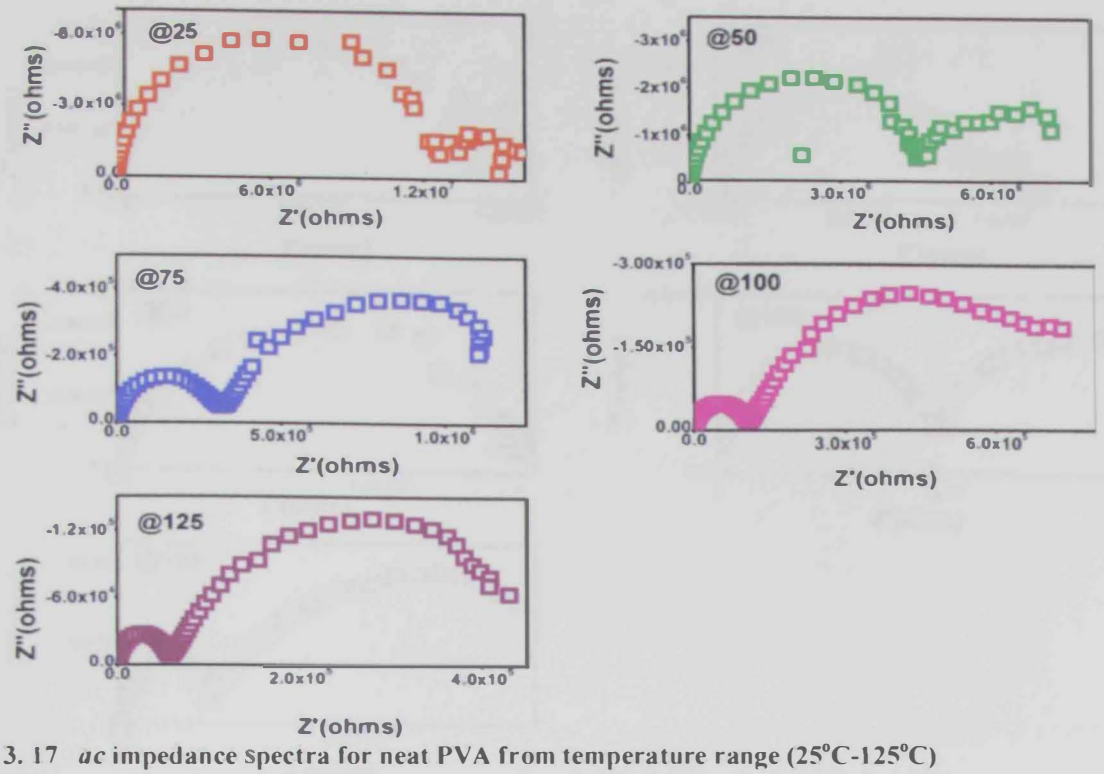

Figure 3. 17 *ac* impedance spectra for neat PVA from temperature range (25°C-125°C)

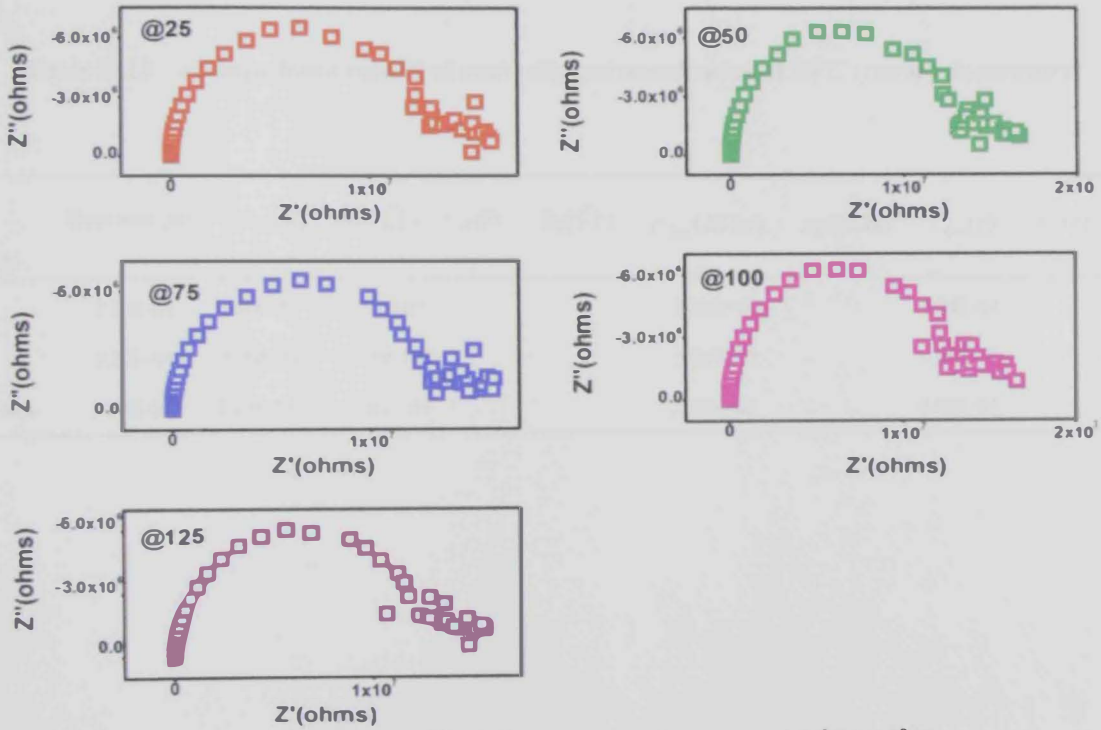

Figure 3. 18 *ac* impedance spectra for neat PAA from temperature range (25°C-125°C)

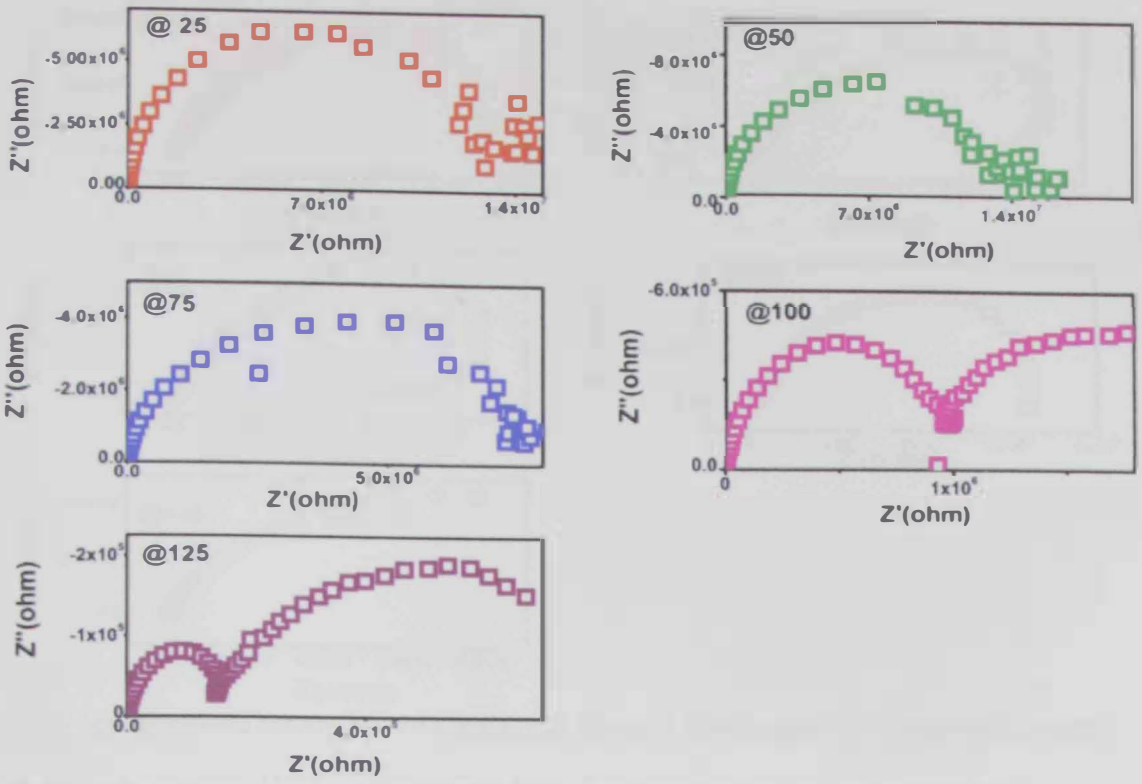

Figure 3. 19 *ac* **impedance spectra for neat PVA-PAA from temperature range (25°C-125°C)**

Table 3. 13 *ac* **impedance results of neat polymer membranes at 25°C (room temperature)**

Sample Description	Thickness (m)	C_{film}(F)	$R_{film}(\Omega)$	C_{dl}(F)	$R_{ct}(\Omega)$	$\rho_{film}(K\Omega m)$	$\rho_{ct}(K\Omega m)$	$\tau_{film}(s)$	$\tau_{ct}(s)$
PVA	3.20E-04	3.60E-11	1.22E+07			3.65E+05		4.34E-04	
PAA	3.20E-04	3.09E-11	1.30E+07			3.91E+05		4.00E-04	
PVA-PAA	3.70E-04	3.17E-11	1.26E+07			3.28E+05		4.00E-04	

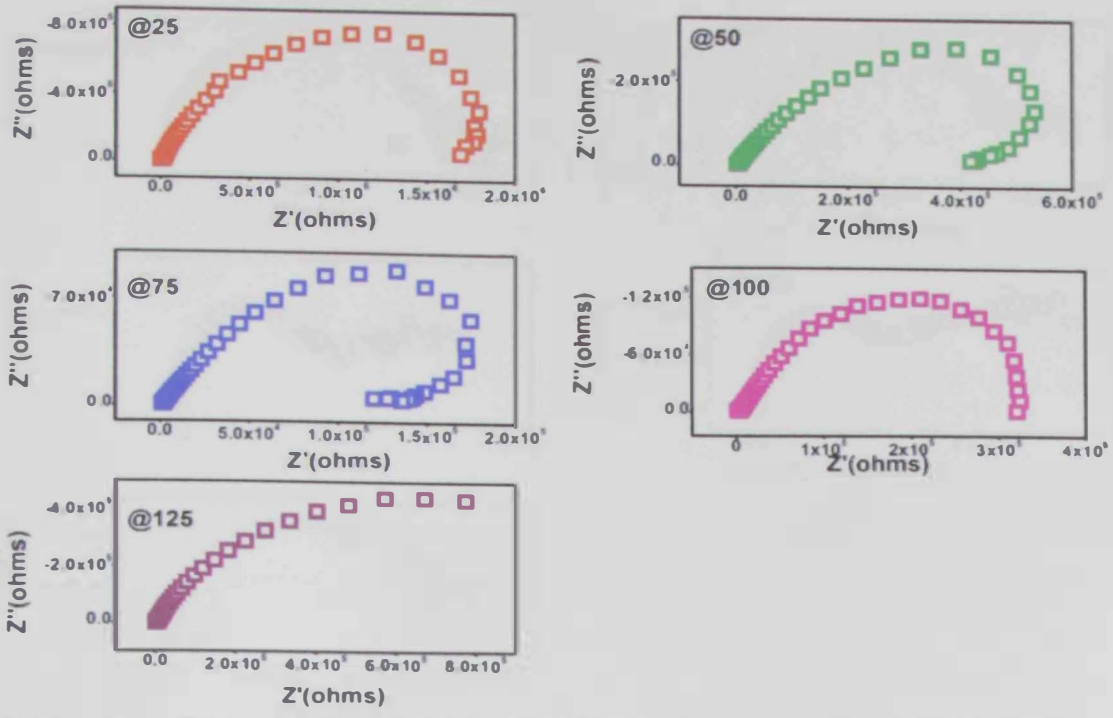

Figure 3. 20 *ac* impedance Spectra for PVA-PAA- 1% Glycerol from temperature range (25°C-125°C)

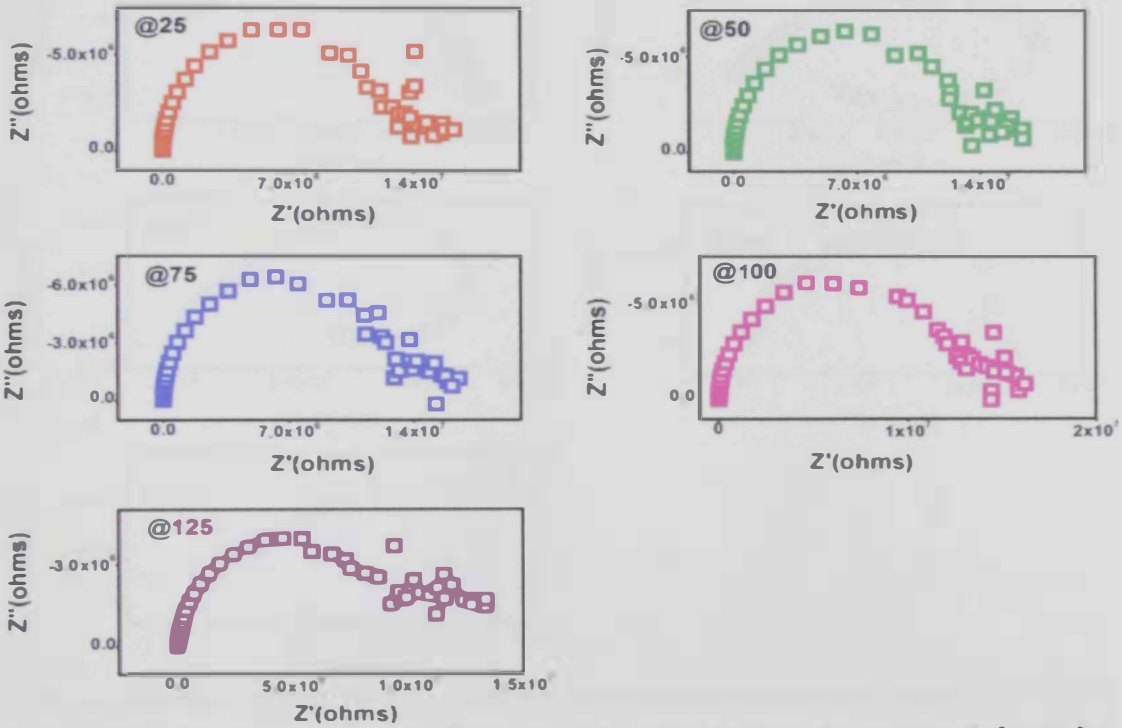

Figure 3. 21 *ac* impedance spectra for PVA-PAA- 2% Glycerol from temperature range (25°C-125°C)

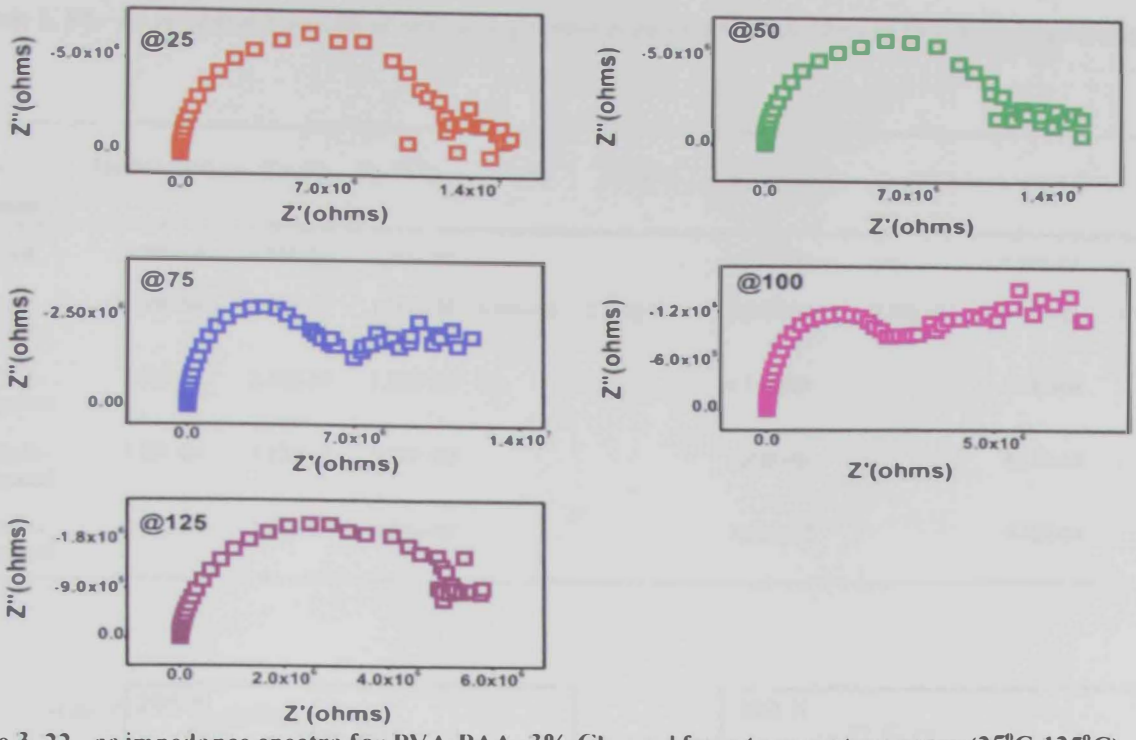

Figure 3. 22 *ac* impedance spectra for PVA-PAA- 3% Glycerol from temperature range (25°C-125°C)

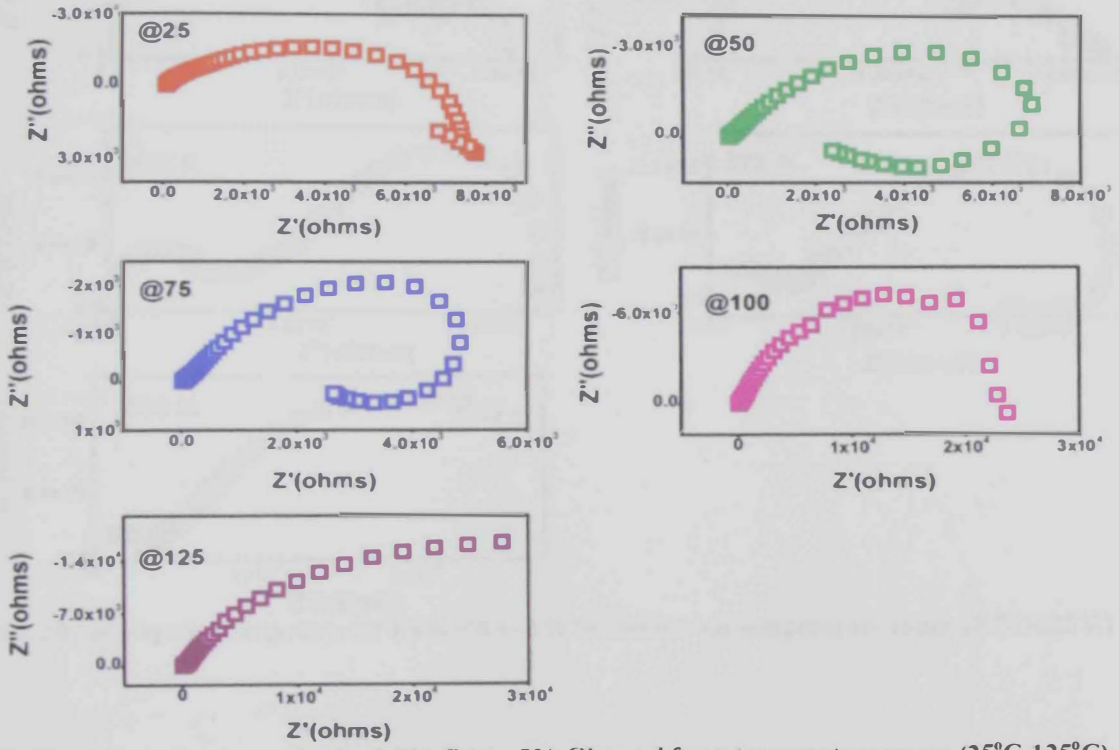

Figure 3. 23 *ac* impedance spectra for PVA-PAA- 5% Glycerol from temperature range (25°C-125°C)

Table 3. 14 *ac* impedance results of neat and glycerol doped PVA-PAA films at 25°C (room temperature)

Sample Description	Thickness (m)	C_{film}(F)	$R_{film}(\Omega)$	C_{dl}(F)	$R_{ct}(\Omega)$	$\rho_{film}(K\Omega m)$	$\rho_{ct}(K\Omega m)$	$\tau_{film}(s)$	$\tau_{ct}(s)$
PVA-PAA	3.70E-04	3.17E-11	1.26E+07			3.28E+05		4.00E-04	
PVA-PAA-1% Glycerol	2.30E-04	4.00E-11	1.69E+04	6.04E-09	2.10E+06	7.07E+02	8.79E+04	6.97E-02	1.34E-02
PVA-PAA-2% Glycerol	2.80E-04	2.59E-10	1.38E+03			4.75E+01		4.14E-04	
PVA-PAA-3% Glycerol	1.80E-04	2.32E-10	9.02E+02			4.82E+01		4.17E-04	
PVA-PAA-5% Glycerol	3.90E-04	1.16E-07	6.56E+03			1.62E+02		9.48E-04	

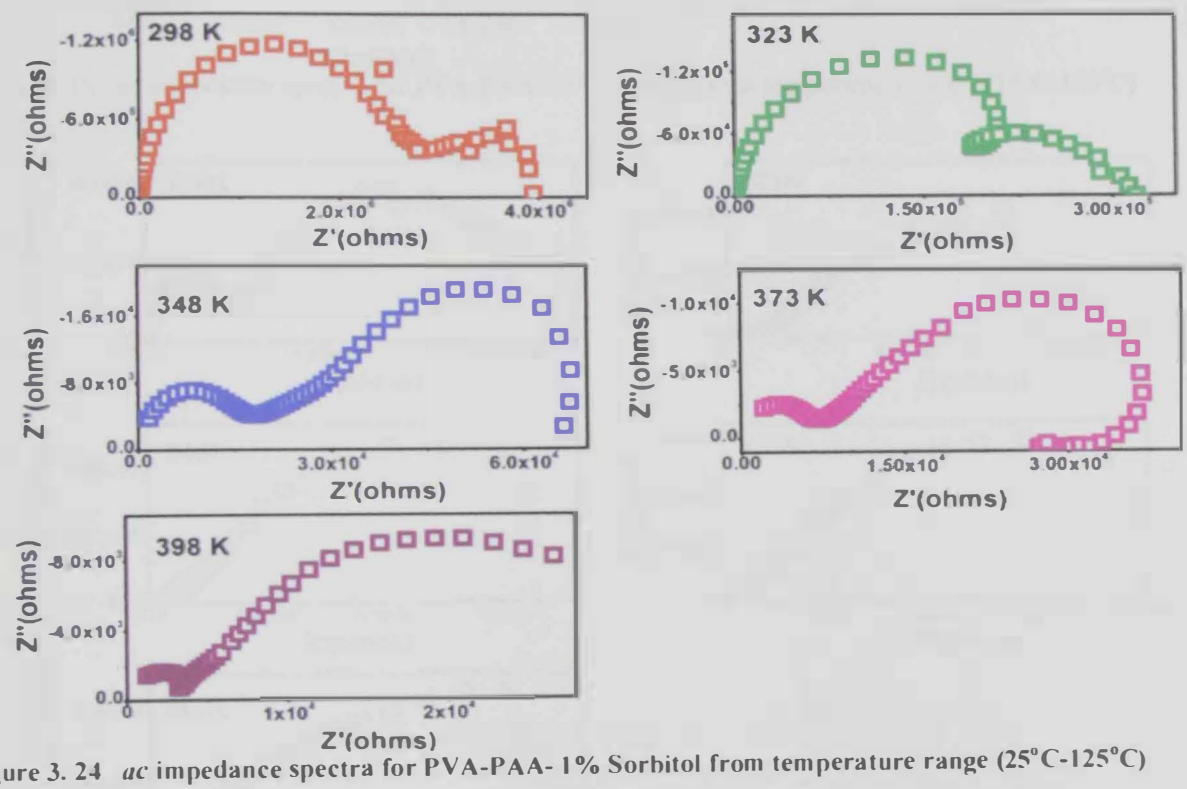

Figure 3. 24 *ac* impedance spectra for PVA-PAA- 1% Sorbitol from temperature range (25°C-125°C)

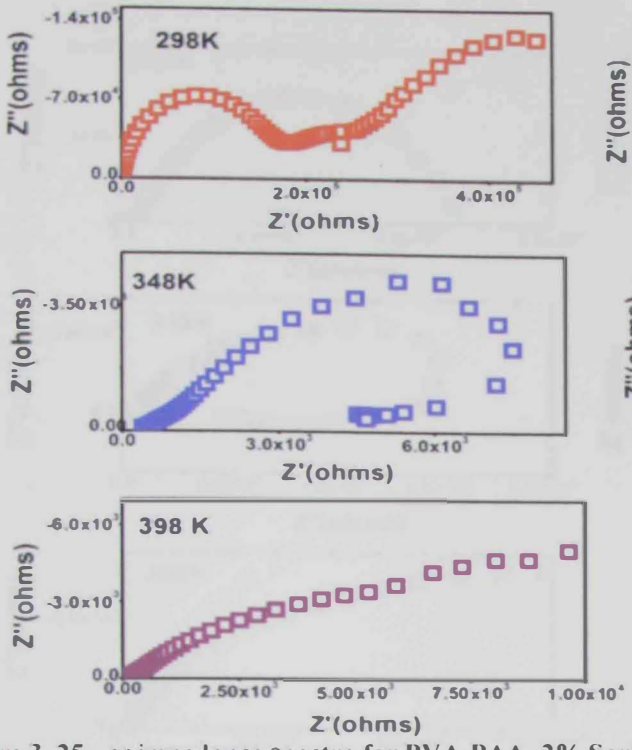

Figure 3. 25 *ac* impedance spectra for PVA-PAA- 2% Sorbitol from temperature range (25°C-125°C)

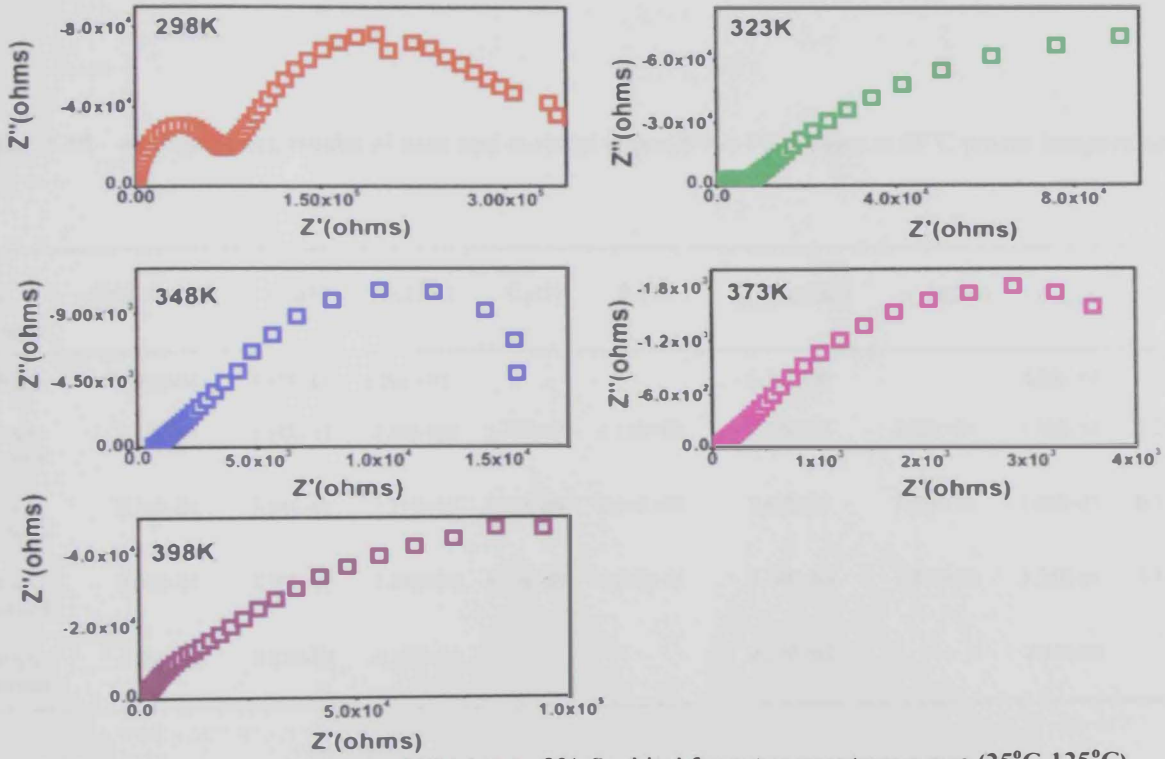

Figure 3.26 *ac* impedance spectra for PVA-PAA- 3% Sorbitol from temperature range (25°C-125°C)

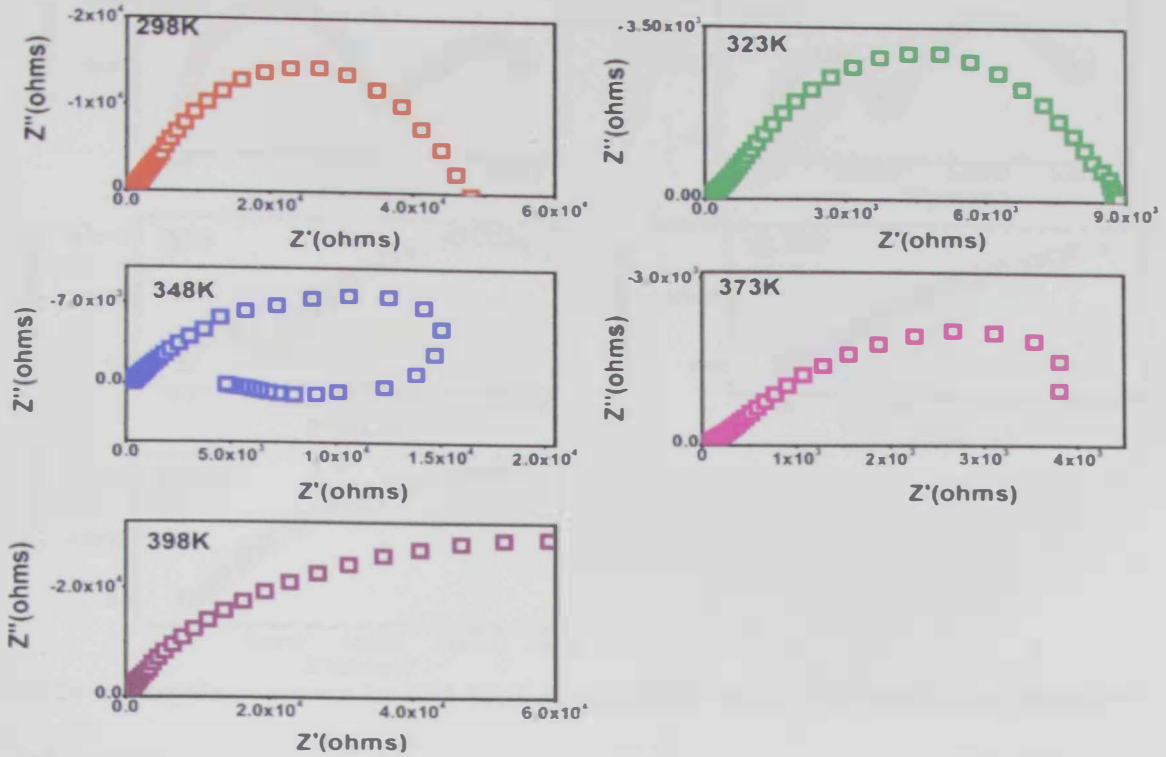

Figure 27 *ac* impedance spectra for PVA-PAA- 5% Sorbitol from temperature range (25°C-125°C)

Table 3.15 *ac* impedance results of neat and sorbitol doped PVA-PAA films at 25°C (room temperature)

Sample Description	Thickness (m)	C_{film}(F)	$R_{film}(\Omega)$	C_{dl}(F)	$R_{ct}(\Omega)$	ρ_{film} ($K\Omega m$)	ρ_{ct} ($K\Omega m$)	τ_{film} (s)	τ_{ct} (s)
PVA-PAA	3.70E-04	3.17E-11	1.26E+07			3.28E+05		4.00E-04	
PVA-PAA-1% Sorbitol	2.10E-04	3.62E-11	2.89E+06	5.79E-09	1.75E+06	1.32E+05	8.02E+04	1.06E-04	1.24E-02
PVA-PAA-2% Sorbitol	2.20E-04	3.94E-11	1.75E+05	1.23E-08	2.86E+05	7.65E+05	1.25E+04	7.00E-07	6.31E-03
PVA-PAA-3% Sorbitol	2.00E-04	4.08E-11	7.87E+04	9.25E-09	2.85E+05	3.78E+03	1.35E+04	3.31E-06	3.11E-03
PVA-PAA-5% Sorbitol	1.90E-04	4.65E-08	4.37E+04			2.21E+03		2.21E-03	

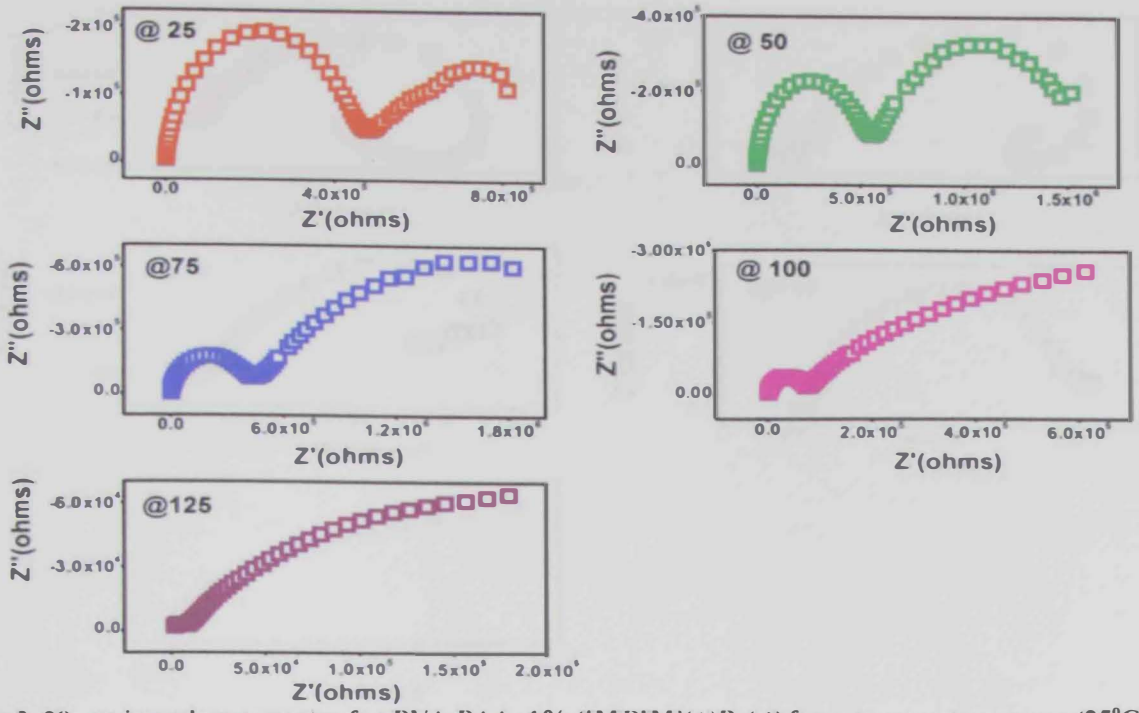

Figure 3. 28 *ac* impedance spectra for PVA-PAA- 1% ([MDIM](+)Br(-)) from temperature range (25°C-125°C)

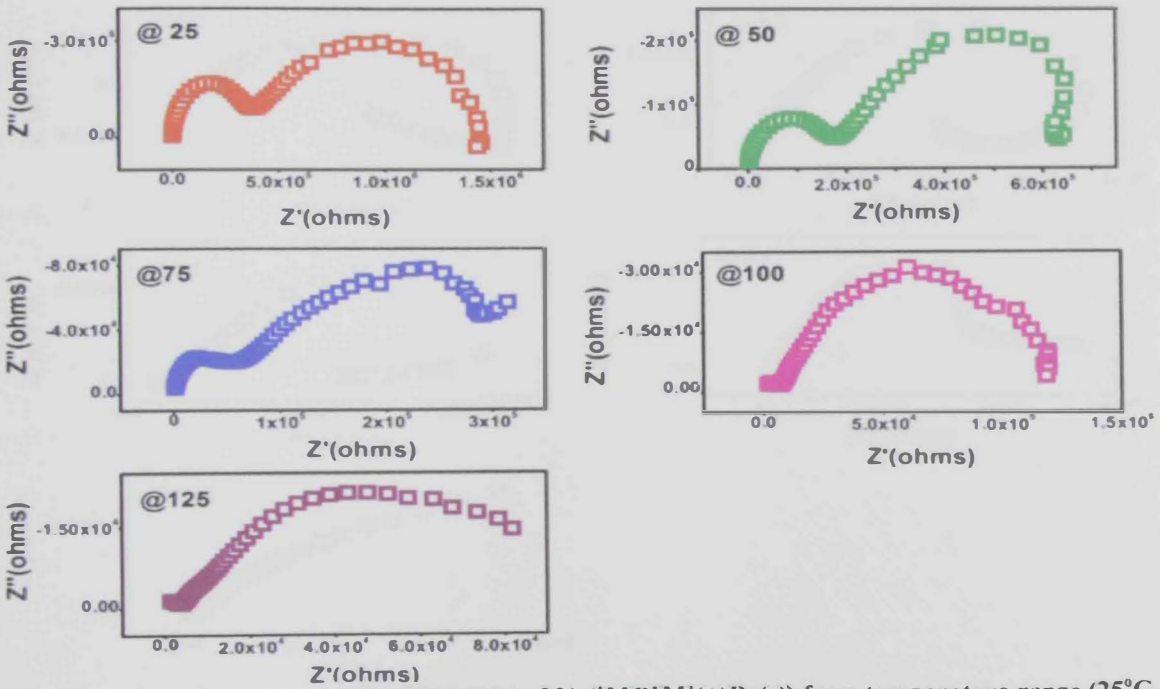

Figure 3. 29 *ac* impedance spectra for PVA-PAA- 2% ([MDIM](+)Br(-)) from temperature range (25°C-125°C)

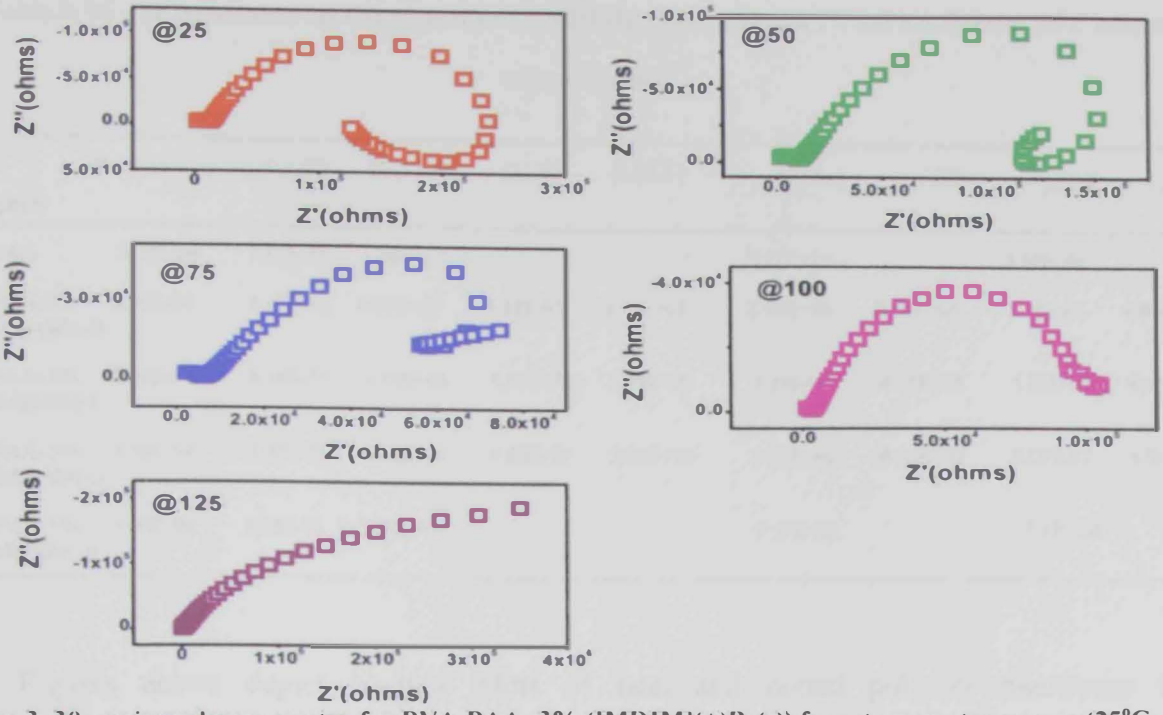

Figure 3. 30 *ac* impedance spectra for PVA-PAA- 3% ([MDIM](+)Br(-)) from temperature range (25°C-125°C)

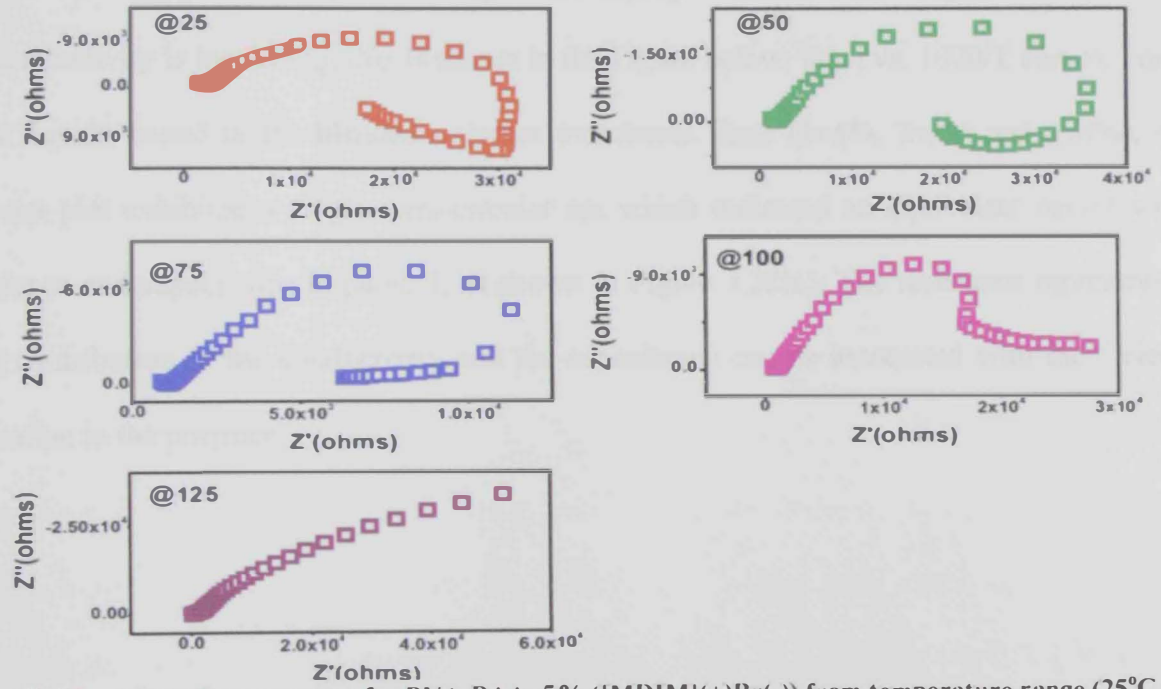

Figure 3. 31 *ac* impedance spectra for PVA-PAA- 5% ([MDIM](+)Br(-)) from temperature range (25°C-125°C)

Table 3. 16 ***ac*** **impedance results of neat and ([MDIM](+)Br(-)) doped PVA-PAA films at 25°C (room temperature)**

Sample Description	Thickness (m)	C_{film}(F)	$R_{film}(\Omega)$	C_{ct}(F)	$R_{ct}(\Omega)$	$\rho_{film}(K\Omega m)$	$\rho_{ct}(K\Omega m)$	$\tau_{film}(s)$	$\tau_{ct}(s)$
PVA-PAA	3.70E-04	3.17E-11	1.26E+07			3.28E+05		4.00E-04	
PVA-PAA-1% ([MDIM](+)Br(-))	2.20E-04	4.17E-11	4.60E+05	1.18E-07	4.93E+05	2.01E+04	2.15E+04	1.94E-05	6.80E-02
PVA-PAA-2% ([MDIM](+)Br(-))	2.80E-04	3.34E-11	3.75E+05	5.31E-09	1.24E+06	1.29E+04	4.28E+04	1.26E-05	8.55E-03
PVA-PAA-3% ([MDIM](+)Br(-))	3.50E-04	3.37E-11	1.16E+04	8.03E-09	2.31E+05	3.20E+02	6.35E+03	4.02E-07	1.90E-03
PVA-PAA-5% [MDIM](+)Br(-))	3.00E-04	1.68E-08	2.99E+04			9.57E+02		5.57E-04	

The Figures above depict Nyquist plots of neat and doped polymer membrane film measurements at temperatures ranging from room temperature 25°C to 125°C. The Tables above show a trend in the resistivity decreasing as the doping increases which implies to the fact that the conductivity is increasing, this is shown in the Figure below; ln(ρ) vs. 1000/T curves. For the ionic liquids doped in the blended polymer membrane films (1wt%, 2wt% and 3wt%), each Nyquist plot exhibited a single semi-circular arc which indicated an equivalent circuit with a resistance and capacitance in parallel, as shown in Figure 3.32(a). The resistance represents the bulk contribution to the conductivity and the capacitance can be associated with the dielectric relaxation in the polymer.

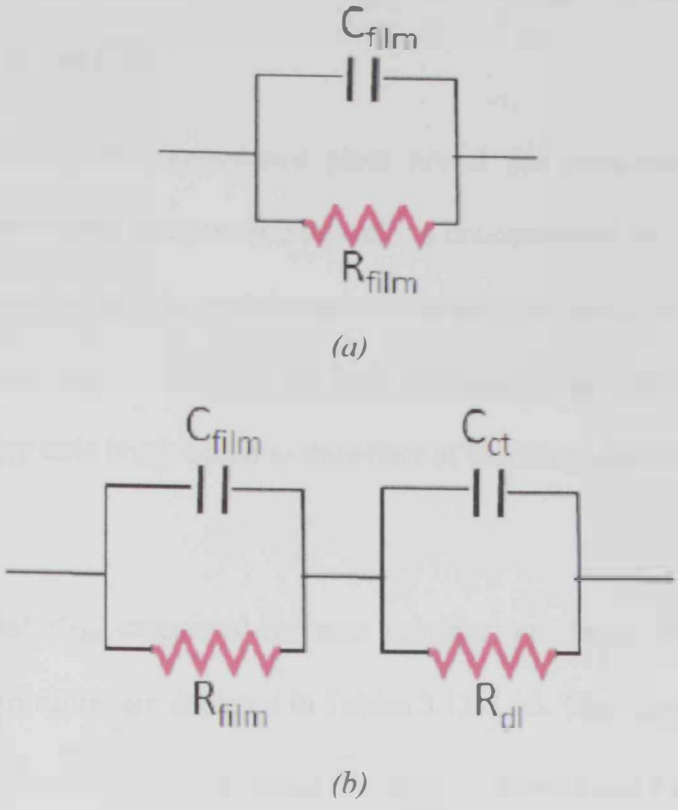

Figure 3. 32 Equivalent circuits of the (a) one semicircle Nyquist plot, and (b) two semicircles Nyquist plots.

Z-view simulation software was used to confirm the equivalent circuit. A semi-circle fitting produces the values of the capacitance (C_{film}) and resistance (R_{film}). R_{film} and C_{film} represent the contribution to resistance and capacitance arising from the grain boundaries and electron depletion regions in the film [72]. The two semicircles shown in the plots above especially for those doped with the ionic liquids at room temperature (25°C) indicate that the sample can be represented by two pairs of parallel RC circuits connected into series as shown in Figure 3.32(b). Z-View simulation was used to confirm this assumption; the first semi-circle corresponds to the resistive and capacitive components (R_{film} & C_{film}) of the film, while the second semi-circle

occurs at low frequency range and related to the interfacial charge transfer resistance and double layer capacitance (R_{ct} & C_{dl}) [73].

As seen from the Figures, the impedance plots reveal the semi-circle response with low frequency tails with increasing temperature as well as concentration of ionic liquids, indicating the double layer response at the electrode/sample interface. The ionic conduction process in the bulk of the polymer electrode is related to the high frequency range. Moreover, the straight line parallel to the imaginary axis is attributed to the effect of blocking electrode at the low frequency range [74, 75].

The values of C_{film} and R_{film} calculated for neat polymer membrane films and for films with different doping concentration are depicted in Tables 3.13-3.16. The values of the resistances are used to calculate the dc resistivity (ρ). Using $\rho = RA/l$, where A and l are the contact area and thickness of measured film, respectively, and R is the resistance. The data presented in the tables above show that increasing the doping ratio decreases the film resistivity which indicates the conductivity is increasing.

The relaxation time (τ) for each semi-circles can be calculated using $\tau = 1/\omega_{max}$, where ω_{max} is the angular frequency ($\omega_{max} = 2\pi f_{max}$) at the semi-circle maximum [76]. The values of τ are shown in the Tables above. The Table show that increasing the concentration percentage ratios doped decreases the film relaxation time, where the 5% doped film exhibits the minimum τ_{film}, where τ_{film} is the relaxation time calculated for the first semi-circle. This is caused from the

addition of the doped plasticizer added to the polymer; the more doped the less the relaxation time.

The first semi-circle can be assigned to the charge transfer process (kinetic process) that occurs at high frequencies, while the second semi-circle is due to the contribution of mass migration process (diffusion). At high frequencies, ions movement is minimal because of their large relaxation time (see Tables). At low frequencies, ionic species with large relaxation time (τ_{ct}) can diffuse towards the electrode and accumulate there [77]. The polarization of this space migration process occurs when an appreciable concentration of the plasticizer is present. Thus, the resistivity of the film decreases noticeably.

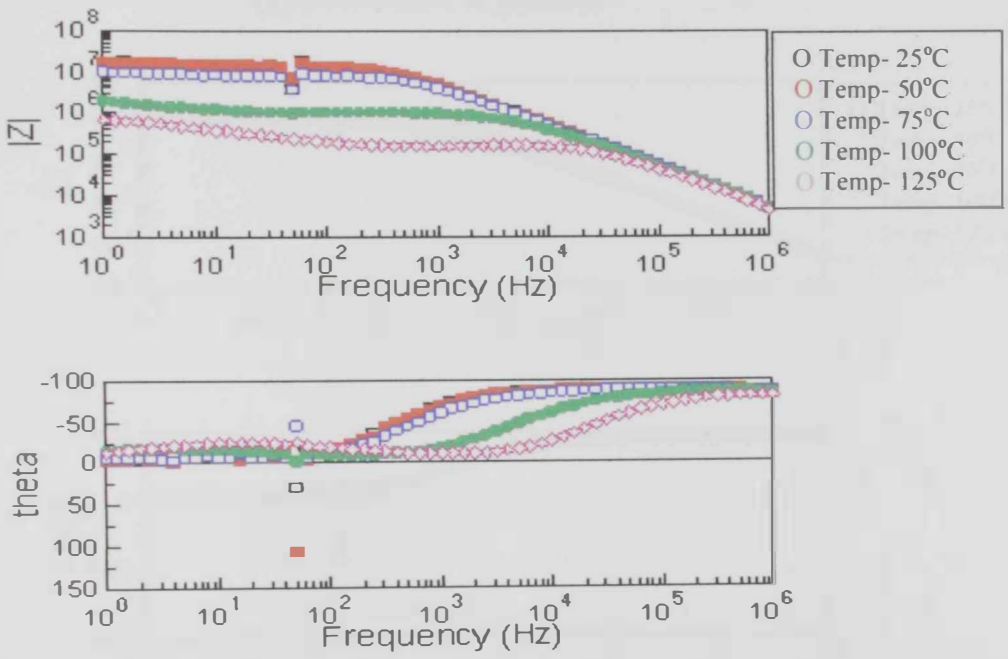

Figure 3. 33 The dependence of the ac impedance (upper curves) and the phase angle of frequency (lower curves) of neat PVA-PAA polymer membranes

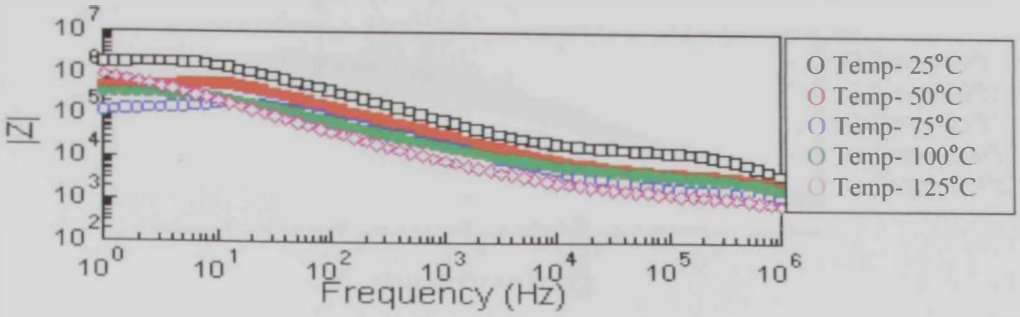

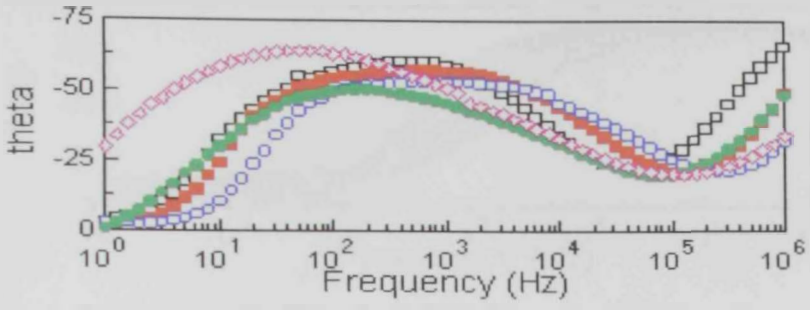

(a) *PVA-PAA-1% glycerol*

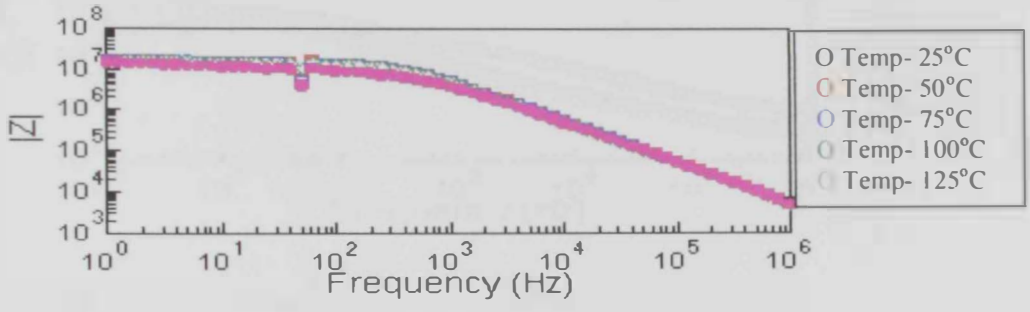

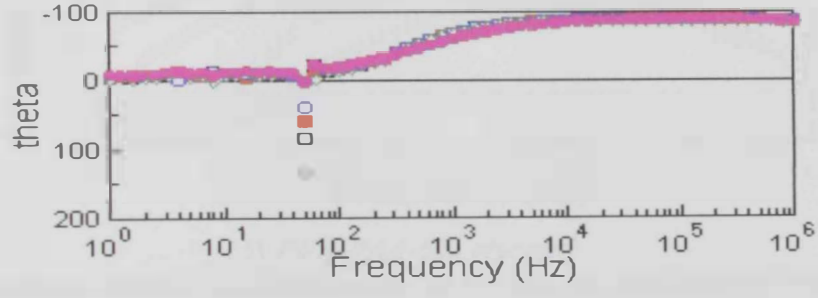

(b) *PVA-PAA-2% glycerol*

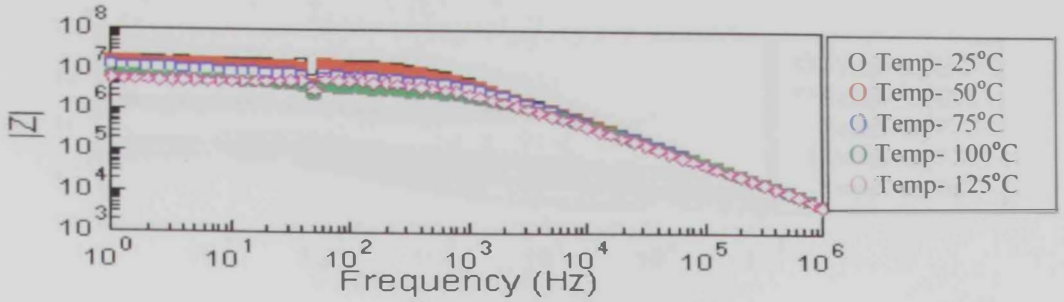

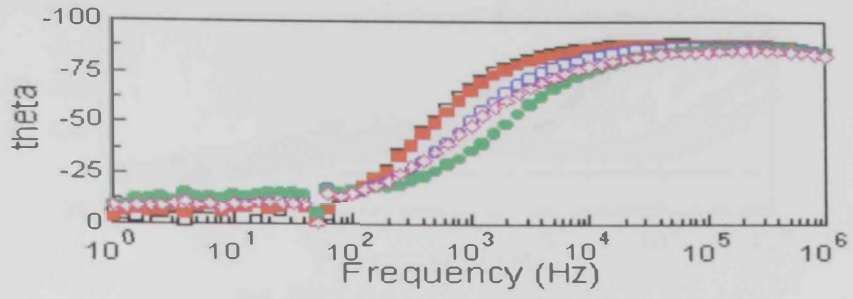

(c) *PVA-PAA-3% glycerol*

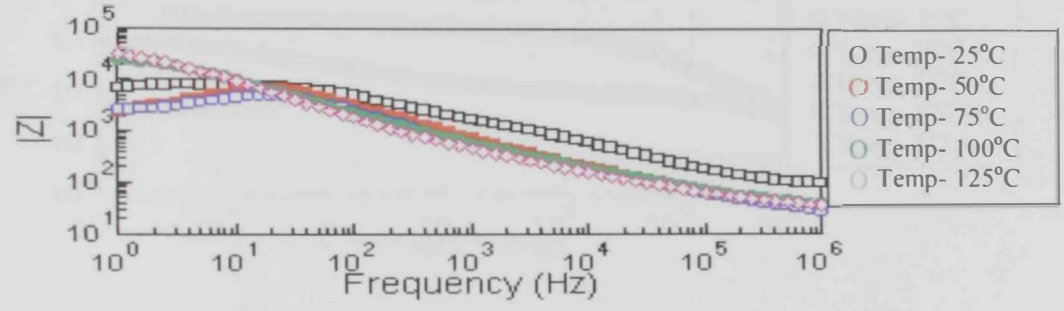

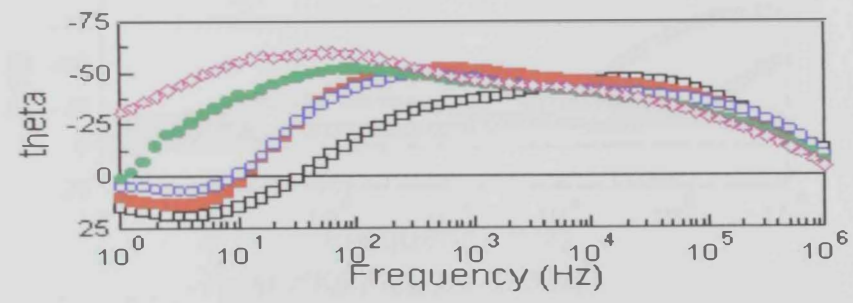

(d) *PVA-PAA-5% glycerol*

Figure 3. 34 The dependence of the ac impedance (upper curves) and the phase angle of frequency (lower curves) of (a) PVA-PAA-1% glycerol, (b) PVA-PAA-2% glycerol, (c) PVA-PAA-3% glycerol, (d) PVA-PAA-5% glycerol polymer membranes.

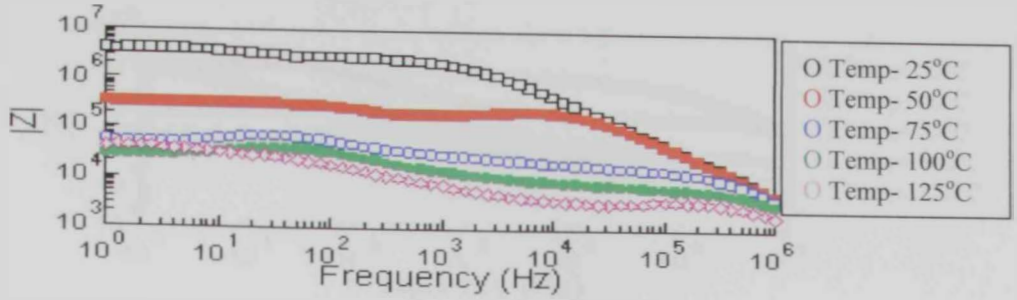

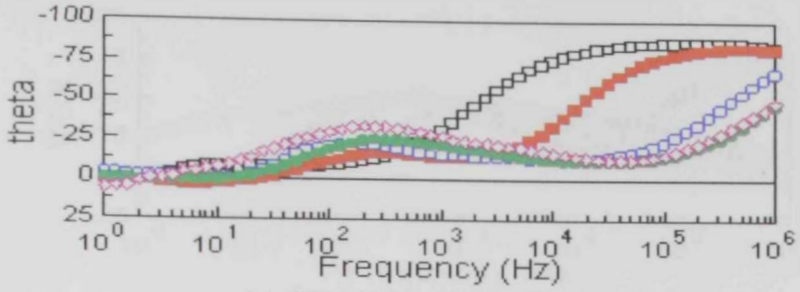

(a) PVA-PAA-1% Sorbitol

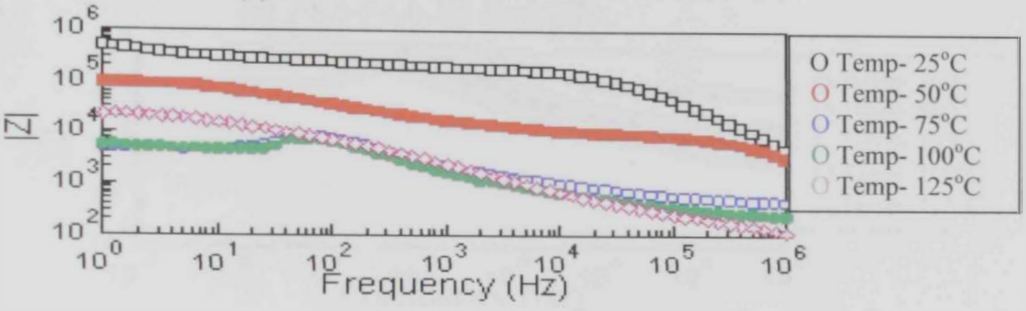

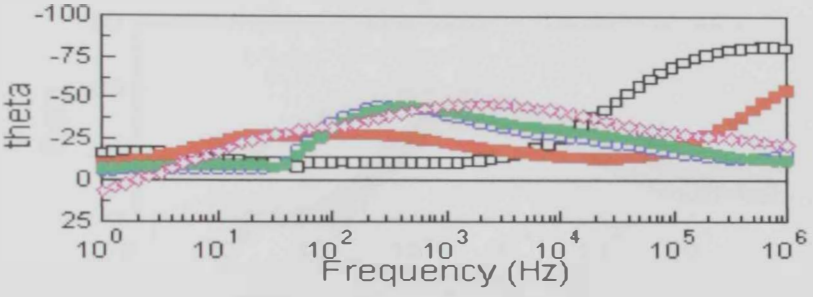

(b) PVA-PAA-2% Sorbitol

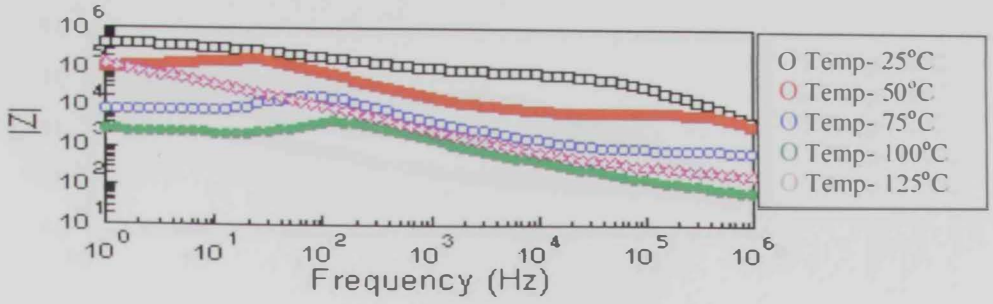

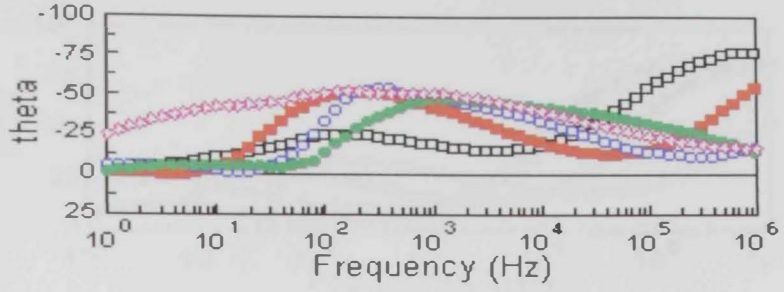

(c) PVA-PAA-3% Sorbitol

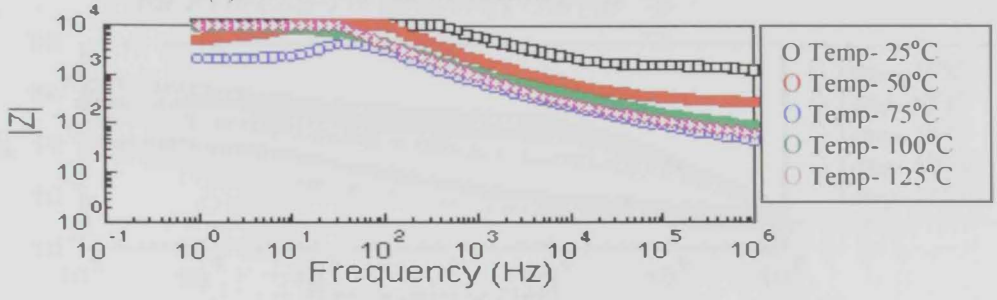

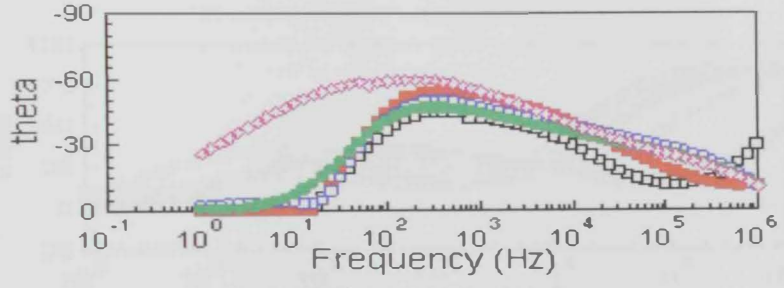

(d) PVA-PAA-5% Sorbitol

Figure 3. 35 The dependence of the ac impedance (upper curves) and the phase angle of frequency (lower curves) of (a) PVA-PAA-1% sorbitol, (b) PVA-PAA-2% sorbitol, (c) PVA-PAA-3% sorbitol, (d) PVA-PAA-5% sorbitol polymer membranes

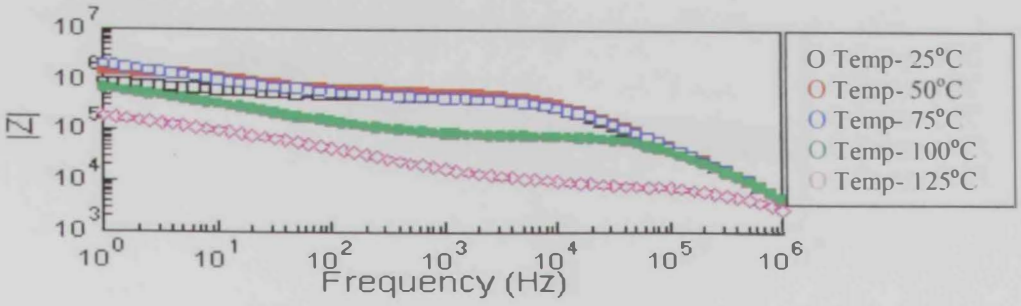

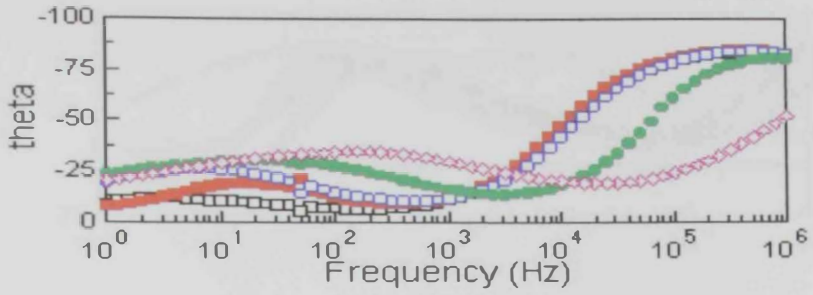

(a) PVA-PAA-1% ([MDIM](+)Br(-))

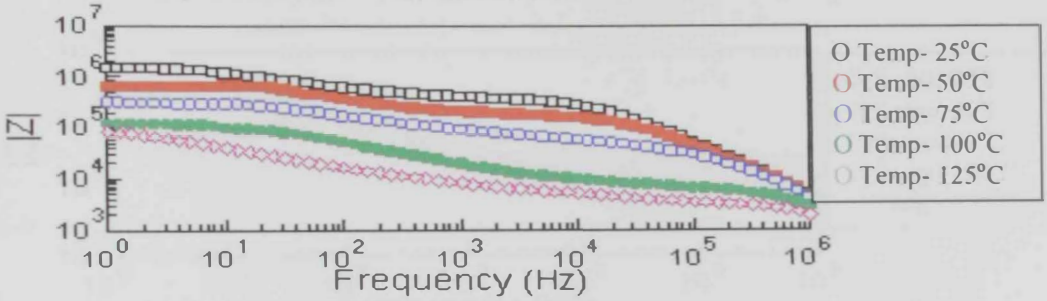

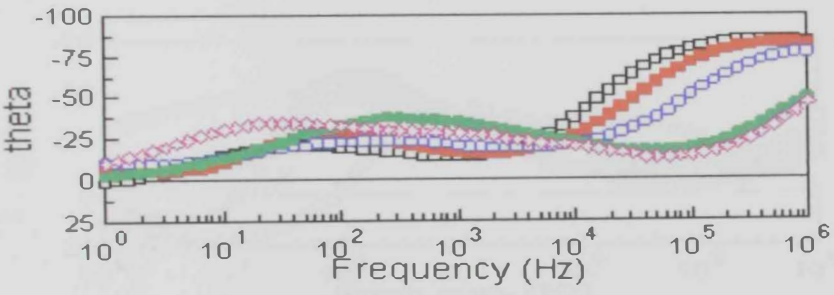

(b) PVA-PAA-2% ([MDIM](+)Br(-))

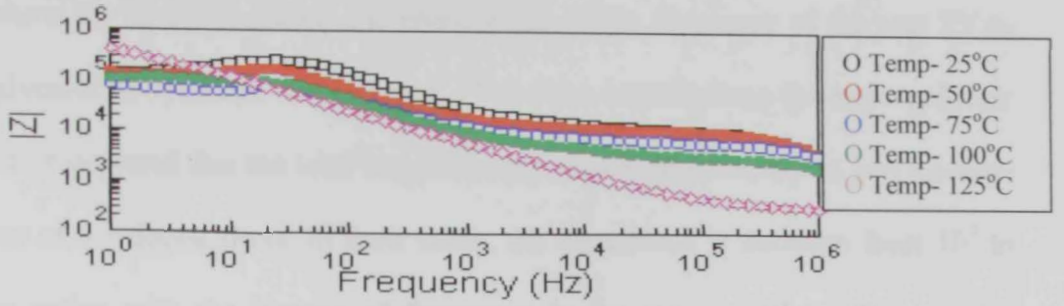

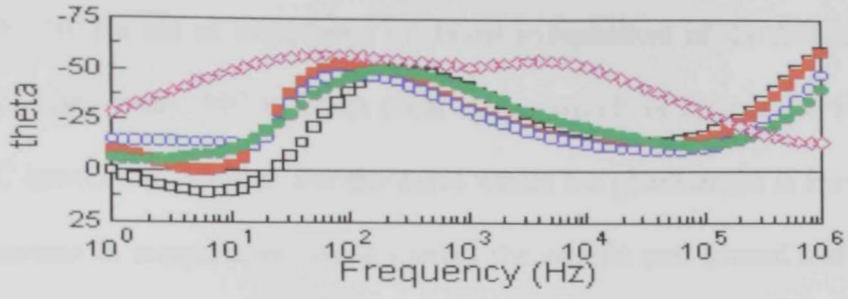

(c) PVA-PAA-3% ([MDIM](+)Br(-))

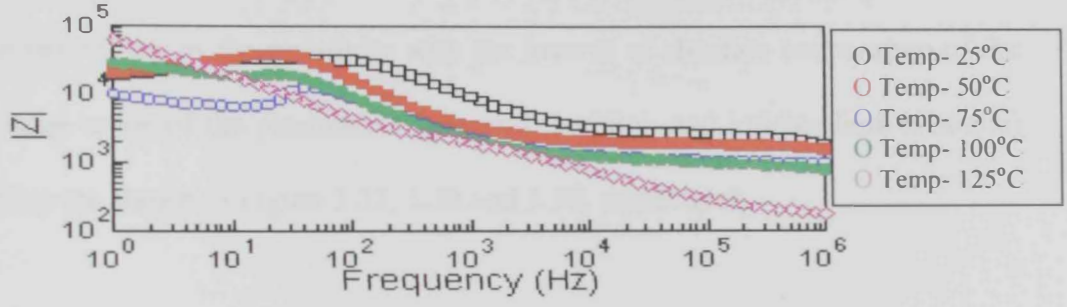

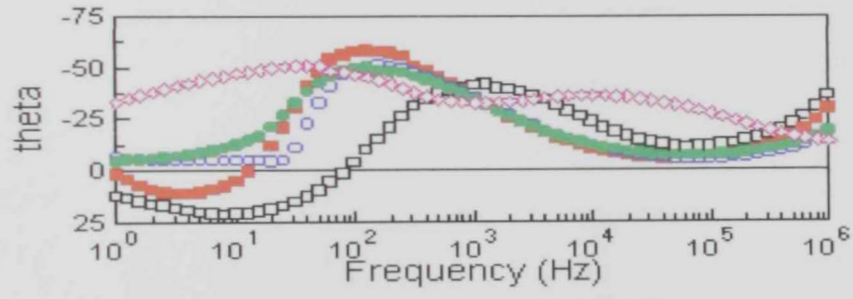

(d) PVA-PAA-5% ([MDIM](+)Br(-))

Figure 3. 36 The dependence of the ac impedance (upper curves) and the phase angle of frequency (lower curves) of (a) PVA-PAA-1% ([MDIM](+)Br(-)), (b) PVA-PAA-2% ([MDIM](+)Br(-)), (c) PVA-PAA-3% ([MDIM](+)Br(-)), (d) PVA-PAA-5% ([MDIM](+)Br(-)) polymer membrane

Figures 3.33-3.36 show the total impedance and phase angle of the frequency of the neat PVA-PAA, PVA-PAA-glycerol, PVA-PAA-sorbitol and PVA-PAA-imidazolium bromide polymer doped membranes. It is depicted that the total impedance decreases dramatically as you increase the percentage ratios of the doped films. In most cases, the impedance is decrease from 10^7 to 10^4; the impedance varies with the inverse of frequency in the range ~10^3-10^6 Hz, and for frequencies less than 10^2 Hz the ac impedance is almost independent of the frequency. For the phase angle which varies from -90° to 0° in most cases, which is typical for films that are equivalent to an RC network in parallel. For the cases where the phase angle is less than 0°, this is caused by the increase in temperature which melted the sample and caused a short circuit to occur.

The variation of the natural log of the resistivity with the inverse of absolute temperature of the neat and the percentage ratios of the plasticizers (glycerol, sorbitol, and imidazolium bromide) doped membrane films are shown in Figure 3.37, 3.38 and 3.39, respectively.

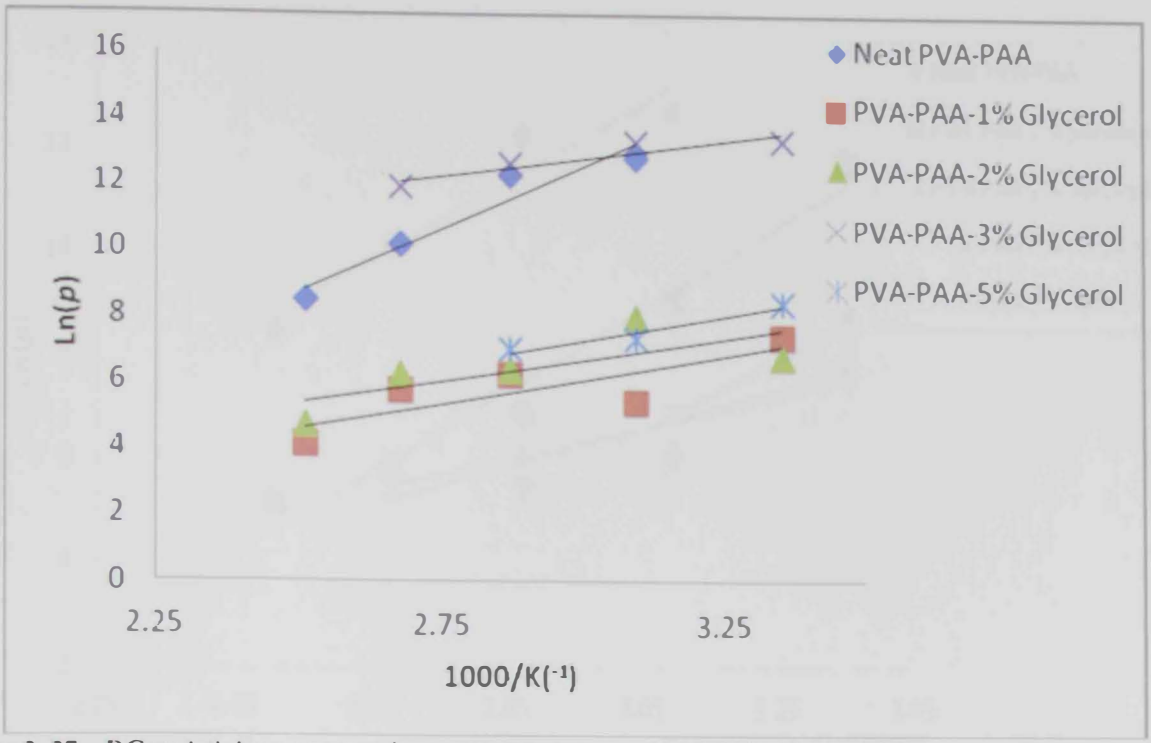

Figure 3. 37 DC resistivity versus reciprocal temperature of neat PVA-PAA and the composition ratios of glycerol doped polymer membranes. The solid line is a linear fit of resistivity $\rho_{(film)}$.

Table 3. 17 Activation energies (Ea) results of the neat PVA-PAA and the Glycerol doped polymer membranes

Sample Description	$E_{a(film)}$ (eV)
PVA-PAA	0.66
PVA-PAA-1% glycerol	0.26
PVA-PAA-2% glycerol	0.22
PVA-PAA-3% glycerol	0.19
PVA-PAA-5% glycerol	0.25

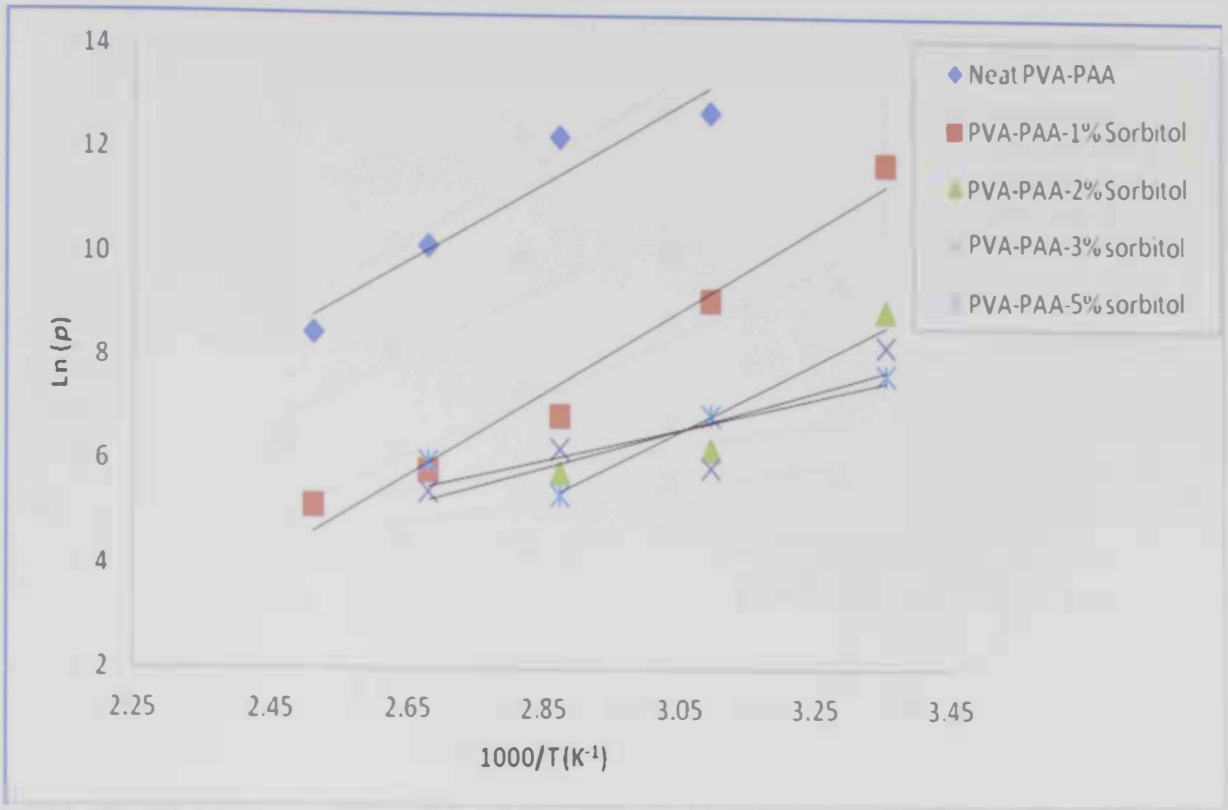

Figure 3. 38 DC resistivity versus reciprocal temperature of neat PVA-PAA and the composition ratios of sorbitol doped polymer membranes. The solid line is a linear fit of resistivity $\rho_{(film)}$.

Table 3. 18 Activation energy (Ea) results of the neat PVA-PAA and the Sorbitol doped polymer membranes

Sample Description	$E_{a(film)}$ (eV)
PVA-PAA	0.66
PVA-PAA-1% sorbitol	0.69
PVA-PAA-2% sorbitol	0.57
PVA-PAA-3% sorbitol	0.31
PVA-PAA-5% sorbitol	0.26

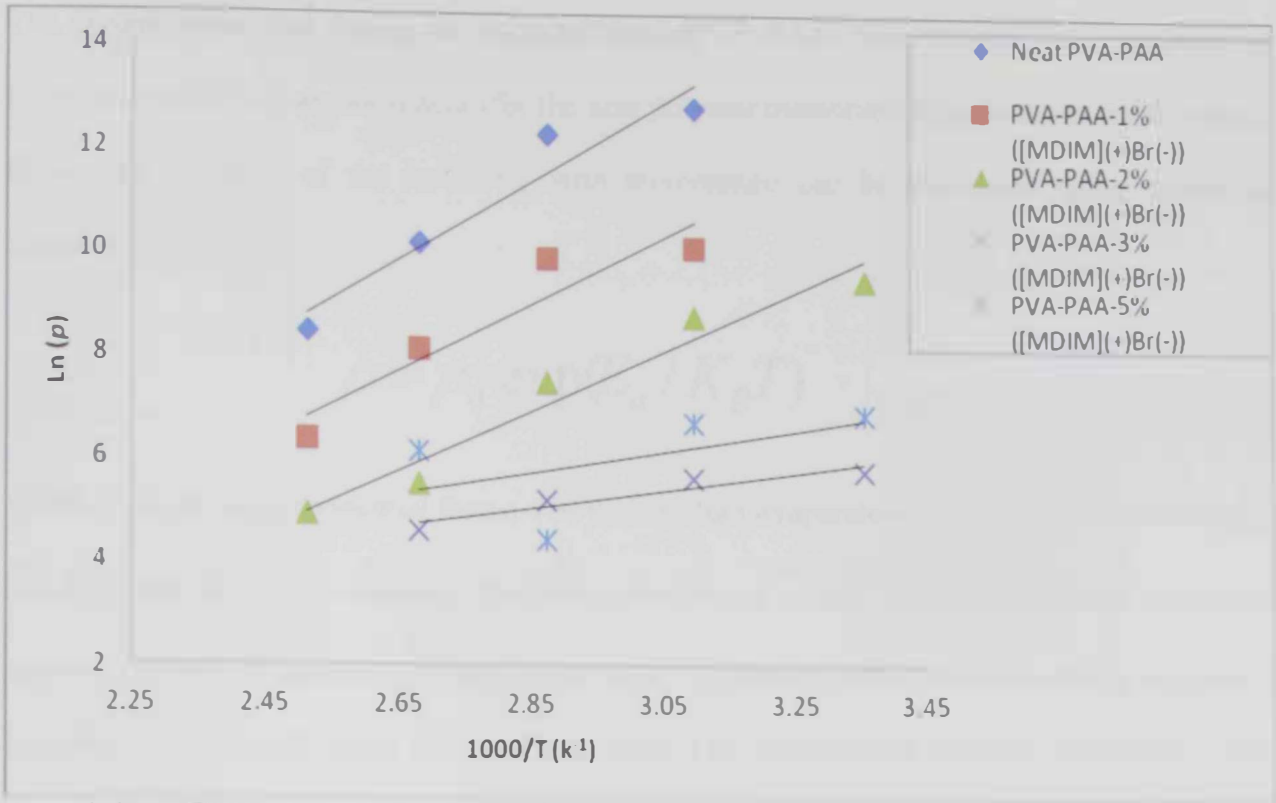

Figure 3. 39 DC resistivity versus reciprocal temperature of neat PVA-PAA and the composition ratios of ([MDIM](+)Br(-)) doped polymer membranes. The solid line is a linear fit of resistivity $\rho_{(film)}$.

Table 3. 19 Activation energy (Ea) results of the neat PVA-PAA and the ([MDIM](+)Br(-)) doped polymer membranes

Sample Description	$E_{a(film)}$ (eV)
PVA-PAA	0.66
PVA-PAA-1% ([MDIM](+)Br(-))	0.56
PVA-PAA-2% ([MDIM](+)Br(-))	0.50
PVA-PAA-3% ([MDIM](+)Br(-))	0.15
PVA-PAA-5% ([MDIM](+)Br(-))	0.18

The Figures reveal that doping the polymer blend (PVA-PAA) films convert the dependence of Ln (ρ) on (1000/T) from non-linear (for the neat polymer membrane film) to linear for the doped films. The variation of the resistivity with temperature can be elucidated using Arrhenius equation below:

$$\rho = \rho_0 \exp(E_a / K_B T) \qquad (5)$$

Where ρ_0 is the pre-exponential factor, T is the absolute temperature, E_a is the activation energy, and K_B is the Boltzmann constant. The linear dependence of Ln(ρ) on (1000/T) can be used to calculate the activation energy for the doped films. The values of the activation energy are shown in Table 3.17; glycerol, Table 3.18; sorbitol, Table 3.19; imidazolium bromide. The Tables show that increasing the doping concentration decreases the E_a which decreases the resistivity of the polymer membrane films and as a result, the conductivity is increased. Increasing the temperature of the doped films increases the carrier concentration inside the film because of the electron transfer from the valance band to the conduction band, which results in decreasing values for both ρ_{film} and ρ_{ct}. In most of the polymer films, it was observed that when increasing the temperatures above room temperature, a second semi-circle appears, this is due to the ions having enough energy to diffuse towards the electrodes under the action of low frequency electric field and accumulate there. The existence of the accumulated charges on the electrodes resist the motion of new ions which increases the interfacial charge transfer resistivity, as noticed in ρ_{ct} when compared with ρ_{film} (see Tables 3.14-3.16).

3.5. Scanning Electron Microscopy (SEM)

SEM micrographs for the polymer membrane with composition ratio of neat PVA-PAA polymer film doped with the ionic plasticizers are shown the in the photos below. They show uniform surface morphology. The cross-section micrographs also exhibit uniform layer structure morphology. The photos also show the domain of the plasticizers is well blended within the polymer matrix and no segregation was observed. It is implied that the ionic liquids used are compatible with the polymer membranes (PVA-PAA) and embeds themselves within the polymer matrix creating an additional free volume. All the polymer membrane film samples appear translucent. This is accordance with the earlier DSC results that there has been only T_m, indicating that the polymer blends form a homogeneous and stable membrane structure. Blending efficiency and compatibility depends on the chemical structure, molecular weight, and functional groups of the plasticizers; therefore, the polymer and the plasticizers have similarities in solubility parameters and polarity (hydrogen bonding) to form a homogeneous blend [78].

(a) Neat PVA-PAA

(b) Neat PVA-PAA

Figure 3. 40 SEM micrographs for the neat PVA-PAA polymer membrane films, (a) SEM captured from top surface (b) SEM captured from cross-section

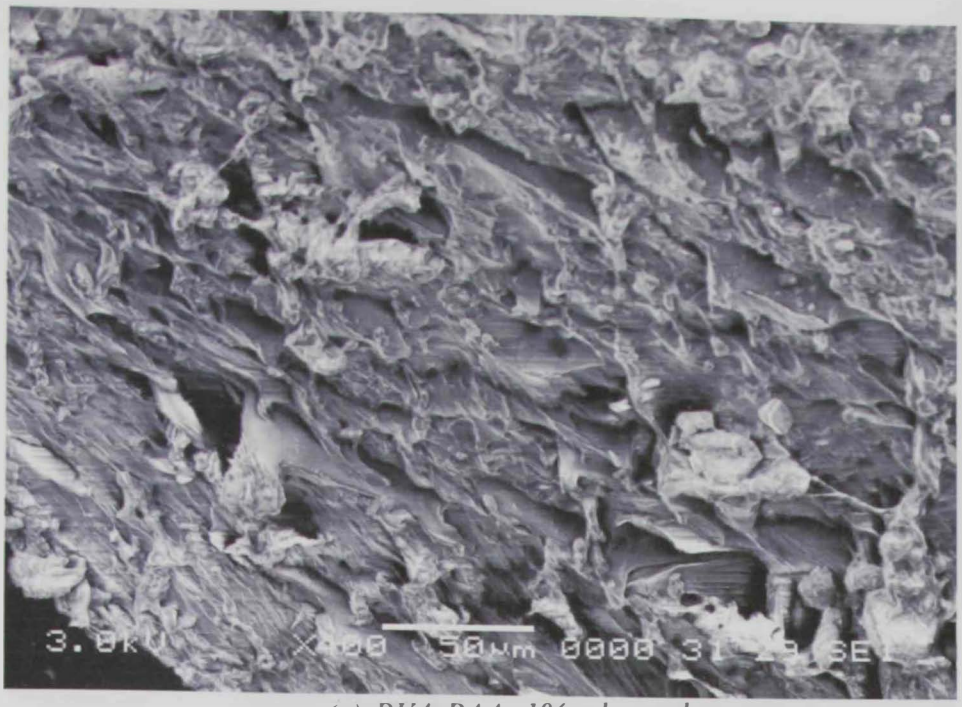

(a) PVA-PAA- 1% glycerol

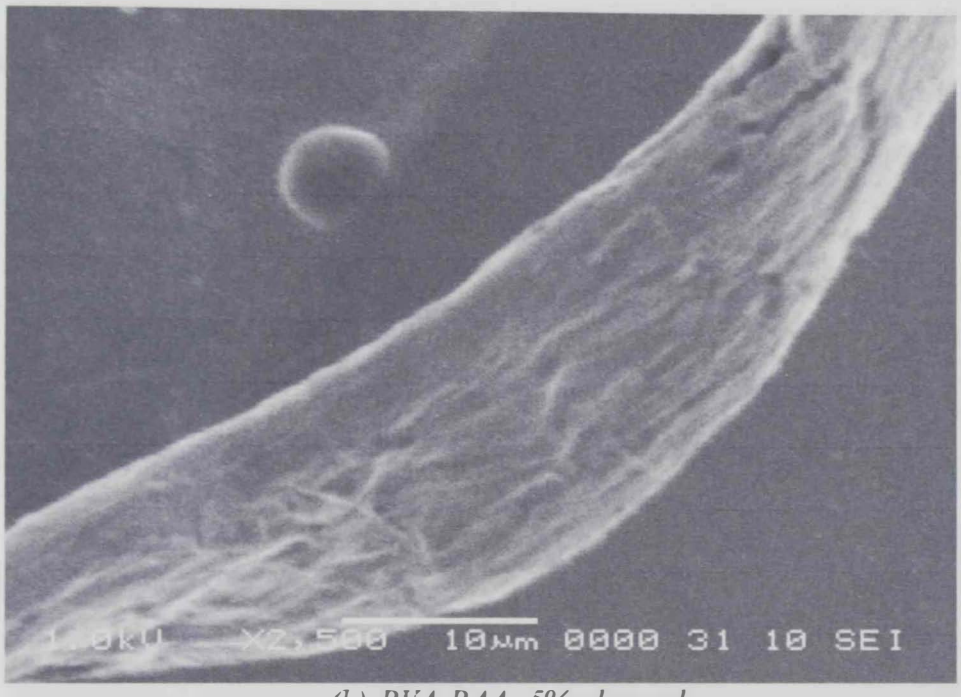

(b) PVA-PAA- 5% glycerol

Figure 3. 41 SEM micrographs for the PVA-PAA with Glycerol doped polymer membrane films, (a) SEM capture of PVA-PAA-1% Glycerol (b) SEM capture of PVA-PAA-5% Glycerol

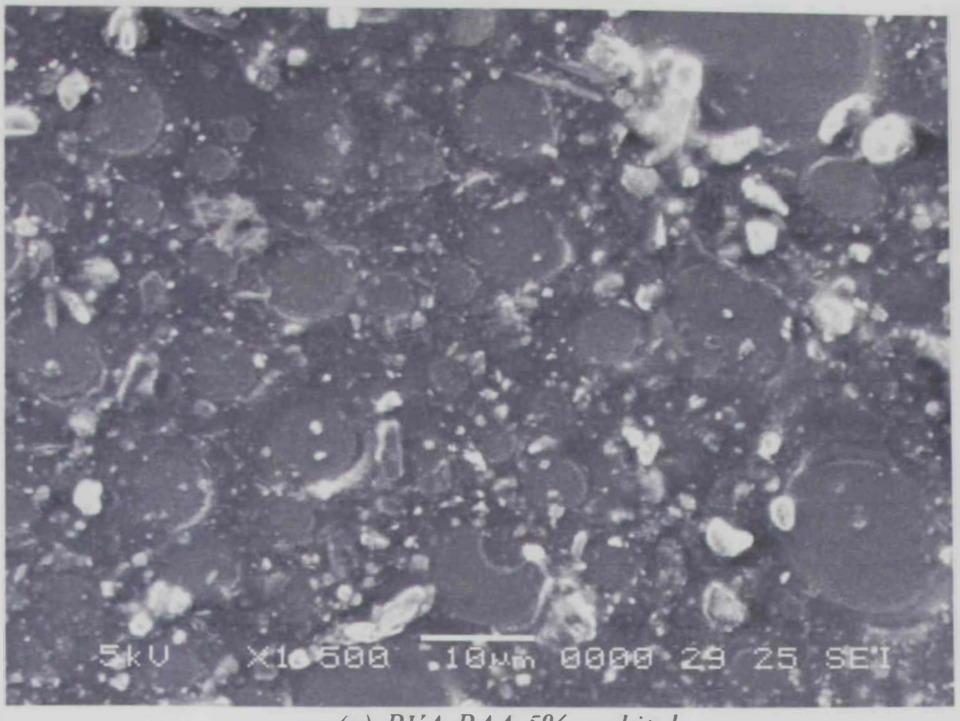

(a) PVA-PAA-5% sorbitol

Figure 3. 42 SEM micrographs for the PVA-PAA with Sorbitol doped polymer membrane films, (a) SEM capture of PVA-PAA-5% Sorbitol

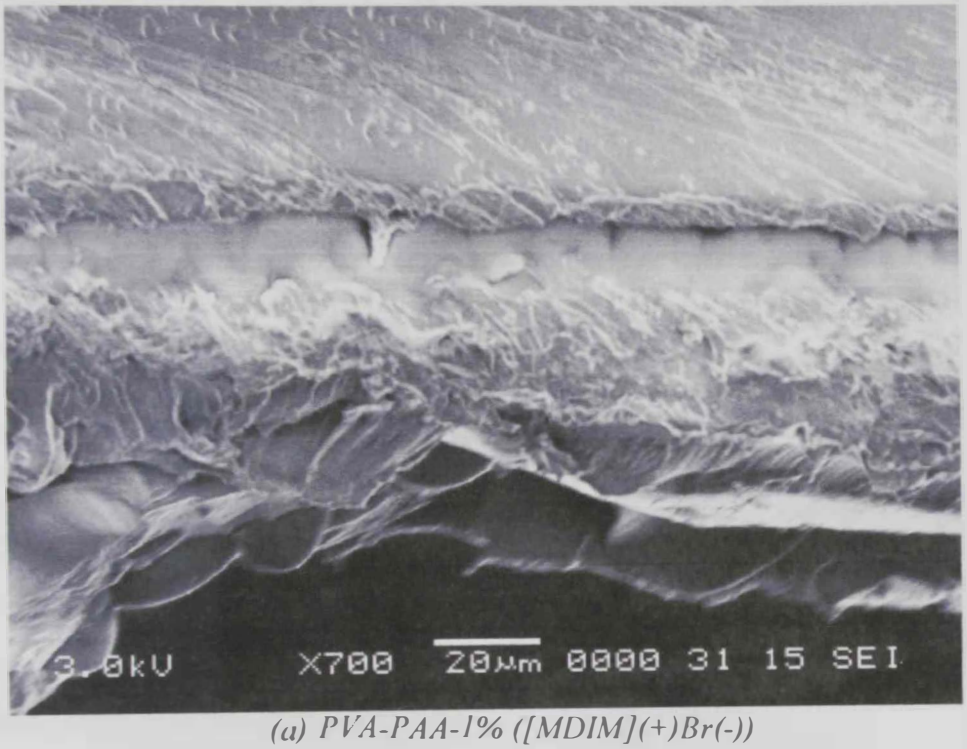

(a) PVA-PAA-1% ([MDIM](+)Br(-))

(b) PVA-PAA-2% ([MDIM](+)Br(-))

(c) PVA-PAA-3% ([MDIM](+)Br(-))

Figure 3. 43 SEM micrographs for the PVA-PAA with(|MDIM|(+)Br(-)) doped polymer membrane films, (a) SEM capture of PVA-PAA-1% (|MDIM|(+)Br(-)), (b) SEM capture of PVA-PAA-2% (|MDIM|(+)Br(-)), (c) SEM capture of PVA-PAA-3% (|MDIM|(+)Br(-)).

The plasticizers when induced into the polymer blends displayed a layer-by-layer deposition that allows the electron movement that interacts with the polymer bonds to create a semiconducting polymer.

Summary of Findings

- TGA, DSC, Nanoindentation, FTIR, and Impedance testing were conducted on all polymeric blended ionic liquid samples.
- TGA and DSC determined the thermal properties of the samples; the TGA results show a three-step degradation process. Dramatic weight loss is also observed. In short, as the percentage of ionic liquids increased, the decomposition decreased respectively.
- DSC results also show a three-step degradation process; the properties show the glass transition temperature (T_g), melting temperature (T_m), and decomposition point (T_d). As the plasticizer ratios is increased the three peaks show a rapid decline in the temperature.
- The thermal properties showed that these polymer blends are relatively stable at very high temperature range which is suitable for fabricating a data-storage memory device.
- FT-IR spectroscopy confirmed the reduction in hydrogen bonding between combined polymer chains in favor of formation new bonding between the plasticizers and the polymer blend chains.
- Nanoindentation was done on the samples to determine their elastic modulus and hardness. It is extremely important to know the ductility and hardness of these polymer

blends. It is observed that when adding the plasticizers, both hardness and elastic modulus decrease rapidly which is caused by reduced the interactions among the macromolecules.

- It is observed that the peaks introduced in the FTIR figures show the same characteristic of both the polymer membranes and that when blended with the ionic liquids. It was observed that the band intensity increases and bandwidth narrowing as the percentage of dopant increased.

- The main reason for determining the molecular structure of the polymer blends using FTIR spectroscopy is to relate the structural changes due to addition of the ionic liquids in order to enhance the electrical properties of the blends due to the cations/anions coupling mechanism which leads to a continuous loss of the hydrogen O-H and the formation of the complications and chain alignment.

- *ac* impedance testing was conducted on all polymeric membranes to determine the electrical properties of the sample membranes. It was observed in most of the polymer membranes two semi-circle arcs which indicate that the sample can be represented by two pairs of parallel RC circuits connected into series. The semi-circles were used to determine the dc resistivity of each semi-circle as a function of temperature.

- It is also noticed, as the composition ratios increase, the resistivity decrease which implies that the conductivity increases. This was noticed in the activation energy, relaxation time curves and tables.

- SEM showed homogeneous mixture of the polymer membrane embedded ionic liquids. It also shows the layer deposition of the polymer blends, which allows the electrons to move freely.

- It has been shown that two out of the three ionic liquids (glycerol and sorbitol) have higher conductivity values and therefore will be used in the fabrication of the organic memory devices.

- The novel conductive polymer presented in this thesis formed a solution to overcome challenges associated with a total organic memory device. The doped polymers were substituted for the silicon base semiconductor in a conventional memory device, however with enhanced performance compared to the silicon based device.

- All the properties tests verify that these polymer blended ionic liquids are appropriate for fabricating a suitable application, such as the one carried out in this project- an organic data storage memory device.

Chapter 4:

APPLICATION: Organic Memory Device

It has been known that research on organic semiconductors and conjugated polymers have attracted widespread interest due to their applications in optical and electronic devices [79]. It has been studied that the conjugated organics can have further applications in switching [80-82] and memory devices [83, 84]. During the past decade, an associated memory effect has been observed in devices based on organic molecules. It was observed that two conducting states at the same applied voltage when a thin metal layer was embedded in the organics [82]. These devices offered possibilities of rewritable memory applications.

Due to their origin and characteristics, two organic plasticizers, namely glycerol and sorbitol, were focused on to be used in fabricating a data-memory device. Hysteresis-type behavior has been observed in the current-voltage characteristics. The work was extended to fabricate a data-storage device based on organic materials. The use of the plasticizers to fabricate such devices is itself of interest. The material's capability to retain the data, and the space charges relaxation dynamics have been studied as well. The conventional spin coating, vacuum-evaporating films and layer-by-layer sequential adsorption films have been used in this work.

A memory device generally consists of sandwiched conductive terminals, semiconducting material and storage element (usually nanoparticles). In here we have employed the unique conductive characteristics of our polymeric blends as semiconductors. We also synthesized different nanoparticles for use as storage elements. The following sections outline the materials and process for fabricating organic memory devices.

4.1. Nanoparticles

The ionic liquids introduced in the polymer film were used as a semiconductor in the device. The storage elements used are single walled carbon nano-tubes (CNT), zinc oxide (ZnO), and gold (Au) nanoparticles. The organic semiconductors were used to form the s-shape of the hysteresis loop, without it; it wouldn't be possible to have achieved the hysteresis loops that are shown below. The organic semiconductors are a replacement of the conventional silicon dioxide used in many memory devices. These single-wall CNTs were obtained from Carbon Nanotechnologies Inc., and are less than 100nm in length and are known to be conductive. ZnO and Au nanoparticles were prepared in house at mechanical engineering department at United Arab Emirates University.

4.1.1. Zinc Oxide Nanoparticles

ZnO where the particle size varying from 50-70nm, was prepared by chemical co-precipitation technique. 1.314 g zinc acetate and 0.48 g NaOH were dissolved in 330 ml ethanol and refluxed at 60°C for 1 h. The acetate group reacted with base, converting zinc acetate into zinc oxide. After reaction, the zinc oxide ethanol dispersion was mixed with DI-water for purification. ZnO particles were then separated from the dispersion supernatant by centrifugation at 7000 rpm for 5 min repeatedly. Finally, the ZnO were dispersed in ethanol and sonicated for 30 seconds to obtain the ZnO-Ethanol dispersion. This procedure was modified from the research article [85]. Zinc oxide (ZnO) was used to send and receive electrical conduction past one electrode from the other.

4.1.2. Carbon Nanotubes

There have been some speculations of carbon nano-tubes to have exhibited remarkably outstanding properties, in all mechanical, thermal and electrical. The stiffness of the Young's modulus was reported to be 1000GPa, which implies it to be five times higher/tougher than that of steel [86]. They have a constant resistivity and high current density. The resistivity has been found to be in the order 10^{-4} $\Omega \cdot$ cm [87]. Such an electrical conductivity suggests that nano-tubes are much better conductors than copper [88]. The chirality or "twist" of the tube can determine their conductivity. Nanotubes are also known to be flexible, extremely light weight, chemically inert and thermally stabile, which make CNTs a suitable material in many potential applications including aerospace, conductive adhesives, energy storage, sensing devices and field-effect transistors. SWNTs have been successfully incorporated into multilayer assemblies to produce conductive thin films [89]. All these reasons clearly justify the use of CNTs as a storage element in the memory devices fabricated and carried out. The layer-by-layer (LbL) technique was chosen to carry out the carbon nanotubes deposition. Commercial SWCNTs (purchased from Carbon Nanotechnologies Inc.) were purified until the impurity content was below 5 wt. %. The purchased SWCNTs have 2/3 semiconducting and 1/3 metallic CNTs according to the manufacturer data. These were combined for the fabrication of the device shown below.

4.1.3. Gold Nanoparticles

Gold (Au) extracted from a 99.999% purity gold specimen was placed as a storage element during the device fabrication. The glass substrate was placed inside the Mantis Deposition

apparatus sealed vacuum deposition chamber. The chamber was then set to a partial vacuum. Once $1x10^{-1}$ Pa was reached, liquid nitrogen was poured into the vessel to activate the high vacuum pump. 10 - 20 minutes were needed until the pressure reached approximately $4x10^{-6}$ Pa. The gold specimen was then placed in place for the thermal evaporation to occur. The rate of evaporation was monitored until the thickness reached 10nm. The system was then turned off and allowed to cool before air was admitted to open the chamber door. The gold layer covered the whole substrate except for a small 2mm square portion to allow the bottom electrode in order to test the device. This procedure is not similar to that of the *Al* dispersion of the bottom and top electrode gates.

4.2. Device Fabrication Procedure

Glass substrate approximately $1cm^2$ in area was first cleaned in a bath of acetone to remove any dust particles that might interfere with the electric current flowing through the device. The substrate was than rinsed in ethanol and finally in de-ionized water. In all steps of the cleaning process, nitrogen gas was diffused on the samples to ensure that there are no impurities on the surface. UV light was used under the vacuum hood to verify this process.

Once the cleaning procedure was completed, a bottom layer of aluminum was placed on top of the substrates as the first electrode contact gate. The glass substrate was placed in the Torr International Inc. apparatus placed onto a holder and the deposition chamber was vacuum sealed. The chamber was then set to a partial vacuum. Nearly 10 – 20 minutes were needed to create a sufficient vacuum, at approximately $4x10^{-6}$ Pa. The aluminum was evaporated by increasing the electrical power through the filament until it had started to glow (bright red color). At that

moment, the shutter was opened to allow the metal vapor to condensate onto the surface of the samples (substrates). The rate of evaporation was monitored and set around 1nm/s until the thickness reached 100nm. The shutter was then closed, the power turned down and the system let to cool before air was admitted to open the chamber door. The aluminum layer covered the whole back/bottom surface of the device. Aluminum top contacts, or gate contacts, were evaporated following the deposition of the organic insulator and semiconductors. The procedure was similar to the first contact evaporation, but in this case, for the samples, a mechanical shadow mask was placed on top, consisting of small circular holes where the contacts would be formed. The thickness of the aluminum top contacts was also approximately 100 nm.

In between the two metal electrodes, a thin layer of polymethyl methacrylate (PMMA) was used as an insulating material and is formed onto the sample by spin coating. This thin film seals in the different charge-storage elements deposited onto the substrates as well as providing a smooth finish before aluminum contacts are evaporated. The PMMA solution is prepared by diluting 8mg of PMMA powder (molecular weight 97,000) for each 1mL of chloroform and left overnight under stirring to ensure a perfect dissolution.

The samples were placed on the spin coater and maintained by a vacuum chuck dispensing a couple drops of PMMA solution onto each of the sample substrates covered with the bottom *Al* layer. To achieve a uniform coverage, the spin coating is initially run at 500 rpm for 10 seconds then 6000 rpm for 50 seconds. The thickness of the layer produced was found to be 85 nm on average. After the PMMA was spin coated on to the substrate and annealed on top of a hot plate for 10-20 minutes, the substrate samples were submerged in a Petri dish filled with

Poly(ethyleneimine) (PEI) with a molecular weight of approximately (M_w=25,000) and CNT. It was immersed in for 15 minutes in each to form a seed layers to facilitate the adhesion of SWCNTs onto the ionic liquids. This procedure was repeated for about 3 times in each.

The SWCNTs were deposited by the layer-by-layer deposition, a technique based on a charge reversal to build up bi-layer assemblies of oppositely charged (functionalized) molecules. The description of this technique is reported elsewhere [90, 91].

For the ZnO disposition procedure, the substrate after the bottom layer of aluminum and PMMA layer have been placed, ZnO was spin coated on the sample with similar procedure to that of the PMMA. It was left to anneal for 10 minutes on top of a hot plate.

After the storage elements were placed, the semiconductors (2% of either glycerol or sorbitol blended with the polymer membranes) were then spin coated, adding another layer on top of the sample (see Schemes below). Causing a layer-by-layer distribution of the sample substrates.

Finally the device sample is left to anneal at 120°C for 20 minutes, before the aluminum top gates are deposited. The top aluminum electrodes were used to supply and allow the current flow through the device. A mechanical mask of area 6mm^2 which defined each device was placed on top of the film during aluminum deposition.

4.3. Schematics and Testing

The Schemes below illustrate the structure of the device in sequence of film coating with sorbitol and glycerol.

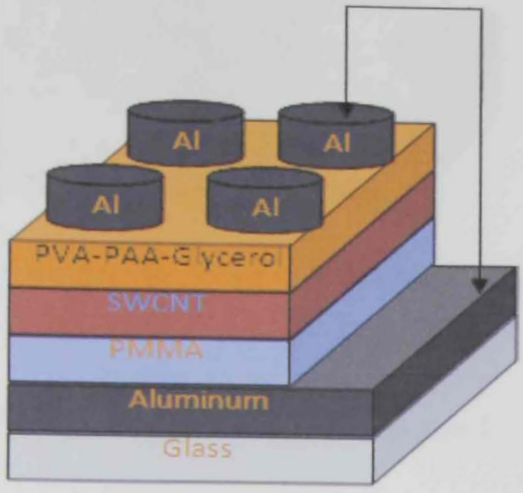

Scheme 4. 1 schematic of a device with CNT and PVA-PAA-2% Glycerol as memory storage elements and semiconductor.

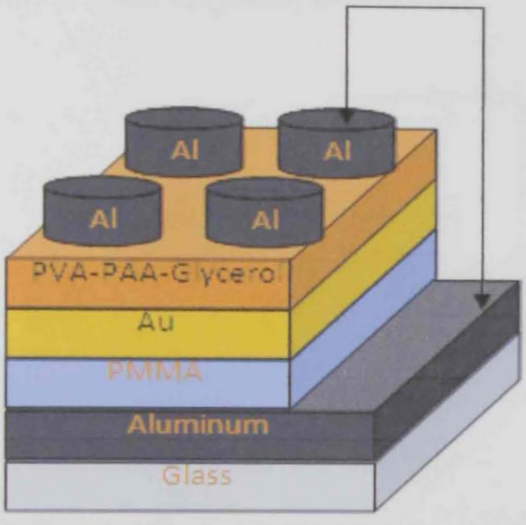

Scheme 4. 2 schematic of a device with Gold (Au) and PVA-PAA-2% Glycerol as memory storage elements and semiconductor.

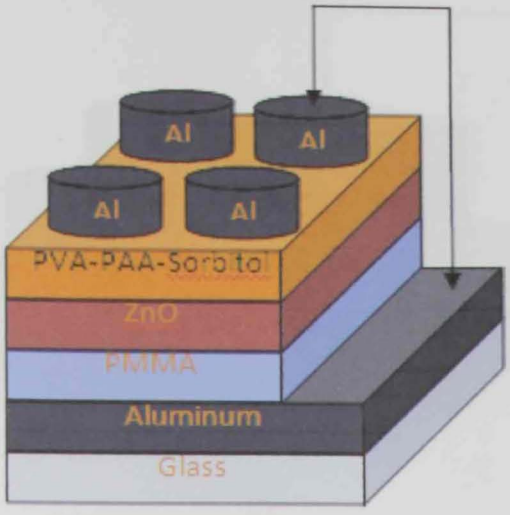

Scheme 4. 3 schematic of a device with ZnO and PVA-PAA-2% Sorbitol as memory storage elements and semiconductor.

A reference device was first fabricated to ensure that any hysteresis loop found will be attributed to the presence of the plasticizers in the bi-layers. This device consists of a glass substrate with *PMMA* spin coating and an aluminum layer on top and bottom to allow the current to pass through. Scheme 4.4 shows the structure of the reference device.

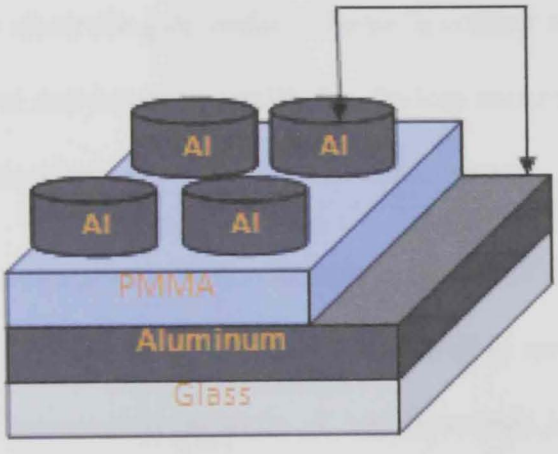

(a)

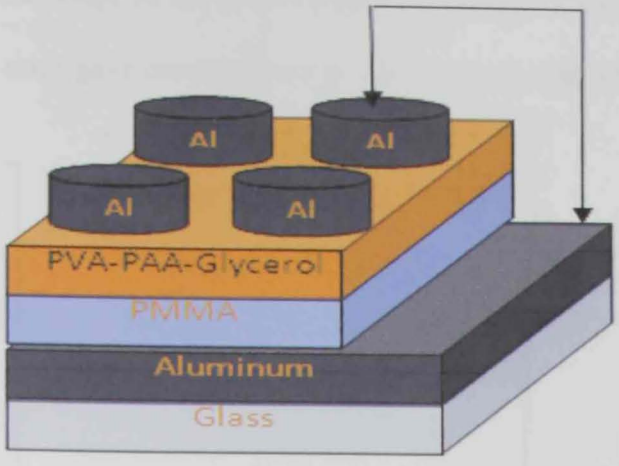

(b)

Scheme 4. 4 schematic of (a) pure reference device and (b) reference device with polymer membranes doped with glycerol.

After the final aluminum evaporation process was done, the devices were ready to be tested. The test was carryout using Keithley 590 CV analyzer instrument and Keithley 590 CV software to extract the data. For the testing, a small portion of the polymer on the bottom *Al* electrode on the glass substrate was washed off using acetone to show the bottom layer of aluminum in order to allow access for the bottom electrode gate probe to come in contact with the aluminum layer to ensure electrical contact, but not interfering with the devices surroundings. The devices were subject to a range of tests using impedance measurement equipment.

Double sweep capacitance-voltage tests were carried out to identify memory properties of the organic semiconductor devices. This was done to show whether or not the devices were working properly by observing the presence or absence of any hysteresis loop and the width of the window gap as a function of the sweep range. A higher sweep rate will produce a larger hysteresis window because any stored charge has not had time to leak away, apart from allowing

a quicker test. However, the shape of the curves obtained are significantly less detailed and more irregular whereas slower rates gave curves closer to ideal, for more accurate results.

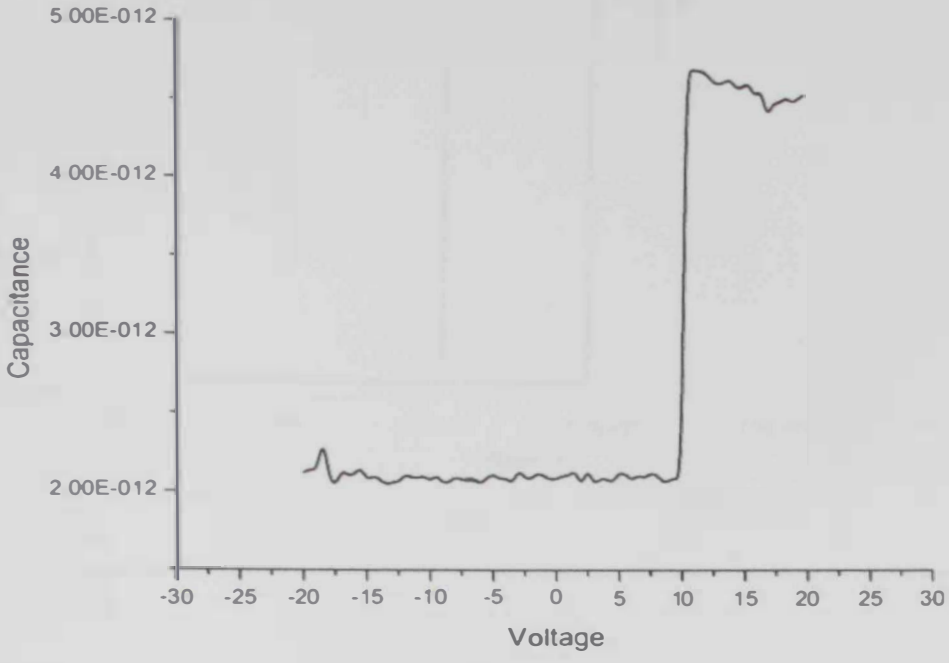

(a)

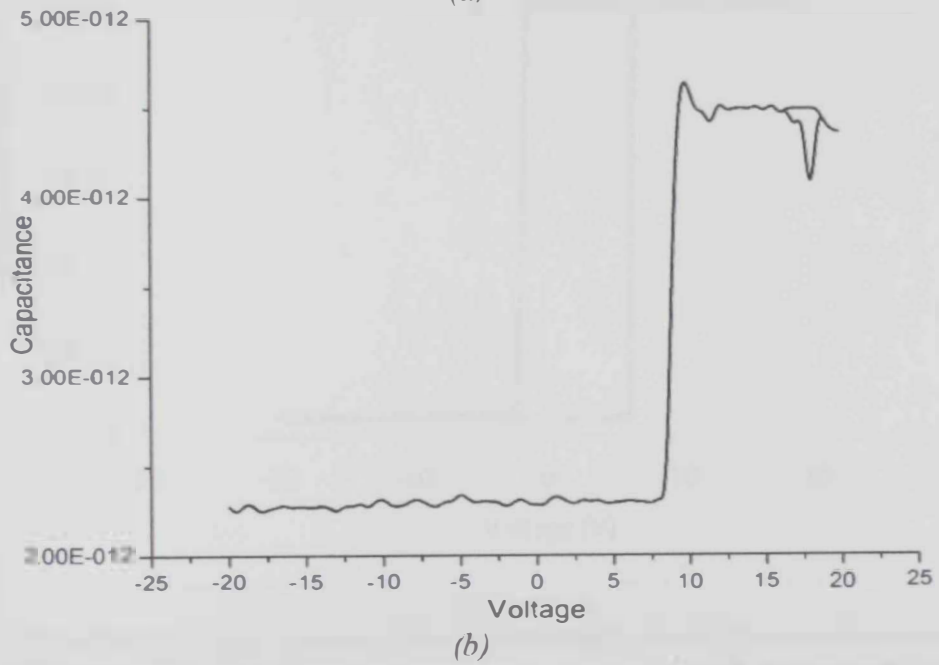

(b)

Figure 44. 1 C-V Characteristic of the latter reference device of scheme 4(with the glycerol). No hysteresis loop shown.

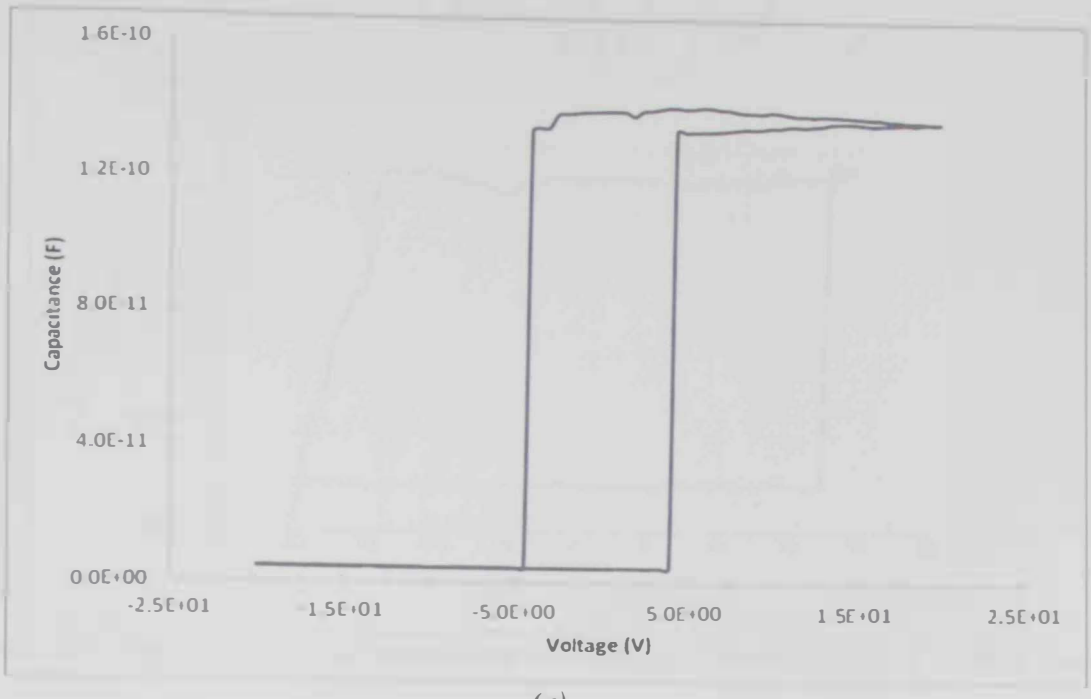

(a)

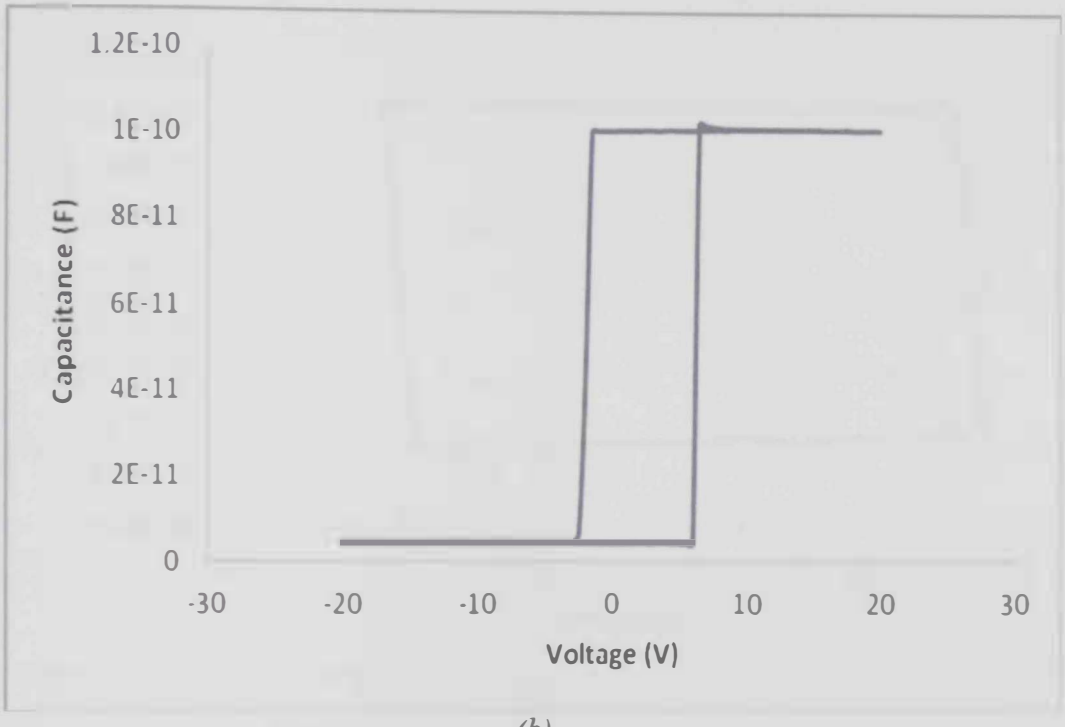

(b)

Figure 45 C-V Characteristic of the Scheme 3 (ZnO is embedded). (a) and (b) are reproducible plots, CV measurements from positive to negative voltage and vise versa were obtained. A hysteresis loop of ± 5V is observed in both.

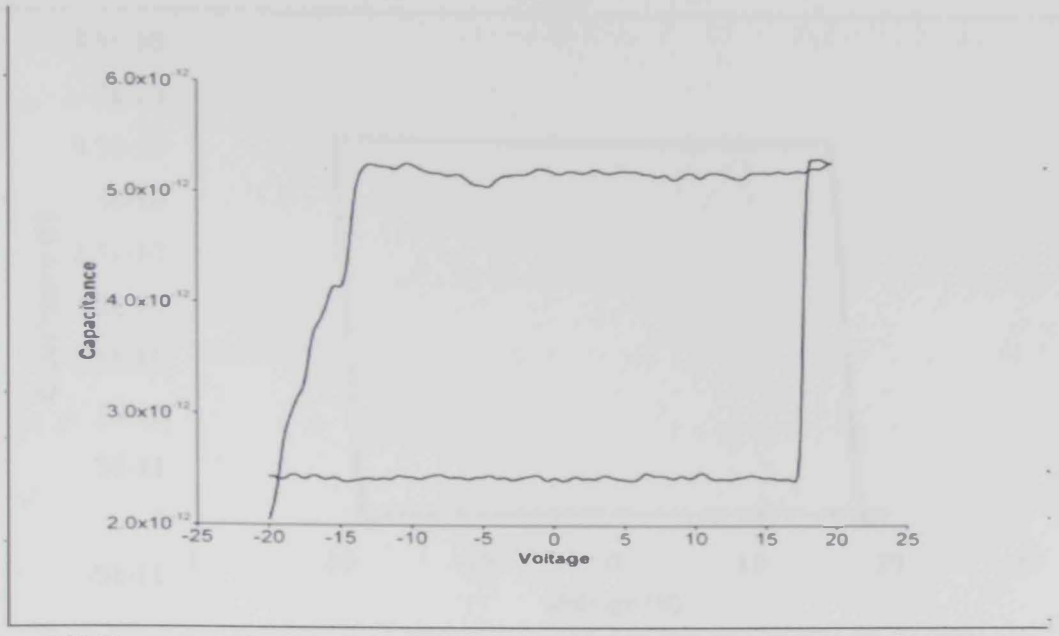

Figure 46 C-V Characteristic of the Scheme 2 (Au is embedded). A hysteresis loop of ± 18V is observed.

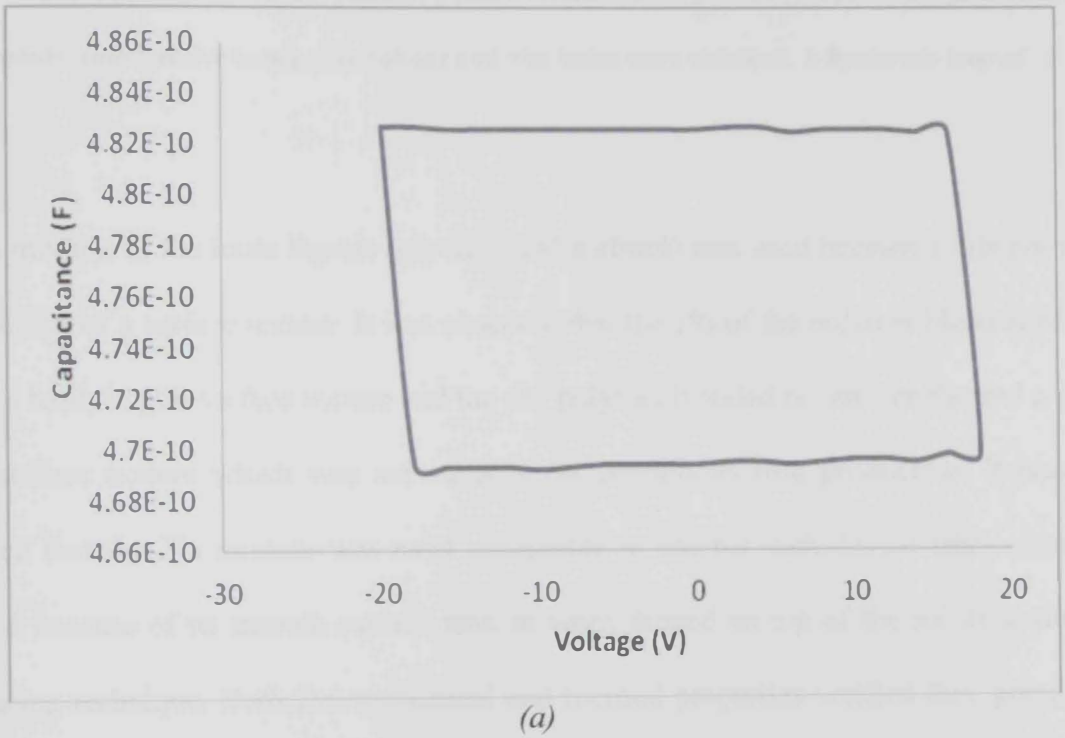

(a)

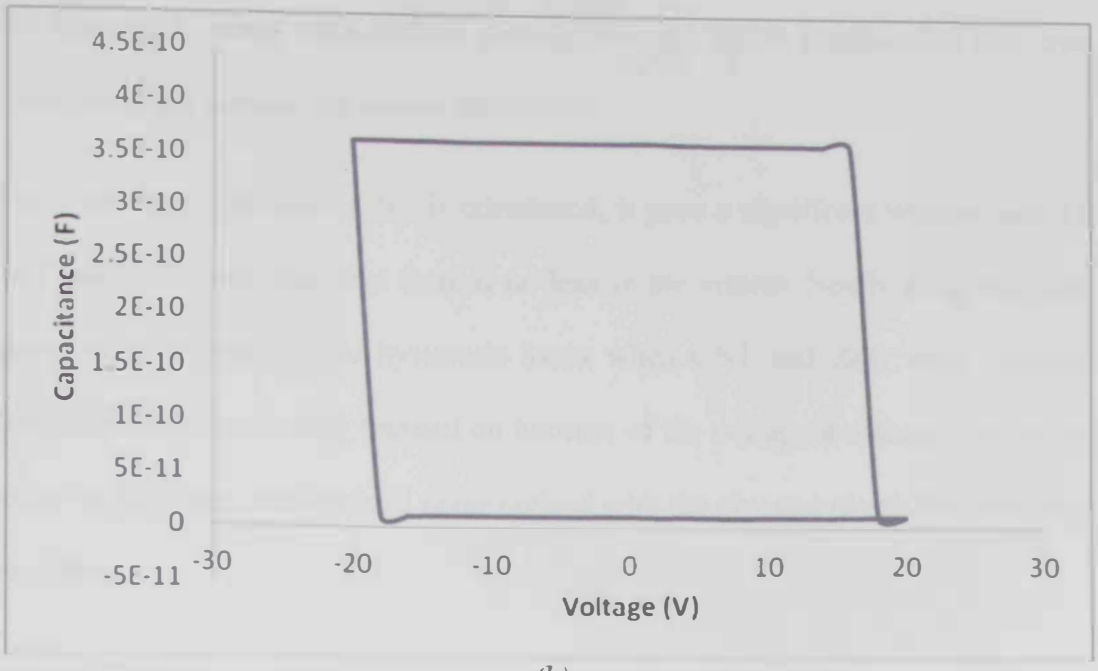

(b)

Figure 47 C-V Characteristic of the Scheme 1 (CNT is embedded). (a) and (b) are both reproducible. CV measurements from positive to negative voltage and vise versa were obtained. A hysteresis loop of ± 20V is observed.

The 2% mixture of the ionic liquids (glycerol and sorbitol) was used because of its not too hard nor a too soft of a surface texture. It was observed that the 1% of the polymer blended plasticizer showed a hard, fragile surface texture and the 5% polymer blended plasticizer showed a very soft elastic surface texture which was not suitable for continuous film production. It was clearly evidenced that the 2% mixture was most reasonable to use for such device fabrication. It was also used because of its smooth surface tension when dipped on top of the substrate during the spin coating technique. Both the mechanical and thermal properties verified this. going beyond the 5% mixture is not sufficient in the fact that the texture of the polymer blends become more

liquefied than rigid, along with that its viscosity lowers which implied that this type of the surface texture is not suitable for device fabrication.

It is clearly observed that when CNT is introduced, it gave a significant window gate of ± 20V (refer to Figure 47), indicating that there is no leak in the system. Nearly all of the devices that were tested gave a reproducible hysteresis loops when CNT and ZnO were embedded. The plasticizer, glycerol, was mainly focused on because of the s-shape it makes. Another important issue to add is that there was minimal noise noticed with the glycerol plasticizer compared to that of the sorbitol.

Summary of Finding:

- PVA-PAA-2% Glycerol blended with CNT showed a wide window gap that indicated no leak occurred during the C-V measurements due it having all ± 20V sweep covered.
- Both ZnO and Au showed smaller window gap of ± 5V sweep, regardless of the semiconductor used.
- Sorbitol when compared with Glycerol displayed more noise.
- It is also shown that the reference samples show that the plasticizers only act as a semiconductor.
- Regardless of direction of voltage sweep, hysteresis loops were obtained.
- In most of the tests, reproducible hysteresis loops were obtained over a period of time.

Chapter 5:

CONCLUSION AND FUTURE WORK

5.1. Conclusion

Solid polymer membranes from poly (vinyl alcohol) PVA and Poly (acrylamide-co-acrylic acid) PAA with varying doping ratios of glycerol, sorbitol, and 1-methyl-3-n-decyl-Imidazolium Bromide were prepared using the solution casting method. It was observed that the residual ionic liquids (glycerol, sorbitol and imidazolium bromide) in the blends played a role as plasticizers, which reduced the interactions among the macromolecules. The chemical compositions of the blends were confirmed using Fourier transform infrared spectroscopy (FTIR) spectral measurements. DSC and TGA measurements states that the membranes show single (T_g) for all the compositions and are relatively stable in the temperature range of 25°C-300°C. As the ionic liquids percentage increased, the melting temperature of the polymer blend decreased along with broadens of endothermic peaks, which indicated that, the ordered association of the polymer blends (PVA-PAA) molecules decreased.

Nanoindentation was performed on the doped polymer membranes films which illustrated that the hardness and the elastic modulus were both decreased when increases doping concentration of the ionic liquids. It is observed that as you increase the ionic liquid content, the texture of the polymer flexions.

ac impedance spectroscopy was used as a powerful tool to investigate the electrical properties of the films. The impedance results also showed that doping the polymer blend films with the ionic liquids decreases their film resistivity due to the addition of the ions; as you increase the doping concentration, the resistivity decreases considerably. The conductivity of the membranes was controlled by controlling the doping level of the ionic liquids. It was found the resistivity

decreases with increasing temperature and plasticizer content. This is due to the increase in the mobility and assistance of polymer segmental motion which would probably be the net effect of the interplay of decreasing crystalline nature and viscosity on the account of higher plasticizer ratio.

The dependence of the resistivity on temperature enabled the calculation of the activation energy. It was demonstrated that the film activation energy can be adjusted by adding or lowering the doping concentration of the ionic liquids in the polymer matrix. Those films could be suitable for the fabrication of organic device in medical applications (such as memory devices or organic sensors) since their resistivity and activation energy could be engineered by proper doping concentration.

This project was taken a step further to fabricate the memory device. It was observed that when the polymer blend with glycerol was introduced with the addition of adding of CNT as the storage element, showed a window gate of ± 20V hysteresis loop when a voltage source of ± 20V was applied.

5.2. Future Work

It was observed that with these ionic liquids and storage elements, large hysteresis loops were obtained. However, in most cases, the storage elements can be very expensive along with that the ionic liquids. I recommend that for future work, that focus should be on obtaining inexpensive materials, such as, to work with conductive polymers without the use of ILs.

References

1- A.J. Campbell. D.D.C. Bradley, E. Werner, W. Brutting, Organic Electronics 1 (2000) 21.

2- H.S. Majumdar, A. Bandyopadhyay, A. Bolognesi, A.J. Pal, J. Appl. Phys. 91 (2001) 2433; Erratum, J. Appl. Phys. 91 (2002) 5508.

3- L.P. Ma, J. Liu, Y. Yang, Appl. Phys. Lett 80 (2002) 2997.

4- G.M. Wu, S.J. Lin, C.C. Yang, Journal of membrane science 257 (2006) 127-133.

5- D.R. Paul, S. Newman, Polymer Blends, Academic, New York, 1978.

6- O. Olabisi, L.M. Robinson, M.T. Shaw, Polymer-Polymer Miscibility, Academic, New York, 1979.

7- Y. Nishio, R.St.J. Manley, Polymer 28 (1987) 1385.

8- Y. Nishio, R.St.J. Manley, Macromolecules 21 (1988) 270.

9- S.N. Cassu, M.I. Felisberti, Polymer 38 (1997) 3907.

10- T. Tanaka, S. Ohnishi, K. Yamura, Polym. Int. 48 (1999) 811.

11- Q. Wang, L. He, Polymer 38 (1997) 3931.

12- T.Kondo, C. Sawatari, R.St.J. Manley, D.G. Gray, Macromolecules 27 (1994) 210.

13- C. Sawatari, T. Kondo, Macromolecules 32 (1999) 1949.

14- J.H. Hong, J.Y. Kim, Y.M. Lee, K.Y. Kim, J. Appl. Polym. Sci. 45 (1992) 1711.

15- K. Lio, N. Minoura, M. Magura, Polymer 36 (1995) 2579.

16- K. Miura, M. Kimura, H. Suzuki, Y. Miyashita, Y. Nishio, Carbohydr. Polym. 39 (1999) 139.

17- O.A.C. Monteir Jr., C. airoldi, Int. J. Biol. Macromol. 26 (1999) 119

18- E.Quartarone, P.Mustarelli, Solid state ionics 110 (1998).

19- D.W. Kim, J.R.Park, H.W. Rhee, Solid State Ionics 83 (1996) 49.

20- W.Wieckzorek, J.R.stevens, J.Phys.Chem., B 101 (1997) 1529.

21- J.Przyluski, W.Wieczorek, Solid state ionics 36 (1989) 165.

22- J.Y.Cherng, M.Z.A.Munshi, B.B.Owens, W.H.Smyrl, Solid State Ionics 28 (1988) 857.

23- H.S. Mansur, C.M. Sadahira, A.M. Souza, A.A.P. Mansur, Mater. Sci Eng. C: Biomim. Mater, Sens, Syst. 28 (2008) 539.

24- M. Mohsin, A. Hossin, Y. Haik, Mat Sci and Eng., A 528 (3) (2011) 925-930.

25- K. Pal, K. Banthia, D.H. Majumdar, Journal of Biomaterials Appls 2006, 21, 75.

26- S.H. Imam, P. Cinelli, S.H. Gordon, E. Chiellini, Journal of Polymers and the Environment 2005, 13,47.

27- W.B. Lui, K. Peng, Journal of Food Engineering 2005, 71,73.

28- E. Chiellini, P. Cinelli, S. H. Imam, L. Mao, Biomacromolecules 2001, 2 1029.

29- R. Jayasekara, I. Harding, I, Bowater, G.B.Y. Christie, G.T. Lonergan, Polymer Testing 2004, 23, 17.

30- Z. Guohua, L. Ya, F. Cuilian, Z. Min, Z. Caiqiong, C. Zongdao, Polymer Degradation and Stability 2006, 91, 703.

31- S.R.Dicharry, M.S. Prasad, K.U. Sankar, Food Hydrocolloids 2003, 17, 245.

32- R.N. Dicharry, P. Ye, G. Saha, E. Waxman, A.D. Asandei, R.S. Parnas, Biomacromolecules 2006, 7 (10), 2837.

33- P. Alexy, D. Bakos, S. Hanzelova, L. Kukolikova, J. Kupec, K. Charvatova, E. Chiellini, P. Cinelli, Polymer Testing 2003, 22, 801.

34- B. Sarti, M. Scandola, Biomaterials 1995, 16, 785.

35- E. Chiellini, P. Cinelli, E.G. Fernandes, E.S. Kenawy, A. LAzzeri, Biomacromolecules 2001, 2, 806.

36- E. Chiellin, P. Xinelli, A. Corti, E.R. Kenawy, Polymer Degradation and Stability 2001, 73, 549.

37- P.V. Bergo, P.J.A. Sobral, Food Hydrocolloids 2007, 21, 1285.

38- http://pslc.ws/macrog/acrylate.htm

39- E. Grzadka, S. Chibowski, Physicochemical Problems of Mineral Processing, 43 (2009), 31-42.

40- M. Tehrani, M. rabiee, M. Parviz, M.R. Tahiri, Z. Fahini, Macromol. Syump. 2010, 296, 457-465.

41- D.E. Fenton, J.M. Parker, P.V. Wright, Complexes of Alkali Mrtal Ions with Poly(ethylene Oxide), Polymer 14 (1973) 589.

42- P.V Wright, Electrical Conductivity in Ionic Complexes of Poly (ethylene Oxide), Brit. Polym. J. 7 (1975) 319.

43- B. Singh, S.S. Sekhon, Chem. Phys. Lett. 414 (2005) 34.

44- J.G. Huddleston, H.D. Willauer, R.P. Swatloski, A.E. Visser, R.D. Rogers, Chem. Commun. 998 (1998) 1765.

45- N. Matsumi, K. Sugai, M. Miyake, H. Ohno, Macromolecules 39 (2006) 6924.

46- S.S. Sekhon, B.S. Lalia, C.S. Kim,W.Y. Lee, Macromol. Symp. 249 (2007) 216.

47- H. Jiang, S.B. Fang, Polym. Adv. Technol. 17 (2006) 494.

48- W. Ogihara, J.Z. Sun, M. Forsyth, D.R. MacFarlane, M. Yoshizawa, H. Ohno, Electrochim. Acta 49 (2004) 1797.

49- K.S. Kim, S.Y. Park, S. Choi, H. Lee, J. Power Sources 155 (2006) 385.

50- J.H. Shin, W.A. Henderson, C. Tizzani, S. Passerini, S.S. Jeong, K.W. Kim, J. Electrochem. Soc. 153 (2006) A1649.

51- H. Cheng, C.B. Zhu, B. Huang, M. Lu, Y. Yang, Electrochim. Acta 52 (2007) 5789.

52- M. Aydinli, M. Tutas, Food Sci. Technol. 33 (1) (2000) 63–67.

53- P.L.M. Barreto, A.T.N. Pires, V. Soldi, Polym. Degrad. Stab. 79 (1) (2003) 147–152.

54- L.H. Cheng, A.A. Karim, C.C. Seow, J. Food Sci. E: Food Eng. Phys. Prop. 71 (2) (2006) 62–67.

55- http://www.covalentassociates.com/Introduction%20to%20Ionic%20Liquids.pdf

56- Teo, G; Suzuki, Y; Uratsu, SL; Lampinen, B; Ormonde, N; Hu, WK; Dejong, TM; Dandekar, AM (2006). "Silencing leaf sorbitol synthesis alters long-distance partitioning and apple fruit quality", Proceedings of the National Academy of Sciences of the United States of America 103 (49): 18842–7.

57. Sobral, P. J. A.; Menegalli, F. C.; Hubinger, M. D.; Roques, M.A. Food Hydrocolloids 2001, 15, 423.

58. Oliver, W. C.; Pharr, G. M. J Mater Res 1992, 7, 1564.

59. Beake, B. D.; Chen, S.; Hull, J. B.; Gao, F. J Nanosci Nanotech 2002, 2, 73.

60. Fang, T. H.; Chang, W. J. Microelectron Eng 2003, 65, 231.

61. Sneddon, I. N. Int J Eng Sci 1965, 3, 47.

62. Cuq, B.; Aymard, C.; Cuq, J. L.; Guilbert, S. J Food Sci 1995, 60, 1369.

63. Simmons, G.; Wang, H. A Handbook; MIT Press: Cambridge,MA, 1971.

64. Cuq, B.; Gontard, N.; Guilbert, S. Polymer 1997, 38, 2399.

65. Pouplin, M.; Redl, A.; Gontard, N. J Agric Food Chem 1999, 47, 538.

66. Sobral, P. J. A.; Menegalli, F. C.; Hubinger, M. D.; Roques, M.A. Food Hydrocolloids 2001, 15, 423.

67. N. Barhani, F. Bertoni, G. Ciardelli, C. Cristallini, D. Silvestri, M.L. Coluccio, P. Giusti, European Polymer Journal 41 (2005) 3004-3010.

68. J.F. Fauvarque, E. Salmon, N. Cassal, Electrochemcial properties of an alkaline slide polymer electrolyte based on P(ECH-co-EO), electochem. Acta 45 (2000) 1527.

69. Yang, C. C. J. Membr Sci, 2007, 288, 51.

70. J.S. Park, J.W. Park, E. Ruckenstein, Polymer 42(9) (2001) 4271-4280.

71. X.Ma, J. Yu, N. Wang, macromol. Mater, Eng. 292 (2007) 723-728.

72. O.K. Varghese, L.K. Malhotra, J. Mater. Eng. 292 (2007) 723-728.

73. T. Tonosaki, T. Oho, K. Isomura, K. Ogura, J. Electoanal, Chem, 520 (2002). 89.

74. M.Venkateswarlu, K.Narasimha Reddy, B. Rambabu, N. Saryanarayana, Solid State Ionics 127 (2000) 177-184.

75. E.Barsoukov, J. Ross McDonald, Hobken, N.J.: Wiley-Interscience, c-2005

76. M.E. Fernandez, J.E. Diosa, R.A. Vargas, Microelectronics J. 39 (2008) 1344.

77. M. Mohsin, A. Hossin, Y. Haik, J. Poym. Sci. 122 (5) (2011) 3102-3109.

78. J.S. Choi, W. H. Park. Polym test 2004, 23, 455.

79. A.J. Campbell, D.D.C Bradley, E. Werner, W. Brutting, Organic electronics 1 (2000) 21.

80. D.M. Taylor, C.A. Mills, J. Appl. Phys. 90 (2001) 306.

81. A. Bandyopadhyay, A.J. Pal, J. Phys. Chem. B 107 (2003) 2531.

82. L. Ma, J. Liu, S. Pyo, Y. Yang, Appl. Phys. Lett. 80 (2002) 362.

83. H.S. Majumdar, A. Bandyopadhyay, A. Bolognesi, A.J. Pal, J. Appl. Phys. 91 (2001) 2433; Erratum, J. Appl. Phys. 91 (2002) 5508.

84. L.P. Ma, J. Liu, Y. Yang, Appl. Phys. Lett. 80 (2002) 2997.

85. Jui Hung Chen, Chu-Yun Cheng, Wen-Yen Chiua,, Chia-Fen Lee, Nai-Yun Liang, "Synthesis of ZnO/polystyrene composites particles by Pickering emulsion polymerization," European Polymer Journal, 2008, 44 Vol. 3271-3279

86. M.F. Yu, B.S. Files, S. Arepalli, R.S. Ruoff. "Tensile Loading of Ropes of Single Wall Carbon Nanotubes and their Mechanical Properties" Physical Review Letters, 2000 Vol. 84, 5552.

87. A. Thess, R. Lee, P. Nikolaev, H. Dai, P. Petit, J. Robert, C. Xu, Y. H. Lee, S. G. Kim, A.G. Rinzler, D.T. Colbert, G.E. Scuseria, D. Tomanek, J.E. Fischer, R.E. Smalley. "Crystalline Ropes of Metallic Carbon Nanotubes" Science, 1996 Vol. 273, 483

88. S. Hong, S. Myung. "Nanotube Electronics: A flexible approach to mobility". Nature Nanotechnology, 2007, Vol. 2 (4): 207–208.

89. M. Palumbo, K.U. Lee, B.T. Ahn, A. Suri, K.S. Coleman, D. Zeze, D. Wood, C. Pearson, M.C. Petty. "Electrical investigations of layer-by-layer films of carbon nanotubes" Institute of Physics 39, 2006, 3077-3085

90. S. Jombert, K. S. Coleman, D. Wood, M. C. Petty, and D. A. Zeze, J. Appl. Phys. 104, 094503 (2008).

91. M. Palumbo, K. U. Lee, B. T. Ahn, A. Suri, K. S. Coleman, D. Zeze, D. Wood, C. Pearson, and M. C. Petty, J. Phys. D: Appl. Phys. 39, 3077 (2006).

ملخص الرسالة

الهدف من هذا المشروع هو تجميع وتوصيف البوليمرات الموصلة مصنوعة من مزج البوليمرات غير الموصلة, مشحونة مع السوائل الأيونية. تطبيق لشرح استخدام هذه البوليمرات الموصلة الغير مألوف هوصنع جهاز ذاكرة عضوي.

تم الاعلان عن محاولات عده لتصنيع وتشكيل البوليمرات الموصله في المنشورات العلمية، العديد من هذه الأساليب تشمل منشطات البوليمر الذي يستعمل كعامل إشابة مع الزرنيخ أو البود القائمة في هذا العمل. وفي هذا البحث تم استخدام السوائل الايونيه، والمعروفة باسم الملدنات كعامل إشابة للبوليمرات الغير موصله. هناك مزايا عدة من لتوظيفالسوائل الأيونية لتشكيل بوليمرات موصله من بوليمرات غير موصله بما في ذلك الحفاظ على الخصائص العضوية (كل من البوليمرات والسوائل الايونية عبارة عن مواد عضوية).

في هذا العمل، تم تشكيل البوليمرات الموصلة بواسطة خليط غير موصل عن طريق مزج بولي فينيل الكحول PVA و بولي الأكريلاميد – كو- الاكريليك اسيد PAA, مع نسب مختلفة الوزن من الجلسرول، السوربيتول, واميدازوليوم بروميد بنسب تصل الى - 5٪ من نسب الوزن. تم استخدام طريقة الصب لتشكيل الأغشية الرقيقة، التي بحثت فيها مع اجهزة نانوانديتيشن، دفرنشول سكانينج كالوريمتري DSC، ثيرمو جرافيمترك انااليسس TGA، فوريير ترانسفورم انفريد اسبكتروسكوبي FT-IR وايسي انبيدنس اسبكتروسكوبي . وقد وجد أن الخواص الحرارية التحويل الزجاجي, ونقطة الانصهار , ودرجة حرارة التحلل) للPVA المخلوطة / PAA انخفاضا يتناسب مع النسب المئوية من المواد البلاستيكية الثلاثة المستخدمة في هذا المشروع. الصلابة ومعامل مرونة التي تم الحصول عليها من اختبار النانوانديتنشين وجد ان هناك تناقص مع زيادة تركيز الملدن. وأكد FT-IR الانخفاض في الرابطة الهيدروجينية بين سلاسل البوليمر المشترك لصالح تشكيل الروابط الجديدة بين المواد البلاستيكية وسلاسل خليط البوليمر

حداثة منشطات البوليمرات الغير موصولة مع الأيونية السائل تنبع من القدرة على تعديل درجة التوصيل الكهربائي، والخواص الميكانيكية والحراريه للخلطات من خلال التحكم في نسبة السائل الايونية التي أدخلت على البوليمر سوف تفتح حقلا جديدا من حقول دراسات البوليمر . وبالتالي يمزج العضوية البوليمر.

عندما تم تحديد مزيج من الخصائص الكهربائية مواتية، واستخدمت بعد ذلك في انتاج ذاكرة تخزين الجهاز العضوي. لوحظ وجود حلقة التباطو واسعة 40 فولت تقريبا كعنصر أساس تحت نطاق الاجتياح 40 فولت عندما كان كاربون نانو توب موجود مع خلطة البوليمرات . ولكن. 10- 20 فولت عندما تم مزج الذهب واكسيد الزنك جنبا إلى جنب مع مزيج من البوليمرات والجلسرين واظهرت قياسات مقاومة التي يمكن السيطرة عليها من الموصلية الايونية من غشاء البوليمر PAA /PVA بواسطة إضافة الملدنات. وبالتالي، شكلت البوليمر موصل إلى حل للتغلب على التحديات المرتبطة جهاز ذاكرة عضوي مجموع. تم استبدال البوليمرات بديل لأشباه الموصلات قاعدة السليكون في جهاز الذاكرة الاصطلاحية، ولكن مع تحسين الأداء بالمقارنة مع جهاز السيليكون القائم.

جامعة الإمارات العربية المتحدة
United Arab Emirates University

UAEU

جامعة الامارات العربية المتحدة
عمادة الدراسات العليا

البوليمرات الموصلة للكهرباء واستخداماتها في أجهزة حفظ المعلومات

رسالة مقدمة من

محمد يوسف الحايك

اشراف:

د. سعود الدعجة
قسم الهندسة الميكانيكية
جامعة الامارات العربية المتحدة

د. احمد عايش
قسم الفيزياء
جامعة الامارات العربية المتحدة

د. محمود محسن
قسم الكيمياء
جامعة الشارقة

رسالة مقدمة الى عمادة الدراسات العليا في جامعة الامارات العربية المتحدة لاستكمال متطلبات الحصول على درجة

الماجستير في الهندسة الميكانيكية

يونيو 2012 م

جامعة الإمارات العربية المتحدة
United Arab Emirates University

UAEU

جامعة الامارات العربية المتحدة
عمادة الدراسات العليا

البوليمرات الموصلة للكهرباء واستخداماتها في أجهزة حفظ المعلومات

رسالة مقدمة من

محمد يوسف الحايك

اشراف:

د. سعود الدعجة
قسم الهندسة الميكانيكية
جامعة الامارات العربية المتحدة

د. احمد عايش
قسم الفيزياء
جامعة الامارات العربية المتحدة

د. محمود محسن
قسم الكيمياء
جامعة الشارقة

رسالة مقدمة الى عمادة الدراسات العليا في جامعة الامارات العربية المتحدة لاستكمال متطلبات الحصول على د جة

الماجستير في الهندسة الميكانيكية

يونيو 2012 م